

LOW-COMPLEXITY ITERATIVE SOFT DETECTION FOR LDPC
CODED MULTI-RELAY CHANNELS

by

ALİ ÇAĞATAY CIRİK

Master of Science

Submitted to the Graduate School of Engineering and Natural Sciences

in partial fulfillment of

the requirements for the degree of

Master of Science

in

Electronics Engineering

Sabanci University

August 2009

LOW-COMPLEXITY ITERATIVE SOFT DETECTION FOR LDPC
CODED MULTI-RELAY CHANNELS

APPROVED BY:

Associate Prof. Dr. Mehmet KESKİNÖZ (Thesis Advisor):

Assistant Prof. Dr. Hakan ERDOĞAN:

Assistant Prof. Dr. İlker HAMZAOĞLU:

Assistant Prof. Dr. Kürşat ŞENDUR:

Assistant Prof. Dr. Yücel SAYGIN:

DATE OF APPROVAL:

© Ali aęatay Cırık 2009

All Rights Reserved

Abstract

Next generation wireless communication applications require reliable transmission of data at high data rates and a guarantee of quality-of-service over wireless links. However, degradations inherent in wireless channels, such as multipath fading, shadowing, path loss, and noise lead to reduction in the communication capacity and range significantly. One way to combat these adverse limitations is to employ spatial diversity, which can be achieved, for example, by transmitting independent copies of the signal over relay nodes, resulting in improvements in the transmission rates, reliability, and the capacity of the channel under pre-mentioned detrimental effects. In addition to exploiting diversity, the capacity of the channel can be further increased by employing an error correction code such as low-density parity check (LDPC) codes and turbo codes, etc.

Throughout this thesis, we consider LDPC coded full-duplex multi-relay channels using Estimate and Forward (EF) and Decode and Forward (DF) protocol. We focus on designing optimal and sub-optimal iterative soft detectors. Although the use of multi-relaying improves the channel reliability, the performance of the system is degraded because of the interference caused by multiple received signals coming from all relay nodes. To reduce the effect of the interference, maximum a posteriori (MAP) detector can be employed. Unfortunately, the complexity of the MAP detector grows exponentially as the number of relays increases. In the literature, two computationally efficient sub-optimal detectors have been proposed based on Taylor expansion or Central Limit Theorem (CLT) assumption to alleviate this problem. However, we find out that the correlation between intrinsic and extrinsic information stemming from these sub-optimal detectors is very high, and this correlation degrades the detector performance. To remedy that, in this thesis, we developed two new detectors: Soft Decorrelating Detection-Taylor (SODED-Taylor) and Soft Decorrelating Detection-CLT (SODED-CLT), which improves the performance of sub-optimal detectors about 0.8 dB - 1 dB.

Özet

Yeni nesil kablosuz iletişim uygulamaları, bilginin (verinin) kablosuz bağlantılar üzerinden yüksek veri hızında, güvenilir ve kaliteli servis garantisi altında iletimini gerektirir. Ancak, çok yönlü sönümlenme, gölgeleme, yol kaybı ve gürültü gibi kablosuz ortamın yapısında var olan bazı sınırlamalar, iletişim kapasitesi ve mesafesinde önemli ölçüde azalmalara sebep olur. Bu olumsuz sınırlamalarla mücadele etmenin bir yolu da sinyalin birbirinden bağımsız kopyalarının röle düğümleri üzerinden iletimiyle elde edilen *uzamsal çeşitlilik*dir. Röle kullanılarak elde edilen *çeşitlilik*, bu sınırlamalar altında bile iletim veri hızında, sinyalin güvenilirliğinde ve kanal kapasitesinde artmalara sebep olur. Çeşitlilikten başka, kanalın kapasitesi ayrıca LDPC, Turbo kodları gibi hata düzeltme kodları kullanılarak da artırılabilir.

Bu tezde, “Tahmin ve İleri” veya “Kod çözme ve İleri” protokollerini kullanarak, LDPC kodlu çift yönlü çoklu röle kanalları için, en uygun ve standart altı özyineli alıcı kod çözme tasarımı üzerine odaklandık. Çoklu röle kullanımı kanal güvenilirliğini ve kapasitesini artırsa da, sistem performansı tüm rölelerden gelen çoklu alınan sinyallerden dolayı oluşan girişim sayesinde bozulur. Girişimin etkisini azaltmak için En Büyük Sonsal (MAP) sezicisi kullanılabilir. Ne yazık ki, röle sayısı arttıkça, MAP sezicisinin karmaşıklığı üstel olarak artar. Literatürde, bu sorunu hafifletmek için, Taylor açılımı veya Merkezi Limit Teoremi varsayımı kullanılarak iki tane sayısal karmaşıklığı az olan standart altı sezici önerildi. Ancak, standart altı detektör kullanmaktan kaynaklanan asıl ve ikincil bilgi arasındaki ilintinin fazla olduğunu ve bunun sezici performansını azalttığını farkettik. Buna çare olarak, bu tezde standart altı sezicilerin performansını 0.8 -1dB artıran iki yeni sezici geliştirdik: Yumuşak İlintisizleştirilen Sezim-Taylor (SODED-Taylor) ve Yumuşak İlintisizleştirilen Sezim-CLT (SODED-CLT).

Acknowledgment

First and foremost, I would like to thank and express my gratitude to my advisor, Associate Professor Mehmet Keskinöz for his support, valuable guidance and patience during my MSc period. His thoughtful feedbacks, careful comments and criticism, and knowledgeable suggestions, have significantly enhanced my thought processes.

I would like to thank all my colleagues in Telecommunications & Networking Laboratory, where I have had the great opportunity to meet high talented people. Kayhan, Yunus, Sarper, Mehmet, Ali, Mumin, Ilgaz, you made this lab a great place to work.

I also thankfully acknowledge the financial support provided by the Scientific and Technological Research Council of Turkey (TÜBİTAK).

Finally, I would like to extend my deepest gratitude to my beloved parents, Mustafa and Elmas, and my brother Kubilay, for their constant love, unconditional support throughout the long path of my academic journey. I owe them all I have ever accomplished.

Dedicated to my beloved parents ...

TABLE OF CONTENTS

Abstract	iv
Özet	v
Acknowledgment	vi
LIST OF FIGURES	x
1. Introduction	1
1.1 Background on Relay Channels	3
1.2 Contributions of the Thesis	5
1.3 Outline of the Thesis	6
1.4 Notation	7
2. LDPC Codes	8
2.1 Linear Block Codes	8
2.2 Low Density Parity Check Codes	10
2.3 LDPC Representation	13
2.4 LDPC Encoding	14
2.5 LDPC Decoding	15
2.5.1 Probability Domain SPA Decoder	19
2.5.2 Log-Domain SPA Decoder	22
3. Cooperative Communications	26
3.1 SISO System	26
3.2 Cooperative Diversity	27
3.2.1 Background	27
3.2.2 Relay Channels	29
3.3 Cooperative Coding	32
4. LDPC Codes over Wireless Relay Channels	35
4.1 Single Relay Channel	36
4.1.1 Channel Model for Full-Duplex Relay Schemes	36

4.1.2	Capacity and Information Rate Bounds	39
4.1.3	Iterative LDPC Decoding for Relay Channels.....	42
4.1.4	Simulation Results	46
4.2	Multiple Relay Channels.....	51
4.2.1	Iterative LDPC Decoding for Multiple Relay Channels.....	52
4.2.2	Simulation Results	56
5.	Low Complexity Iterative Soft Detection	61
5.1	Approximation based on Taylor Expansion.....	62
5.2	Approximation based on Central Limit Theorem (CLT).....	67
5.3	Soft Decorrelating Detection (SODED)	73
6.	Conclusion	84
6.1	Future Work	85
References		87

LIST OF FIGURES

Figure 2.1: A regular matrix: $k = 3, j = 2, M = 4; N = 6, K = N - M = 2; R = 1/3$	12
Figure 2.2: An irregular matrix.....	12
Figure 2.3: LDPC code: A matrix representation.....	13
Figure 2.4: LDPC Code: Tanner Graph Representation.....	14
Figure 2.5: Illustration of message-passing algorithm on a bipartite graph	16
Figure 2.6: Message passing from variable node to check node	18
Figure 2.7: Message passing from check node to variable node	18
Figure 2.8: Illustration of message passing half-iteration for the computation of $q_{ij}(b)$.	20
Figure 2.9: Illustration of message passing algorithm for the computation of $r_{ji}(b)$	21
Figure 2.10: Demonstration of encoding with a rate 1/2 Gallager code. The encoder is derived from a very sparse 10000 x 20000 parity-check matrix with three 1's per column. (a) The code creates transmitted vectors consisting of 10 000 source bits and 10 000 parity-check bits. (b) Here, the source sequence has been altered by changing the first bit. Notice that many of the parity-check bits are changed. Each parity bit depends on about half of the source bits. (c) The transmission for the case $s = (1,0,0,\dots 0)$. This vector is the difference (modulo 2) between transmissions (a) and (b). (Reproduced from [22])	24
Figure 2.11: Iterative probabilistic decoding of a Gallager code. The sequence of figures shows the best guess, bit by bit, given by iteration decoder, after 0,1,2,3,10,11,12 and 13 iterations loop. The decoder halts after the 13th iteration when the best guess violated no parity check set. This final decoding is error free. (Reproduced from [22])	25
Figure 3.1: Communication block diagram.....	26
Figure 3.2: Cooperative Relay System	30
Figure 4.1: Basic Relaying System.....	36
Figure 4.2: Block Diagram of the Relay System.....	37
Figure 4.3: Capacity for Three Transmissions	41
Figure 4.4: Information Rates for Three Transmissions.....	41
Figure 4.5: Block Diagram of the coding scheme for the relay channels.....	43
Figure 4.6: Block Diagram of the Decoder	44
Figure 4.7: Bit error rate for three transmissions using LDPC decoding	47

Figure 4.8: BER of single relay channel for different number of global iteration using EF	49
Figure 4.9: BER of single relay channel for different number of global iteration using DF	49
Figure 4.10: BER comparison of EF and DF techniques for different number of global iteration	50
Figure 4.11: Multiple Relaying Systems	51
Figure 4.12: Block Diagram of the Decoder for Multiple Relays	54
Figure 4.13: Bit Error Rate for one, two and three relays using DF	57
Figure 4.14: Bit Error Rate for one, two and three relays using EF	58
Figure 4.15: BER comparison of EF and DF techniques for multi-relay channels	59
Figure 5.1: BER comparison of MAP detector and sub-optimal detector obtained by Taylor expansion for 1 global iteration	66
Figure 5.2: BER comparison of MAP detector and sub-optimal detector obtained by Taylor expansion for 2 global iterations	66
Figure 5.3: BER comparison of MAP detector and sub-optimal detector obtained by CLT assumption for 1 global iteration	70
Figure 5.4: BER comparison of MAP detector and sub-optimal detector obtained by CLT assumption for 2 global iterations	70
Figure 5.5: Comparison of sub-optimal detectors obtained by Taylor expansion and CLT assumptions for two relay network	72
Figure 5.6: Comparison of sub-optimal detectors obtained by Taylor expansion and CLT assumptions for eight relay network	72
Figure 5.7: Soft Decorrelating Detection (SODED)	76
Figure 5.8: BER Comparison of MAP, Taylor and SODED-Taylor detectors	83
Figure 5.9: BER Comparison of MAP, CLT and SODED-CLT	83

1. Introduction

Wireless communication is one of the most vibrant and rapidly growing area of the communications industry that provides a high-speed and a high-quality information exchange between devices when the use of wires are impossible or impractical to implement. Potential applications enabled by this technology include cell phones, smart homes, video teleconferencing, distance learning, and wireless sensor networks. However, supporting these applications using robust wireless techniques is challenging, since a transmitted signal encounters various obstacles, such as interference, propagation path loss, delay spread, Doppler spread, shadowing, and fading, due to the randomness in wireless channel, and limited transmission resources. These obstacles make it difficult to support high data rates with continuous coverage at a reduced cost, which is the main requirement in today's wireless broadband networks. Increasing the transmission bandwidth or transmit power is not a feasible solution to increase the transmission data rates due to high system deployment costs, an increased interference to other transmissions, and also reduction in the battery life-time [1].

Apart from increasing transmission bandwidth or transmit power, the scarcity of wireless spectrum allows the allocation of the high frequency bands to support high data rates. But, in high frequency bands, power attenuation with distance is more severe, leading to reduction in the coverage of a base station significantly. Therefore, increasing the density of base stations is also suggested to overcome fast decay of power to get improvements in the capacity and the coverage of networks. However, this trivial solution leads to the high infrastructure and deployment costs. As a result, we face a situation in which the wireless systems can achieve any two, but not all three, of high capacity, high coverage, and low cost [2].

Diversity was introduced as a pragmatic solution to mitigate the limitations imposed by wireless channel [3]. There are three main diversity techniques in the literature, which are temporal diversity, frequency diversity, and spatial diversity. Among these, spatial diversity provides a more robust and reliable communication, since it provides a higher system capacity without requiring any additional power or bandwidth.

Spatial diversity is exploited by transmitting signals via several independent diversity branches to get independent copies of the signal at the destination. Cooperative communication generates this diversity via multiple spatially separated antennas and multiple geographically separated users or relay nodes. Therefore, using relay nodes is a more practicable solution to increase the data rate, coverage range, and enhance the reliability, compared to employing additional antennas on mobile terminals and/or deploying base stations.

To grasp the impact of relay channels, a realistic example should be given. We've all had that annoying experience: the strength of your signal may suddenly weaken when you're in the middle of a cell phone conversation, making it difficult for you to perpetuate your chat. The reason is that the wireless channel suffers from fading, leading to severe variations in signal attenuation within the duration of any given call. Therefore, you never know when your conversation will be interrupted or cut off.

In today's mobile communication, cell phones and base stations form a one to one communication. When an obstacle comes between the cell phone and a base station, the phone either increases its signal power to maintain continuous contact with the base station or the communication is cut off. But, as it is mentioned above increasing transmit power results in reduced battery life and an increased interference to other transmissions.

The fact that numerous people use cell phones simultaneously allows the creation of a cooperative network protocol that phones communicate with a base station through the help of other phones. When your cell phone has some difficulties to maintain contact with the base station, the fellow behind you may have a perfectly strong signal.

Therefore, by exploiting cooperative communication, your phone sends its signal through that fellow's cell phone, and the strength of your signal becomes stronger than before. Therefore, the overall signal power is strengthened and an interactive, reliable, and cooperative mode of uninterrupted communication is generated. This cooperative communication scheme is not designed for only cell phones, but also for any wireless devices operating in a network.

In the next section, the communication techniques enabling spatial diversity are introduced and specifically background on relay networks, which is one of those communication techniques, is provided.

1.1 Background on Relay Channels

Spatial diversity can be generated via multiple antennas that are physically separated from one another. The receiver antenna diversity, where the receiver has more than one antenna is the first spatial diversity technique proposed in the literature [4]. The antennas must be separated on the order of wavelength to have independently faded versions of the transmitted signal to use receiver combining techniques, i.e., maximum-ratio combining (MRC), equal gain combining (EGC), and selection combining (SC) effectively. But, the size of the mobile terminals puts a constraint to employ multiple antennas. To overcome this constraint, a simple transmit diversity scheme is invented by Alamouti [5], which involves the transmission of multiple redundant copies of data to combat for fading. Alamouti's transmit diversity scheme for two transmit antennas is used to develop Space-Time Block Coding (STBC). A generalized study of STBC is given in [6], [7].

Again, due to the limitations in size and hardware complexity, transmit diversity methods are not applicable to many wireless systems. A conventional example is ad-hoc networks and sensor networks, where size, complexity, and power are all constraints that prevent the presence of a large number of transmit antennas. In such wireless networks,

geographically separated users can be used to help forward the data of their partners, resulting in diversity. If only one user in the network has information to transmit and the other nodes are only present to help the user by forwarding its data, such networks are called relay networks [8]. With this approach, the full connectivity between the nodes in the network is exploited.

The use of relays can significantly improve the channel capacity, reduce the power cost and enhance the system reliability. In relay networks, the basic idea is that a relay node helps a source node transmit its data to a destination that is out of reach of the source node [9]. Relay channels are important building blocks of next generation wireless systems and will play a central role in various applications including cellular systems and wireless ad hoc networks. From a physical layer point of view, there are two main research directions on wireless relaying: information theoretical work aiming at the evaluation of theoretical limits of relay channels [10], and the development of practical wireless relaying protocols. This thesis focuses on the latter research direction, where an appropriate receiver structure is designed for LDPC coded full-duplex relay channels and works on increasing the system performance by employing multi-relays, as well as decreasing the system complexity as relay number increases

Some practical relaying strategies have been proposed in the literature. The “coded cooperation” technique was proposed using convolutional codes [11] and later extended to space-time codes [12], [13]. However, these codes could not approach the capacity limits of the relay channel. That leads to incorporation of Turbo codes [14]-[15]. In [14]-[15], the authors propose turbo coded cooperation schemes for both half-duplex and full-duplex relaying and it is shown that these schemes approach the capacity limits very closely by employing a multi-access channel detector and iterative decoding at the destination. LDPC codes which have superior error correction capability and capacity approaching capability as compared to Turbo codes have not been considered in a significant amount of research for relay channels. Specifically, [16] proposes the design of a compress and forward scheme for the half-duplex Gaussian relay channel based on Wyner-Ziv coding where LDPC codes are not given a special attention, but only treated

as an error protection method at the source node. The authors in [17] present an efficient LDPC code design approach for full-duplex Gaussian relay channels and corresponding decoding based on a partial factor graph. From information theoretical perspective, the authors in [18] and [19] show that carefully-designed LDPC codes can approach the capacity limits in a non-fading environment by developing different coding schemes for half-duplex and full-duplex relay channels. In [20], authors design appropriate coding/decoding strategies based on LDPC codes using the decode-and-forward protocol for single relay channel for both full-duplex and half-duplex relay channels. In this thesis, we have implemented appropriate receiver structures for full-duplex LDPC coded-multi relay channels using DF and EF protocol.

There are a number of contributions in the literature on relay channels. We add to that knowledge by developing some ideas, which are mentioned in the next section.

1.2 Contributions of the Thesis

This thesis is concerned with decoding scheme of full-duplex multiple relay channels for fading channels. The contributions of this thesis can be classified into three categories

1. We extend full-duplex single relay channel to full-duplex multiple relays for flat fading channels. The destination observes a superposition of the codewords transmitted from source and relay nodes. The iterative receiver structure between maximum a posteriori (MAP) detector and LDPC decoder is designed to extract the transmitted data from source node by using these superimposed signals.
2. As we increase the relay number, the computational complexity of MAP detector increases exponentially. Therefore, two sub-optimal detectors based on Taylor expansion or Central Limit Theorem (CLT) approaches are investigated.

The performances of these low complex detectors are compared with optimal MAP detector with respect to number of relays in the network.

3. Using sub-optimal detectors result in degradation of system performance due to high correlation between intrinsic and extrinsic information of detectors. Therefore, we propose two detectors named SODED-Taylor and SODED-CLT which decorrelate these two values by using attenuators at the output of the detector and get improvements.

1.3 Outline of the Thesis

The rest of this thesis is organized as follows:

Chapter 2 Presents an overview of LDPC codes. The representation of LDPC codes, encoding and decoding processes are provided in detail.

Chapter 3 Provides a background on cooperative communication and cooperative diversity relaying. In addition, background on coding for relay channels is presented.

Chapter 4 Studies the performance of single relay networks where the source, the destination and relay node are all equipped with single antennas. Full-duplex channel model and capacity and information rates of this scheme, as well as the direct and multi-hop transmission schemes are discussed. At the receiver side, the iterative decoding process between MAP detector and LDPC decoder is analyzed. Moreover, single relay system is extended to multi-relay systems and an appropriate receiver structure is designed accordingly. The performance of this system is investigated and compared to single-relay systems.

Chapter 5 Two sub-optimal detectors with low computational complexity are obtained by approximating MAP detector using Taylor expansion or CLT assumption. These sub-

optimal detectors are compared with optimal MAP detector and the worse performance of these sub-optimal detectors compared to MAP is alleviated by decreasing the correlation between intrinsic and extrinsic information using attenuators. The reduction in decorrelation of intrinsic and extrinsic information allows us to achieve two detectors, named SODED-Taylor and SODED-CLT.

Chapter 6 Provides concluding remarks and discuss possible future work based on the ideas developed in this thesis.

1.4 Notation

In the thesis, we use following notations. T stands for transposition . Bold uppercase letters describe matrices while bold lowercase letters describe row vectors of appropriate dimensions. We denote the expectation operator as $E[\cdot]$. \mathbf{I}_N is the $N \times N$ identity matrix.

2. LDPC Codes

This chapter introduces a detailed overview of LDPC codes. The representation, encoding and principles of iterative LDPC decoding, which will be used throughout this thesis, are provided. Before we begin a discussion of LDPC codes, some basics of linear block codes are reviewed.

2.1 Linear Block Codes

In error control codes, extra redundant bits are added to the information data to help the receiver detect and correct errors of the received data. The main characterization of a block code is the division of the transmitted data into blocks of fixed length of K bits. A linear block code is an important type of block codes used in detection and correction of errors. In linear block coding, each symbol can be written as a linear combination of other bits or symbols in the transmitted data. The encoder maps block of K source bits into blocks of N coded bits, where N is greater than K . That would provide the recipient of the message block enough redundancy to detect and correct errors. The rate of the code is expressed as $R=K/N$, where it states the fraction of the total amount of information that is useful (non-redundant).

When K bits are used to form an information data, there are 2^K distinct information data possible. Each K bit information data is attributes to the N bit codeword. An arbitrary encoding, an encoder requires the storage of a table of 2^K entries each of length N , which is not practical as K increases. Linear block codes alleviate the non-practicality and the complexity of the arbitrary encoding by using a linear generator matrix to transform information data to codewords. In this work, we consider binary linear block codes.

A binary code is linear if and only if the modulo-two sum of any two codewords is a codeword, which allows to find a generator matrix (\mathbf{G}), defining the code. The generator matrix consists of K linearly independent row vectors of size N , $g_1, g_2 \dots g_K$, such that it can be defined as

$$\mathbf{G} = \begin{bmatrix} g_1 \\ \cdot \\ \cdot \\ \cdot \\ g_K \end{bmatrix} \quad (2.1)$$

The encoder generates a codeword \mathbf{c} by multiplying the message bits \mathbf{u} with the generator matrix \mathbf{G} as, $\mathbf{c}=\mathbf{uG}$, where \mathbf{c} is the codeword and \mathbf{u} is the vector of message bits. As it is mentioned above, in arbitrary encoding the complexity of the encoder is $2^K \times N$, whereas now the complexity reduces to the size of \mathbf{G} , that is $K \times N$, since it is enough for the encoder to just store \mathbf{G} . Also a parity-check matrix \mathbf{H} can be deduced from the generator matrix \mathbf{G} , where the relation of the matrices are expressed as $\mathbf{GH}^T=0$. To check whether the received data, \mathbf{y} , is a codeword or not, the receiver uses the \mathbf{H} matrix, by utilizing the expression

$$\mathbf{yH}^T = \mathbf{0} \quad (2.2)$$

since $\mathbf{uGH}^T=0$. That is, a codeword is orthogonal to each row of \mathbf{H} . This expression is used by the decoder for error detection and correction.

Systematic encoding, where the message bits and redundant bits are explicitly extracted from the codeword, is convenient to be used in encoders. Designing a generator matrix that allows systematic encoding, is possible by performing row reductions and column reordering on \mathbf{G} until obtaining an identity matrix. Thus \mathbf{G} can be expressed as

$$\mathbf{G} = [\mathbf{P} | \mathbf{I}_K] = \begin{bmatrix} p_{1,1} & \cdots & p_{1,N-K} & 1 & 0 & \cdots & 0 \\ p_{2,1} & \cdots & p_{2,N-K} & 0 & 1 & \cdots & 0 \\ \vdots & \ddots & \vdots & \vdots & \vdots & \ddots & \vdots \\ p_{K,1} & \cdots & p_{K,N-K} & 0 & 0 & \cdots & 1 \end{bmatrix} \quad (2.3)$$

where \mathbf{P} is an $K \times (N-K)$ sub-matrix, and \mathbf{I}_K is the $K \times K$ identity matrix

It is easy to determine the parity check matrix \mathbf{H} , when \mathbf{G} is systematic. It is simply

$$\mathbf{H} = [\mathbf{I}_{N-K} | -\mathbf{P}^T] = \begin{bmatrix} 1 & 0 & \cdots & 0 & -p_{1,1} & \cdots & -p_{K,1} \\ 0 & 1 & \cdots & 0 & -p_{1,2} & \cdots & -p_{K,2} \\ \vdots & \vdots & \ddots & \vdots & \vdots & \ddots & \vdots \\ 0 & 0 & \cdots & 1 & -p_{1,N-K} & \cdots & -p_{K,N-K} \end{bmatrix} \quad (2.4)$$

where \mathbf{I}_{N-K} is the $(N-K)$ identity matrix and \mathbf{P}^T is the transpose matrix of \mathbf{P} . For binary codewords, $-\mathbf{P}^T = \mathbf{P}^T$.

After providing some basics of linear block codes, the next section introduces one of the most powerful error correcting codes, LDPC codes, which are a class of linear block codes.

2.2 Low Density Parity Check Codes

Designing practical coding schemes approaching the capacity very closely has always been a central challenge in coding theory. In recent years, understanding and the ability to design iterative decoding schemes have improved such that all aspects of the telecommunication network can be included in the iterative processing: source coding channel coding, modulation, equalization, multiple access, and transmission via multiple antennas; and so on. Coding techniques, such as turbo codes or LDPC codes, also use iterative decoding based approach, that give a performance close to the Shannon limit within a factor of a dB.

LDPC codes were discovered by Robert Gallager in the 60s in his Ph.D. thesis [21]. But, his ideas of iterative decoding using message-passing algorithm has been forgotten for almost 30 years until Mackay-Neal [22] and Wiberg [23] rediscovered the capability of this error correcting code. With an appropriate degree distribution, LDPC codes were shown to demonstrate the properties of good codes capable of asymptotically approaching Shannon limit. They have a threshold within 0.0045dB of the Shannon limit of AWGN channel (At BER 10^{-6} and block length 10^7) [24]. LDPC codes were further extended in [25] to include irregular LDPC codes, outperforming the Turbo codes, in terms of bit-error rates.

The interest of researchers on LDPC codes has boosted due to its surpassing the performance of Turbo codes and having lower hardware complexity than Turbo codes. Therefore, a number of next generation communication standards, such as mobile phones and next-generation satellite digital video broadcasting standard, DVB-S2 has been considering LDPC codes for error correction standard [26].

LDPC codes are linear block codes specified by a sparse $M \times N$ parity check matrix, \mathbf{H} where $N > M$ and $M = N - K$. Despite the fact that these codes can be generalized to non-binary symbols, in this thesis we only consider binary codes. The parity check matrix contains a small number of 1's per column and per row, both of which are very small compared to block length, making it sparse. In particular, an (N, j, k) low-density code is a code of block length N . The number of 1's in a parity check matrix row is called the row weight, k , and the number of 1's in a column is the column weight, j . Regular LDPC codes have same row weight and same column weight on parity check matrix, whereas, irregular LDPC codes have different row and column weight on parity check matrix.

- A regular LDPC code is characterized by two values: k , and j .

j is the number of ones in each column of the parity check matrix $\mathbf{H} \in \mathbb{F}_2^{M \times N}$.

k represents the number of ones in each row. $\mathbb{F}_2^{M \times N}$ represents binary finite field, consisting of $M \times N$ elements 0 and 1, where addition is exclusive OR (XOR) and multiplication is AND.

- The rate of parity check matrix is the fraction of information bits in the codeword. It is given by $R = \frac{K}{N} = \frac{N-M}{N} = 1 - \frac{M}{N}$

The number of 1's in the parity check matrix \mathbf{H} is given by Mk or Nj . From $Mk=Nj$, we get $\frac{M}{N} = \frac{j}{k}$. Hence the rate of matrix can also be expressed as $R = 1 - \frac{j}{k}$.

Figure 2.1 represents a regular (6, 2, 3) LDPC code with its parameters

$$\mathbf{H} = \begin{bmatrix} 1 & 1 & 0 & 1 & 0 & 0 \\ 1 & 0 & 1 & 0 & 1 & 0 \\ 0 & 1 & 1 & 0 & 0 & 1 \\ 0 & 0 & 0 & 1 & 1 & 1 \end{bmatrix}$$

Figure 2.1: A regular matrix: $k = 3, j = 2, M = 4; N = 6, K = N - M = 2; R = 1/3$

- An irregular LDPC code has different numbers of ones in each row and columns. It is known to be better than the regular one in terms of bit error rate (BER) and its performance is close to Shannon limit [27].

Figure 2.2 shows an irregular parity check matrix. The number of ones in some columns is 3 and in others it is 2. We have also the same situation for rows, a row has 4 ones and others have 3 ones.

$$\mathbf{H} = \begin{bmatrix} 1 & 0 & 1 & 0 & 0 & 0 & 1 \\ 1 & 1 & 0 & 0 & 1 & 0 & 1 \\ 1 & 1 & 0 & 0 & 0 & 1 & 0 \\ 0 & 0 & 1 & 1 & 1 & 0 & 0 \\ 0 & 0 & 0 & 1 & 0 & 1 & 1 \end{bmatrix}$$

Figure 2.2: An irregular matrix

2.3 LDPC Representation

R.M. Tanner, in [28] used the basic techniques of graph theory to facilitate the design algorithms for encoding and decoding. He proposed an approach to the construction of codes which generalized the LDPC code construction, using recursive techniques. In addition, he suggested a bipartite graph, also known as a Tanner graph for a graphical representation of LDPC codes, rather than using a sparse matrix for representation. In a bipartite graph, nodes are partitioned into two subsets such that an edge connects each node in a set to a node in the other set. In the context of LDPC coding, the two subsets of nodes in a Tanner graph are referred to as check nodes and variable nodes. Figure 2.3 shows a parity check matrix with a corresponding Tanner graph, Figure 2.4. An edge exists between the c^{th} check node and the v^{th} variable node if and only if $\mathbf{H}_{c,v}$ is 1. Check nodes $c_1 \dots c_5$ represent the five rows of the matrix, whereas $v_1 \dots v_{10}$ are the columns.

A cycle in a Tanner graph is formed by starting from a node and alternating through “1” entries between variable and check nodes, and then ending in the starting node. The number of edges in the complete path determines the length of the cycle and is always even; but it cannot be two. A cycle of four is shown in bold in the graph of Figure 2.4. The smallest cycle in a Tanner graph is called its girth. The smallest possible girth is four.

$$\mathbf{H} = \begin{bmatrix} 1 & 1 & 1 & 1 & 1 & 1 & 0 & 0 & 0 & 0 \\ 0 & 0 & 1 & 1 & 1 & 1 & 1 & 1 & 0 & 0 \\ 0 & 1 & 0 & 1 & 0 & 1 & 0 & 1 & 0 & 1 \\ 1 & 0 & 1 & 0 & 1 & 0 & 1 & 0 & 1 & 0 \\ 1 & 1 & 0 & 0 & 1 & 0 & 1 & 0 & 1 & 1 \end{bmatrix}$$

Figure 2.3: LDPC code: A matrix representation

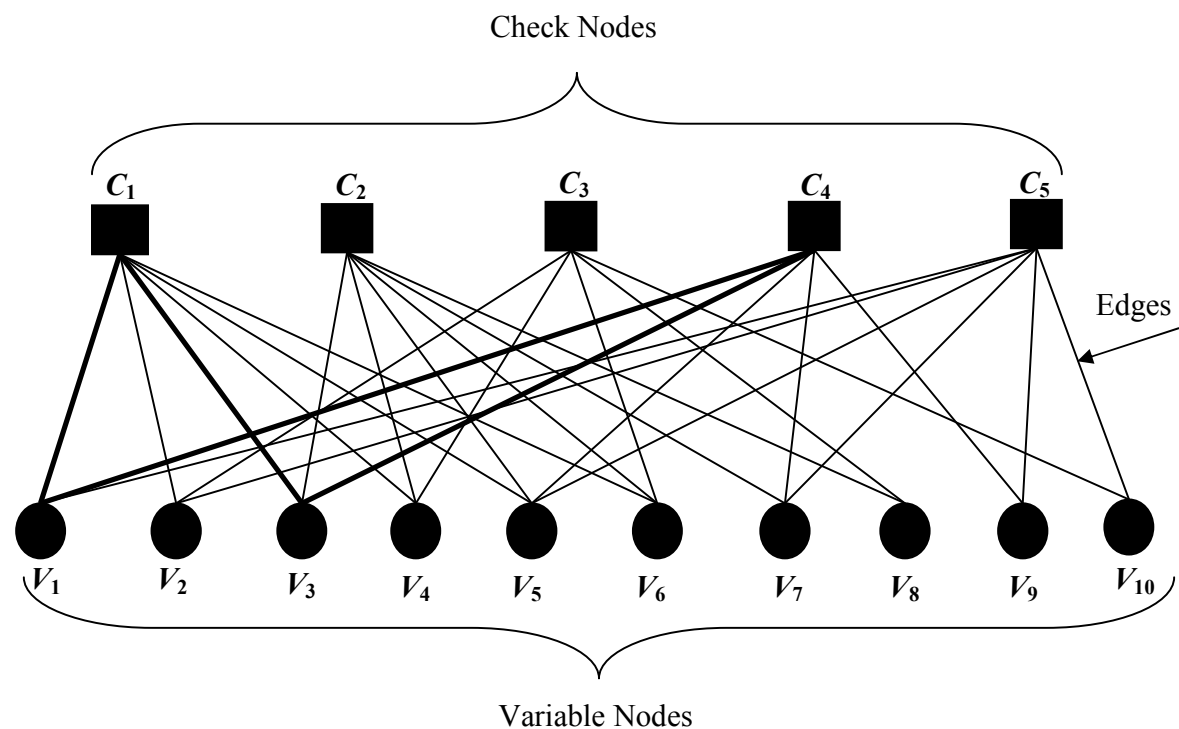


Figure 2.4: LDPC Code: Tanner Graph Representation

2.4 LDPC Encoding

The encoding of LDPC codes is similar to encoding of linear codes, which is briefly discussed in Section 2.1. From a given parity check matrix, \mathbf{H} , a generator matrix, \mathbf{G} , is derived. The encoding of data $\mathbf{u} = u_1 \dots u_N$ is performed by multiplying \mathbf{u} with the generator matrix, $\mathbf{c} = \mathbf{u}\mathbf{G}$ where \mathbf{u} is a vector of message bits and \mathbf{c} is the codeword to be transmitted. Converting \mathbf{H} matrix in systematic form, using Gaussian elimination and column permutations $\mathbf{H} = [\mathbf{I}_M \mid \mathbf{P}^T]$, eliminates the sparseness of the parity check matrix, since it has no longer fixed column or row weights and \mathbf{P} is very likely to be dense. The computational complexity of the encoder increases due to this denseness of \mathbf{P} , since the multiplication of message bits with the dense generator matrix requires a large number of operations. Performing Gaussian elimination takes about $O(N^3)$ and afterwards the

actual encoding it takes $O(N^2)$, or more precisely $N^2(\frac{R(1-R)}{2})$ operations, where R is the code rate [29], since the \mathbf{H} matrix is dense after the Gaussian elimination.

Richardson and Urbanke [30] took advantage of the sparsity of the \mathbf{H} matrix to decrease the quadratic complexity of the encoding process by parity-check matrix preprocessing. They found that the encoding complexity is either linear or quadratic, but quite manageable without performance degradation. For example, for a (3,6) regular code of length N , even though the complexity is still quadratic, the actual number of operations required is $O(N)$ in addition to $0.017^2 N^2$. But 0.017^2 is a small number, so the complexity of the encoder is still manageable for large N .

2.5 LDPC Decoding

In addition to introducing LDPC codes, Gallager also proposed an iterative decoding algorithm with a computational complexity that is linear in the block length [22]. The decoding algorithm works iteratively and computes the distributions of variables by passing messages on the edges of bipartite graph. Depending on the context, decoding algorithm has different names which include sum-product algorithm (SPA), the message passing algorithm (MPA) and the belief propagation algorithm (BPA). In this thesis, we will use “message passing” term, which usually covers SPA, BPA and their approximations. In message-passing algorithm, message, which is an estimate of the bit associated with that edge, is passed along the edges of the graph as shown in Figure 2.5.

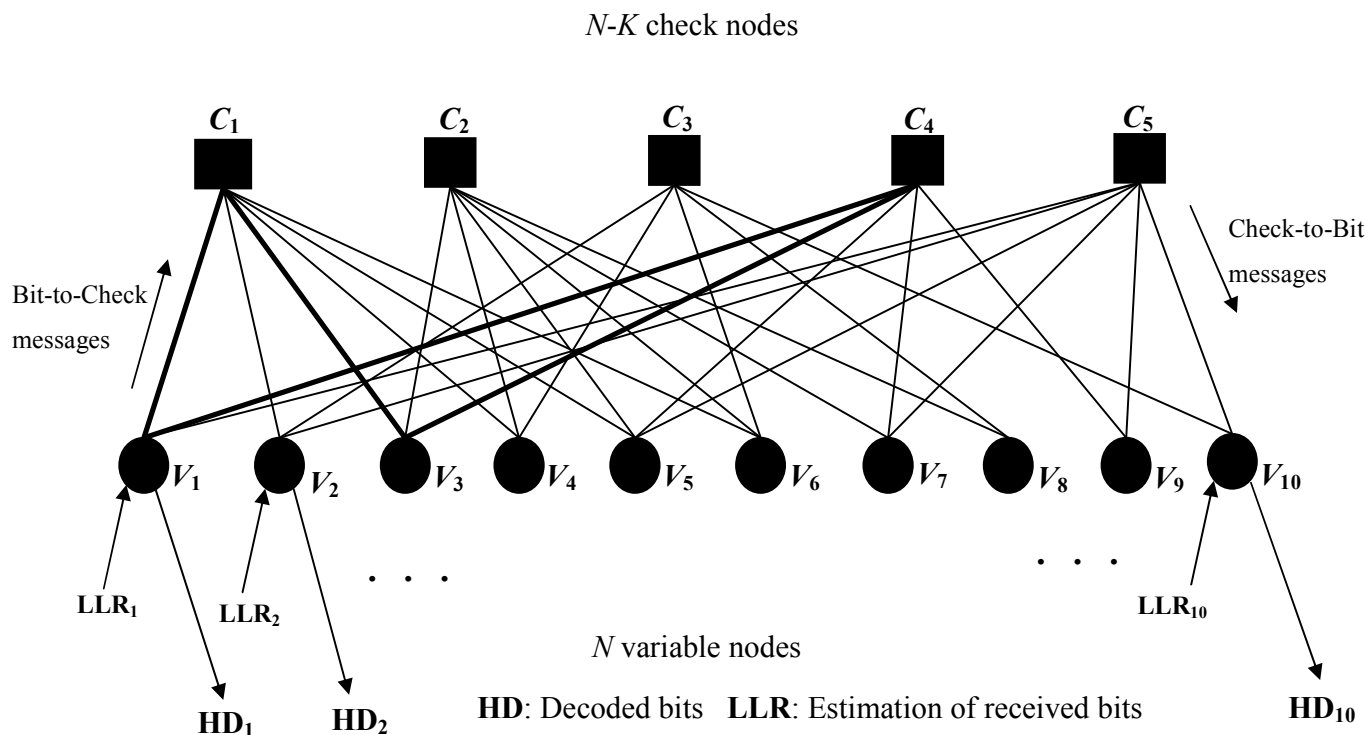


Figure 2.5: Illustration of message-passing algorithm on a bipartite graph

These decoders can be understood by focusing on one bit as follows:

A codeword which is encoded by LDPC codes encounter noisy communication channel during transmission and some of its bits are corrupted by noise. Each variable node at the decoder has to determine whether the bit that arrived is error free or not. Therefore the variable node asks all bit's neighboring check nodes (two nodes are said to be neighbors if they are connected by an edge) about the value of the bit. Afterwards, each neighboring check node asks its other neighbors their values and modulo two sums of those values is sent back to the variable node.

The variable node now has several estimations coming from check nodes. It can take a majority vote, but as the iteration number increases, the true value of the bit can be obtained easily.

Each node obtains estimates from all its neighbors and forwards its estimate to each neighbor with the help of the estimates of the other neighbors. This is what message-passing algorithm is. This iterative algorithm goes on until either all parity-check equations are satisfied or a pre-determined iteration number runs out.

The decoding analysis of LDPC codes is given in detail in [31].

Similar to symbol by symbol decoding of trellis codes, the value of the a posteriori probability (APP) that a given bit in the transmitted codeword $\mathbf{c} = [c_1 \ c_2 \ \dots \ c_N]$ equals 1, given the received word $\mathbf{y} = [y_1 \ y_2 \ \dots \ y_N]$ is important.

For the decoding of bit c_i , the APP is computed as

$$P(c_i = 1 | \mathbf{y}) \tag{2.5}$$

or the APP ratio (also called the likelihood ratio, LR)

$$LR(c_i) = \frac{P(c_i = 0 | \mathbf{y})}{P(c_i = 1 | \mathbf{y})} \tag{2.6}$$

or the log-APP ratio (also called the log-likelihood ratio, LLR).

$$LLR(c_i) = \log\left(\frac{P(c_i = 0 | \mathbf{y})}{P(c_i = 1 | \mathbf{y})}\right) \tag{2.7}$$

In one half iteration, each variable node v processes its input messages and sends its output messages to its neighboring check nodes c . This is shown in Figure 2.6 for the message m_{13} from variable node v_1 to check node c_3 . The information passed is (2.5) or (2.6) or (2.7). Note that all the information coming to v_1 from the channel and its neighbors, except c_3 is passed to c_3 . That means only extrinsic information is exchanged. Such extrinsic information is computed for each connected variable-check node pair.

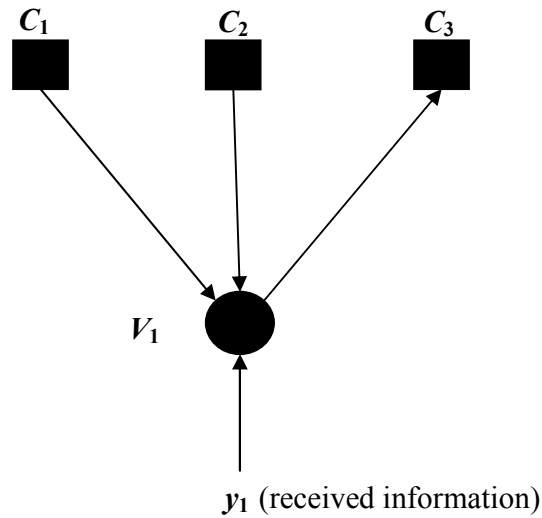


Figure 2.6: Message passing from variable node to check node

In the other half iteration, each check node processes its input messages coming from variable nodes and sends its output messages to its neighboring variable nodes. This is shown in Figure 2.7 for the message m_{14} from check node c_1 to variable node v_4 . The information passed is $\Pr(\text{check equation } c_1 \text{ is satisfied} \mid \text{input messages})$. Similar to the previous case, only extrinsic information is passed to variable node v_4 . That is all the information coming to c_1 from its neighbors, except v_4 is passed to v_4 . Such extrinsic information is computed for each connected check-variable node pair.

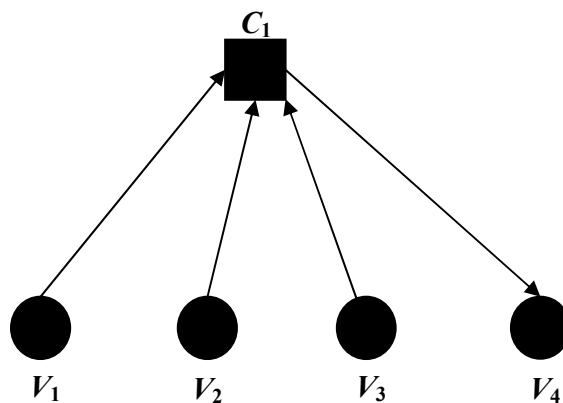


Figure 2.7: Message passing from check node to variable node

After a pre-determined number of iterations or all parity check equations are satisfied, the decoder computes the APP and decides the bits transmitted from this APP value. One example of stopping criterion is to stop iterating when $\hat{\mathbf{c}}\mathbf{H}^T = 0$, where $\hat{\mathbf{c}}$ is a decoded codeword.

2.5.1 Probability Domain SPA Decoder

We start by introducing the following notation:

- $V_j = \{\text{variable nodes connected to check node } c_j\}$
- $V_{j\setminus i} = \{\text{variable nodes connected to check node } c_j\} \setminus \{\text{variable node } i\}$
- $C_i = \{\text{check nodes connected to variable node } v_i\}$
- $C_{i\setminus j} = \{\text{check nodes connected to variable node } v_i\} \setminus \{\text{check node } j\}$
- $M_v(\sim i) = \{\text{messages from all variable nodes except node } v_i\}$
- $M_c(\sim j) = \{\text{messages from all check nodes except node } c_j\}$
- $P_i = \Pr(v_i = 1 | y_i)$
- $S_i = \text{event that the check equations involving } v_i \text{ are satisfied.}$
- $q_{ij}(b) = \Pr(v_i = b | S_i, y_i, M_c(\sim j))$, where $b \in \{0, 1\}$. For the APP algorithm $m_{ij} = q_{ij}(b)$; for the LR algorithm $m_{ij} = q_{ij}(0) / q_{ij}(1)$; and for the LLR algorithm $m_{ij} = \log[q_{ij}(0) / q_{ij}(1)]$
- $r_{ji}(b) = \Pr(\text{check equation } c_j \text{ is satisfied} | v_i = b, M_v(\sim i))$, where $b \in \{0, 1\}$. For the APP algorithm $m_{ji} = r_{ji}(b)$; for the LR algorithm $m_{ji} = r_{ji}(0) / r_{ji}(1)$; and for the LLR algorithm $m_{ji} = \log[r_{ji}(0) / r_{ji}(1)]$

$q_{ij}(0)$ is expressed as

$$\begin{aligned}
 q_{ij}(0) &= \Pr(v_i = 0 | S_i, y_i, M_c(\sim j)) \\
 &= (1 - P_i) \Pr(S_i | v_i = 0, y_i, M_c(\sim j)) / \Pr(S_i) \\
 &= K_{ij} (1 - P_i) \prod_{j' \in C_i \setminus j} r_{j'i}(0)
 \end{aligned} \tag{2.8}$$

where the Bayes' rule is used twice to obtain the second line and the independence assumption is used to obtain the third line. Similarly,

$$q_{ij}(1) = K_{ij} P_i \prod_{j' \in C_i \setminus j} r_{j'i}(1) \quad (2.9)$$

The constants K_{ij} are chosen to ensure that $q_{ij}(0) + q_{ij}(1) = 1$
 Calculation of q_{ij} is shown in Figure 2.8

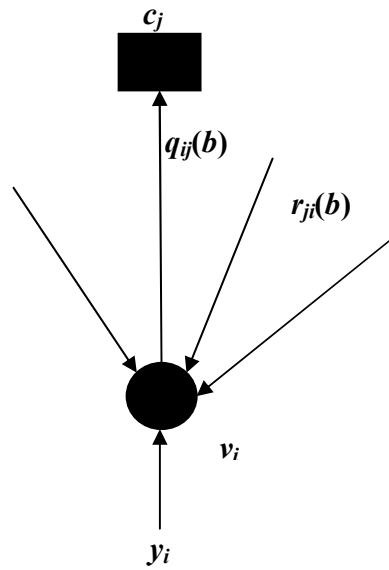


Figure 2.8: Illustration of message passing half-iteration for the computation of $q_{ij}(\mathbf{b})$

To find an expression for the $r_{ji}(b)$, the following result is used.

Result: (Gallager [21]) Consider a sequence of M independent binary digits a_i for which $\Pr(a_i=1)=p_i$. Then the probability that $\{a_i\}_{i=1}^M$ contains an even number of 1's is

$$\frac{1}{2} + \frac{1}{2} \prod_{i=1}^M (1 - 2p_i) \quad (2.10)$$

Proof: Induction on M

Using this result and the correspondence $p_i \rightarrow q_{ij}(1)$, we get

$$r_{ji}(0) = \frac{1}{2} + \frac{1}{2} \prod_{i' \in \mathcal{V}_j \setminus i} (1 - 2q_{i'j}(1)) \quad (2.11)$$

Clearly,

$$r_{ji}(1) = 1 - r_{ji}(0) \quad (2.12)$$

The calculation of r_{ji} is shown in Figure 2.9

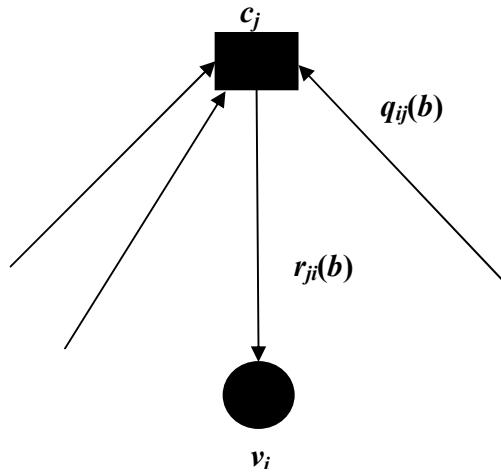


Figure 2.9: Illustration of message passing algorithm for the computation of $r_{ji}(b)$

Summary of the Probability-Domain SPA Decoder

- 1) For all variable nodes, $P_i = \Pr(v_i = 1 | y_i)$ is calculated, where y_i is the i^{th} received channel symbol. Then, set $q_{ij}(0) = 1 - P_i$ and $q_{ij}(1) = P_i$ for all i, j .
- 2) Update $r_{ji}(b)$ using equations (2.11) and (2.12).
- 3) Update $q_{ji}(b)$ using equations (2.8), (2.9) and solve for the constants K_{ij}
- 4) Compute

$$Q_i(0) = K_i (1 - P_i) \prod_{j \in \mathcal{C}_i} r_{ji}(0) \quad (2.13)$$

and

$$Q_i(1) = K_i P_i \prod_{j \in C_i} r_{ji}(1) \quad (2.14)$$

where the constant K_i is chosen to ensure that $Q_i(0) + Q_i(1) = 1$

$$5) \text{ Set } \hat{c}_i = \begin{cases} 1 & \text{if } Q_i(1) > Q_i(0) \\ 0 & \text{else} \end{cases}$$

If $\hat{\mathbf{c}}\mathbf{H}^T = 0$ or the number of iterations equal to the pre-determined iteration, stop; else go to Step 2.

2.5.2 Log-Domain SPA Decoder

For binary codes, the sum-product algorithm can be performed more efficiently in log-domain, where the probabilities are equivalently characterized by the log-likelihood ratios (LLR).

Initialization: Each variable node v_i is assigned an a posteriori probability $P_i = \Pr(v_i=1|y_i)$. In the case of equiprobable inputs for a memoryless AWGN channel

$$L(v_i) \triangleq \log \frac{\Pr(v_i = 0 | y_i)}{\Pr(v_i = 1 | y_i)} = \log \frac{1 - P_i}{P_i} = \frac{2}{\sigma^2} y_i \quad (2.15)$$

$$L(q_{ij}) \triangleq \log \frac{q_{ij}(0)}{q_{ij}(1)} = L(v_i) \quad (2.16)$$

$$L(r_{ji}) \triangleq \log \frac{r_{ji}(0)}{r_{ji}(1)} = 0 \quad (2.17)$$

Checks to variable nodes: Each check node c_j gathers all the incoming information and updates the belief on the bit i based on the information from all *other* bits connected to the check node c_j .

First replace $r_{ji}(0)$ with $1-r_{ji}(1)$ in (2.12) and rearrange to obtain

$$1 - 2r_{ji}(1) = \prod_{i' \in V_j \setminus i}^M (1 - 2q_{i'j}(1))$$

Now, using the fact that $\tanh[\frac{1}{2} \log(\frac{p_0}{p_1})] = p_0 - p_1 = 1 - 2p_1$, the equation above is written as

$$\tanh\left(\frac{1}{2} L(r_{ji})\right) = \prod_{i' \in V_j \setminus i}^M \tanh\left(\frac{1}{2} L(q_{i'j})\right),$$

and rearranging the equation gives

$$L(r_{ji}) = 2 \tanh^{-1}\left(\prod_{i' \in V_j \setminus i} \tanh(L(q_{i'j})/2)\right) \quad (2.18)$$

Variable to Check nodes: Each variable node v_i passes its probability to all the check nodes that connect to it. The initial information P_i and the “extrinsic” information, r_{ji} coming from the connected check nodes are used to calculate the probability. The belief that the v_i propagates back to the check node c_j should not include the information coming from c_j .

First divide equation (2.8) by (2.9) and taking the logarithm of both sides gives

$$L(q_{ij}) = L(v_i) + \sum_{j' \in C_i \setminus j} L(r_{ji'}) \quad (2.19)$$

Check stop criterion: The decoder obtains the total *a posteriori* probability for the bit i by summing the information from all the check nodes that connect to the bit i .

$$L(Q_i) \triangleq \log \frac{Q_i(0)}{Q_i(1)} = L(v_i) + \sum_{j \in C_i} L(r_{ji}) \quad (2.20)$$

Hard decision is made based on $L(Q_i)$ and the resulting decoded input vector $\hat{\mathbf{v}}$ is checked against the parity-check matrix \mathbf{H} . If $\hat{\mathbf{v}}\mathbf{H}^T = 0$, the decoder stops and outputs \mathbf{v} . Otherwise, it repeats the steps after the initialization.

Figure 2.10 and Figure 2.11 illustrate the full LDPC coding and decoding process.

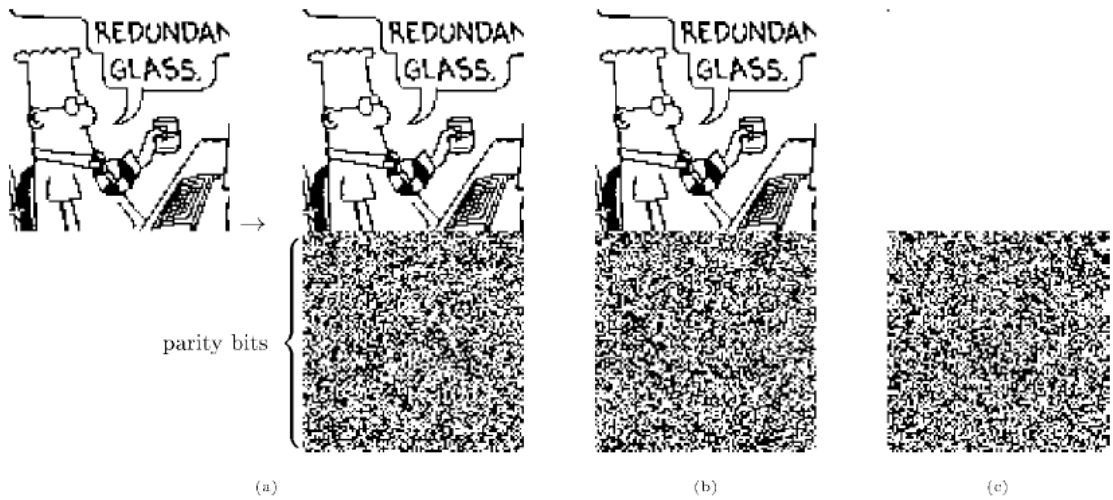


Figure 2.10: Demonstration of encoding with a rate 1/2 Gallager code. The encoder is derived from a very sparse 10000 x 20000 parity-check matrix with three 1's per column. (a) The code creates transmitted vectors consisting of 10 000 source bits and 10 000 parity-check bits. (b) Here, the source sequence has been altered by changing the first bit. Notice that many of the parity-check bits are changed. Each parity bit depends on about half of the source bits. (c) The transmission for the case $\mathbf{s} = (1,0,0,\dots, 0)$. This vector is the difference (modulo 2) between transmissions (a) and (b). (Reproduced from [22])

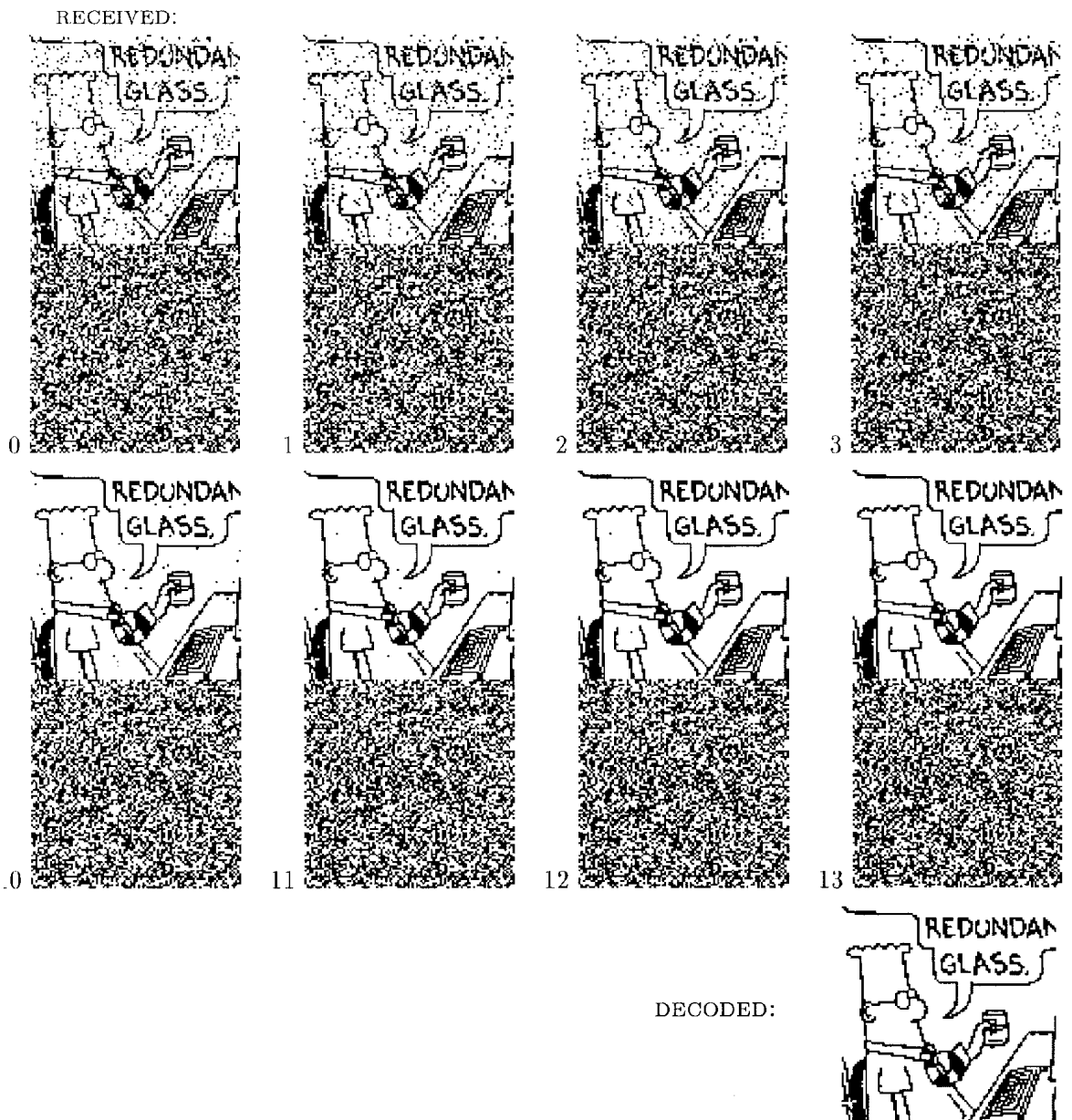


Figure 2.11: Iterative probabilistic decoding of a Gallager code. The sequence of figures shows the best guess, bit by bit, given by iteration decoder, after 0,1,2,3,10,11,12 and 13 iterations loop. The decoder halts after the 13th iteration when the best guess violated no parity check set. This final decoding is error free. (Reproduced from [22])

3. Cooperative Communications

This chapter provides a background on cooperative communication and cooperative diversity relaying. First, SISO system where the network only consists of a single source and destination node is introduced. Then, SISO system is extended to cooperative communication scheme where other nodes help forward data to the destination. Moreover, background on coding for relay channels is presented.

3.1 SISO System

SISO system consists of a bit source; transmitter, channel, receiver, and a bit sink, as shown in Figure 3.1.

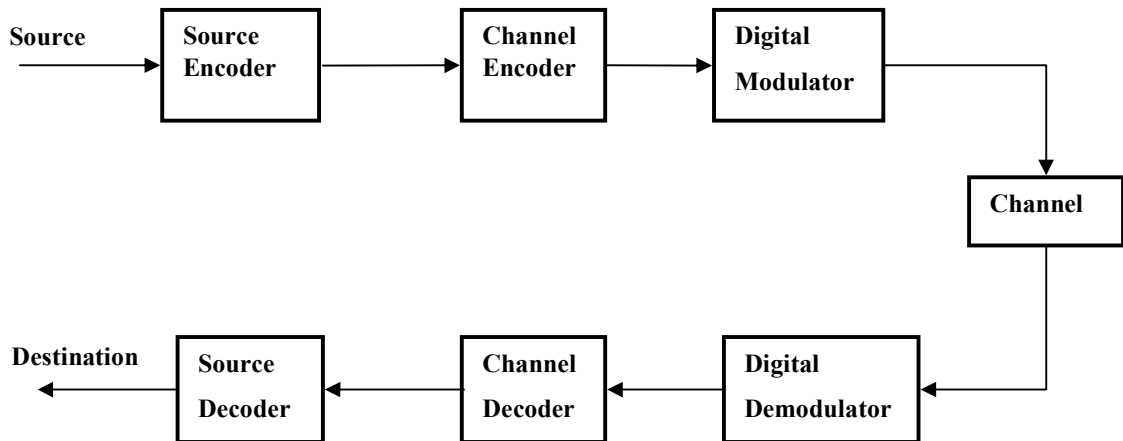


Figure 3.1: Communication block diagram

The bit source generates a vector of information bits to be transmitted. Normally in simulations, a random bit generator is employed as a bit source.

Channel encoder: The transmitter encodes the message bits into coded bits by using the channel encoder, which attaches redundancy to message bits to protect against channel-induced errors.

Modulator: Transforms discrete symbols into analog signals that can be transmitted across the channel.

Communication Channel: A communication channel provides a way to communicate at large distances, which contains external signals like noise that effects transmission.

Signal detection: Receiver decides which message was sent based on noisy received signal, depending on the signal transmission methods as well as the communication channel. Optimum detector minimizes the probability of an erroneous receiver decision.

Channel Decoder: Performs error correction techniques to recover transmitted information

The cooperative system consists of source and destination similar to SISO system, but also includes a partner node (relay node or another user). This system will be investigated in the next section.

3.2 Cooperative Diversity

3.2.1 Background

In a conventional cellular radio network, wireless terminals communicate directly with a base station via a single hop. However, most times the area that base stations cover

cannot include the terminals; hence terminals cannot be approached by their base stations via single hop. For example, the user may be in some place shadowed by a building, or in a subway station or tunnel. Therefore, present wireless systems are incapable of supporting the intended coverage, quality of service and transmission rates expected of future wireless systems.

The inefficiency and inadequacy of conventional cellular architecture do not seem to be reduced enough by the advances in signal processing techniques, smart antennas and MIMO systems. Therefore, present wireless systems require design and deployment of promising signal processing techniques to alleviate the inefficiency. The incorporation of diversity techniques in the current wireless networks is one of the novel and feasible strategies, allowing the support of high data rate, quality of service and coverage.

Due to the wireless environmental factors and limited resource constraints, a transmitted signal encounters various detrimental effects, such as interference, propagation path loss, delay spread, Doppler spread, shadowing and fading that result in high error and outage rates of wireless systems. Therefore, these detrimental effects make diversity techniques appealing to increase robustness. MIMO technology has aroused interest in wireless communications, since it promises improvements in data rate, range, and reliability without additional bandwidth and transmit power. That will enhance the usefulness of wireless applications significantly. MIMO produces link reliability, or in other word, diversity by increasing bit rate which reduces fading. To achieve diversity using MIMO, the transmitter should use multiple antennas at both receiver and transmitter. However, size, cost or hardware limitations limit multiple antennas at many wireless devices that MIMO technology cannot be exploited.

When spatial diversity through multiple antennas is not feasible, cooperative communications provide a new form of spatial diversity, called *cooperative diversity* without utilization of multiple transmit or receive antennas. In a cooperative system, transmitted signal between source and destination can be overheard at neighboring nodes due to the broadcast nature of wireless medium. The neighboring nodes process this

information and re-transmit to collaborate and create spatial diversity. Therefore, it allows single antenna mobiles in a multi-user environment to share their antennas and to produce virtual multiple-antenna system. With this scheme, the detrimental effects of fading are mitigated, since independent copies of the original source signal are forwarded to the destination. As a result, higher throughput, channel capacity and reliability are obtained.

One of the first studies that introduced the concept of cooperative diversity is [32] by Sendonaris et al, in which two users cooperate and form a partnership to forward partner's data. The authors demonstrated the potential of cooperative diversity in increasing the achievable rate region of the two users, as well as improving error probability, outage capacity and coverage. The work of Laneman and Wornell [33] approaches cooperative communication scheme in a conceptual manner and put the user cooperation in a mathematical framework. In this seminal paper, the authors discuss a cooperative protocol for alleviating multipath fading of wireless networks by exploiting the spatial diversity available among terminals that have agreed to forward each other's data.

3.2.2 Relay Channels

Novel and promising strategies at various layers must be improved to support high data rate services needed by future wireless networks. Recently, the use of relay nodes to help source node transmit its information to the destination is considered and received a significant attention due to its application in wireless networks, since it offers higher quality of service, power savings, extended coverage, and improve reliability in BER. It is closely related with MIMO system, which has been widely employed to achieve a diversity gain. But, as it is discussed above, some wireless devices cannot support more than one antenna, since the separation between antennas must be at least on the order of half the wavelength of the carrier frequency to prevent correlated fading. In contrast, relaying enables single antenna mobiles in a multi-user environment to share their

antennas and generate a virtual multiple-antenna transmitter. This is known as cooperative relaying, where the relay node virtually becomes another transmitter and helps the source transmit source data to the destination. Since the copies of source information are transmitted through independent wireless links, a diversity gain is achieved.

A wireless relay network is generally composed of a source node, a destination node, and a variable number of intermediate relay nodes, where these relay nodes participate in the communication between source and destination node by passing information to destination node coming from the source node. Therefore relay nodes cooperate with a source node by forwarding source message and thus help the destination node successfully decode the original information message.

The simple relay system consists of three nodes, as shown in Figure 3.2.

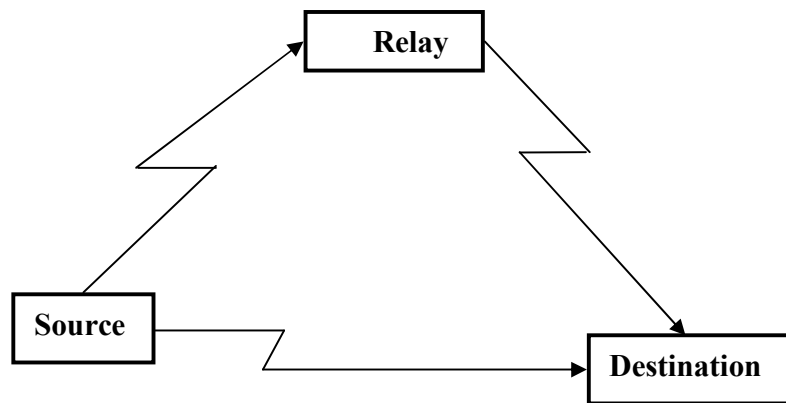


Figure 3.2: Cooperative Relay System

- *The source:* A node that transmits information.
- *The relay:* A node that both receives and transmits information to aid the communication between the source and destination node.
- *The destination:* A node that receives information from both relay and source.

Note that each terminal has one antenna and thus cannot generate spatial diversity individually.

The wireless relaying protocols are classified into three main types *amplify-and-forward* (AF), *decode-and-forward* (DF) and *estimate and forward* (EF) [34].

3.2.2.1 Amplify-and-Forward Method

In this method, each relay receives a noisy version of the transmitted signal and acts like analog repeater. It simply amplifies its received signal, to satisfy its own power constraints, and forwards it to the destination node. The destination can decode received signal by combining the two independently copies of the signals.

Source and the relay nodes are assumed to have power constraints of $E[x_S x_S^*] = E[x_R x_R^*] = E_S$, respectively. And channels are Rayleigh fading with $E[|h|^2] = 1$.

Source node broadcasts its message and the signal received by the relay node is

$$y_R = \sqrt{E_S} h_{SR} x_S + n \quad (3.1)$$

The receiver sends an amplified version of (3.1) to the destination and the transmitted signal is given by

$$x_R = \sqrt{\frac{E_S |h_{SR}|^2}{E_S |h_{SR}|^2 + N_0}} x_S + \sqrt{\frac{1}{E_S |h_{SR}|^2 + N_0}} n \quad (3.2)$$

In AF mode, storage element is required because of the operation on analog signals, and the fact that noise is also amplified and retransmitted to destination, make AF mode be expensive in applications.

3.2.2.2 Decode-and-Forward Method

The relay first decodes the received signal. It re-encodes the data and forwards it to the destination. It uses either the same code as the one used at the transmitter or a new one.

When the relay fails to decode the data correctly, it cannot help the source for the current cooperation and it may select staying silent to save energy

3.2.2.3 Estimate-and-Forward Method

In this strategy, the relay sends an estimate of its channel output to the destination, without decoding the source message. When the relay node is close to the destination, at low SNR estimate and forward relaying is shown to provide substantially higher rates compared to both direct and two-hop communication [35].

3.3 Cooperative Coding

The work of Meulen [8], and Cover and El-Gamal [34] on relay channels is the pioneer of the idea behind cooperative communication, which provides the basis for the cooperative schemes and protocols that recently have received attention. However, they focused on information theoretical perspective, rather than practical perspective. The authors in [34] evaluates the maximum achievable rate of Gaussian channels for with or without feedback to the source or relay node.

Although the area of cooperative communications has seen significant improvements and advancements, it still requires study on practical distributed coding strategies that can approach the capacity limits of the relay channels, derived by information theoretical perspective. Along with the advancements in information theoretic relay channels, practical transmission schemes for relay systems have also been developed [19]-[20], [32]-[42]. Among them, it has been proven that the integration of cooperation with coding is a very useful technique to improve the system performance.

Despite the fact that the implementation of repetition-based protocols proposed in [33] is very simple, they are not efficient with respect to bandwidth utilization. Therefore, more promising schemes that enhance the spectral efficiency must be developed to alleviate the inefficient use of bandwidth of repetition-based protocols. For example, coded cooperative schemes, where signals are not repeated, are proposed using convolutional codes [11]-[12], [36]-[37]. Hunter and Nosratinia [11] proposed a coded cooperation scheme that N bit long codeword of each user is divided into two frames of size N_1 and N_2 via puncturing techniques, using convolutional codes. Each user transmits the N_1 bit frame to its partner. Partner node decodes the received signal and extracts the punctured bits, which are the second frame of size N_2 . Then the users transmit the N_2 bit frame of their partner to the destination node. The receiver combines the two frames N_1 and N_2 to decide the original size N codeword. Due to the fact that first (N_1) and second frames (N_2) for each user are transmitted through independent channels, diversity can be exploited. This technique is extended to space-time codes in [12], [13], [38]. It has been clearly shown that coded cooperative diversity can achieve full diversity order for an arbitrary number of cooperating nodes at higher data rates than repetition-based schemes [37], [38].

However, these distributed coding strategies still have not approached the capacity limits of the relay channel, which motivates the incorporation of turbo codes [14], [15], [39]–[41]. In [39], [40], distributed turbo coding structures are proposed for the half-duplex relay channel, where the destination receives the signals transmitted from the source and the relay nodes via orthogonal sub channels. Later, an improved scheme utilizing the channel adaptivity is developed in [41]. All these strategies take an orthogonal channel between the source and the relay into consideration. That would result in a simpler receiver structure, but inefficient spectral efficiency.

To achieve a higher capacity, the authors in [14], [15] propose several practical turbo coded cooperation schemes for both full-duplex relaying and time-division based half-duplex relaying where the destination receives a superposition of source and relay transmission. These turbo coded cooperation schemes are shown to approach capacity

bounds very closely, by designing an efficient multi-access channel detector and iterative decoding at the destination between detector and decoder.

LDPC codes, which are one of the strongest error correcting codes with its capacity achieving performance, has not been considered for relay channels extensively, except for some preliminary work. Specifically, [42] proposes the design of a compress and forward scheme for the half-duplex Gaussian relay channel based on Wyner-Ziv coding where LDPC codes are not given a special attention, but only treated as an error protection method at the source node. The authors in [17] present an efficient LDPC code design approach for full-duplex Gaussian relay channels and corresponding decoding based on a partial factor graph. From information theoretical perspective, The authors in [18] and [19] show that carefully-designed LDPC codes can approach the corresponding capacity limits in a non-fading environment by developing different coding schemes for half-duplex and full-duplex relay channels. In [20], authors design appropriate coding/decoding strategies based on LDPC codes using the decode-and-forward protocol for single relay channel for both full-duplex and half-duplex relay channels.

Based on the decoding scheme proposed in [20] for single relay channels, in the next section we extend this model to multi-relay channels for full duplex scheme using DF and EF transmission protocols. The iterative receiver structure between detector and LDPC decoder is developed for our scheme.

4. LDPC Codes over Wireless Relay Channels

With the increased interest in wireless ad-hoc networks, next generation wireless systems must provide increased high data rate and improved coverage [10]. To meet these objectives, the intermediate nodes that relay data from a sender to the receiver in a dense environment have been developed. The use of relays can significantly improve the channel capacity, reduce the power cost and enhance the system reliability. In relay networks, the basic idea is that a relay node helps a source node transmit its data to a destination that is out of reach of the source node [9], as shown in Figure 4.1. Relay channels are important building blocks of next generation wireless systems and will play a central role in various applications including cellular systems and wireless ad hoc networks. Therefore, channel capacity and coding for relay channels have been receiving significant attention recently [10].

Some practical relaying strategies have been proposed. The “coded cooperation” technique was proposed using convolutional codes [11] and later extended to space-time codes [12], [13]. However, these codes could not approach the capacity limits of the relay channel. That leads incorporation of Turbo codes [14], [15]. In [14], [15], the authors propose turbo coded cooperation schemes for both half-duplex and full-duplex relaying and it is shown that these schemes approach the capacity limits very closely by employing a multi-access channel detector and iterative decoding at the destination. LDPC codes which have superior error correction capability and capacity approaching capability compared to Turbo codes have not been considered in a significant amount of research for relay channels. In [20], authors design appropriate coding/decoding schemes for single relay based on LDPC codes using the DF protocol for both full-duplex and half-duplex relay channels.

This chapter exploits the capacity approaching of LDPC codes to design a decoding scheme for full duplex channels using EF and DF protocol, where the source, the destination and relay node are all equipped with a single antenna. The chapter is organized as follows. First, the channel models for the single relay system, as well as the direct and multi-hop transmission schemes are presented. In addition, the capacity bounds and the information rate bounds are provided. Then, the iterative decoding process between MAP detector and LDPC decoder at the receiver side is analyzed and some simulation results for Rayleigh fading channels are provided. Moreover, single relay system is extended to multi-relay systems and an appropriate receiver structure is designed. The performance of this system is investigated and compared to single-relay systems

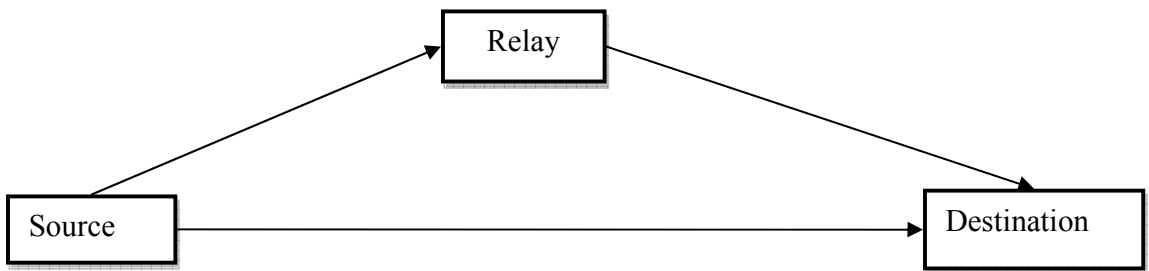


Figure 4.1: Basic Relaying System

4.1 Single Relay Channel

4.1.1 Channel Model for Full-Duplex Relay Schemes

In a simple relay system, there are three directed transmission links as shown in Figure 4.2, which are from source to destination, from source to relay and from relay to destination. Signal to noise ratio (SNR) is γ for source-destination link, $g_1\gamma$ for source-relay link and $g_2\gamma$ for relay-destination link, where g_1 and g_2 are the relative gains of the source-relay link and the relay-destination link over the source-destination link

obtained by strong line of sight of signals (LOS) or by short transmission distances. Typically, the source to relay and the relay to destination links have a larger SNR than the direct link, i.e., $g_1 \geq 1$ and $g_2 \geq 1$.

The overall SNR is defined as $\gamma = P_0 / (N_0 R)$, where R is the code rate. Each node is assumed as to have only one transmit and/or receive antenna, and destination observes the superposition of that the source and relay transmissions, which means source and relay do not transmit through orthogonal channels.

In addition, we neglected Doppler spread, which allows to have independently and identically distributed (i.i.d.) statistics. Moreover, we assume that the coherence bandwidth of the channel is much larger than the bandwidth of the signal, such that each channel is flat faded. Therefore, all frequency components of the signal experience the same magnitude of fading.

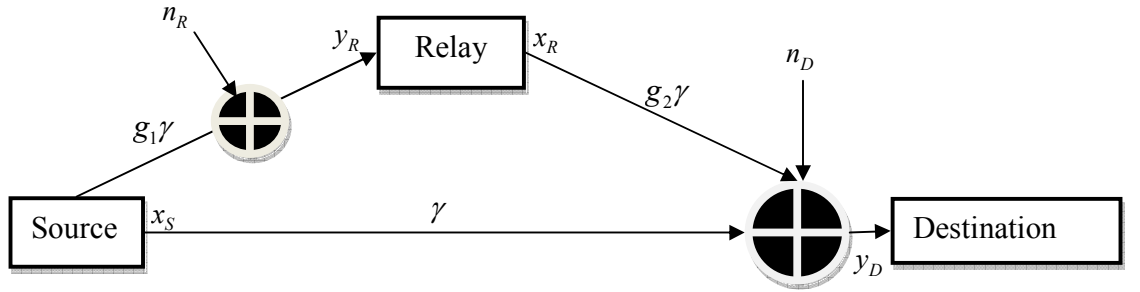


Figure 4.2: Block Diagram of the Relay System

The received signal at the relay node is denoted by y_R which is given by

$$y_R = \sqrt{g_1} h_{SR} x_S + n_R \quad (4.1)$$

where x_S is the transmitted symbol from the source with power P_0 . n_R is an AWGN term, which is a real Gaussian random variable with variance $N_0 / 2$ and h_{SR} is the

channel coefficient between source and relay node, which is considered as 1 when AWGN channel is considered and zero-mean complex Gaussian random variable with unit variance when Rayleigh fading channel is considered.

We considered Rayleigh fading in our simulations, since it is most applicable signal propagation model when relay lies in the non-line-of-sight (NLOS) scenario of both the source and the destination, which is the situation for urban environments. There are many obstacles in the environment that scatter the signal before it arrives at the receiver. Thus, the magnitude of the signal passing through this wireless medium will vary randomly according to a Rayleigh distribution, which can be modeled by generating the real and imaginary parts of a complex number according to independent normal Gaussian variables.

The received signal at the destination is denoted by y_D , which is given by

$$y_D = h_{SD}x_S + \sqrt{g_2}h_{RD}x_R + n_D \quad (4.2)$$

where x_R is the transmitted symbol from the relay node. h_{SD} , h_{RD} are independent channel coefficients between source-destination and relay-destination link, respectively. They are complex Gaussian distributed random variables having zero mean and unit variance. n_D denotes a AWGN term with zero mean and variance of $N_0/2$ per dimension.

The links between source-relay, relay-destination and source-destination are assumed as independent and flat Rayleigh fading channels. In addition, it is assumed that receivers know the channel coefficients, but the transmitters do not know.

The original relay channel model of [8] is used for the full-duplex relay scheme, since this channel model provides a higher channel capacity than the half duplex relay schemes or relaying schemes that source and relay transmit through orthogonal channels.

The authors in [14] assume that source and relay nodes have the same power constraint (P_0), but using a total power constraint and splitting the total power smartly between relay and source node, higher capacity and information rates can be achieved, leading to an improved performance.

For comparison purposes, the signal transmission using direct transmission and multi-hop schemes are considered. In direct transmission, no relay node is considered, the transmission occurs only between source and destination. The channel model is given by

$$y_D = h_{SD}x_S + n_D \quad (4.3)$$

where it is assumed that source transmits with $2P_0$ for a fair comparison.

In multi-hop transmission, only relay node is considered and source to destination link is ignored. The channel model for this scheme is given by,

$$y_D = \sqrt{g_2} h_{RD}x_R + n_D \quad (4.4)$$

where it is assumed that relay node can both receive and transmit simultaneously.

4.1.2 Capacity and Information Rate Bounds

A general upper and lower bound on the capacity of the relay system is derived in [34], which is given by

$$C \leq \max_{p(x_S, x_R)} \min\{I(X_S, X_R; Y_D), I(X_S; Y_R, Y_D | X_R)\} \quad (4.5)$$

and

$$C \geq \max_{p(x_S, x_R)} \min\{I(X_S, X_R; Y_D), I(X_S; Y_R | X_R)\} \quad (4.6)$$

where $p(x_S, x_R)$ is the joint probability of the signals transmitted at the source and the relay nodes.

In addition to capacity bounds, the achievable information rates for relay channels with i.u.d. binary inputs are evaluated.

The upper and lower information-rate bounds are given by

$$I \leq \min\{I_b(X_S, X_R; Y_D), I_b(X_S; Y_R, Y_D | X_R)\} \quad (4.7)$$

and

$$I \geq \min\{I_b(X_S, X_R; Y_D), I_b(X_S; Y_R | X_R)\} \quad (4.8)$$

where x_S and x_R are i.u.d. binary random variables, which are independent of each other.

Furthermore, for comparison purposes, the capacity and information rates of direct and multi-hop transmission are evaluated. Due to the fact that direct transmission consists of only source-destination link, it is easy to evaluate the information rates. For the multi-hop transmission, the capacity or the achievable information rate is computed by the worse link, either between source to relay or relay to destination.

As shown in [20], when g_1 is much larger than g_2 , both the upper and lower bounds are limited by the achievable rate of relaying part, thus convergence is achieved.

If a practical case is considered, which means, the source-to relay link is imperfect ($g_1=12\text{dB}$), and so is the relay-to-destination link ($g_2=4\text{dB}$). The capacity bounds converge for the relay system over the i.i.d. Rayleigh flat-fading channel in this case, and are given in Figure 4.3 together with the capacities of the multi-hop and direct transmission schemes. As it is seen in Figure 4.4, the lower and upper bounds converge in the low-to-medium SNR region and the gain in terms of achievable information rates is very large by using the relay system, instead of the direct transmission. The intuition behind this gain is that, the asymptotical rate for the relay system is two bits per channel use, whereas it is one bit per channel use for the direct transmission, using binary signaling. For example, there is a gain of 6.5 dB over the multihop transmission and 7.5 dB over the direct transmission promised by these information theoretical limits.

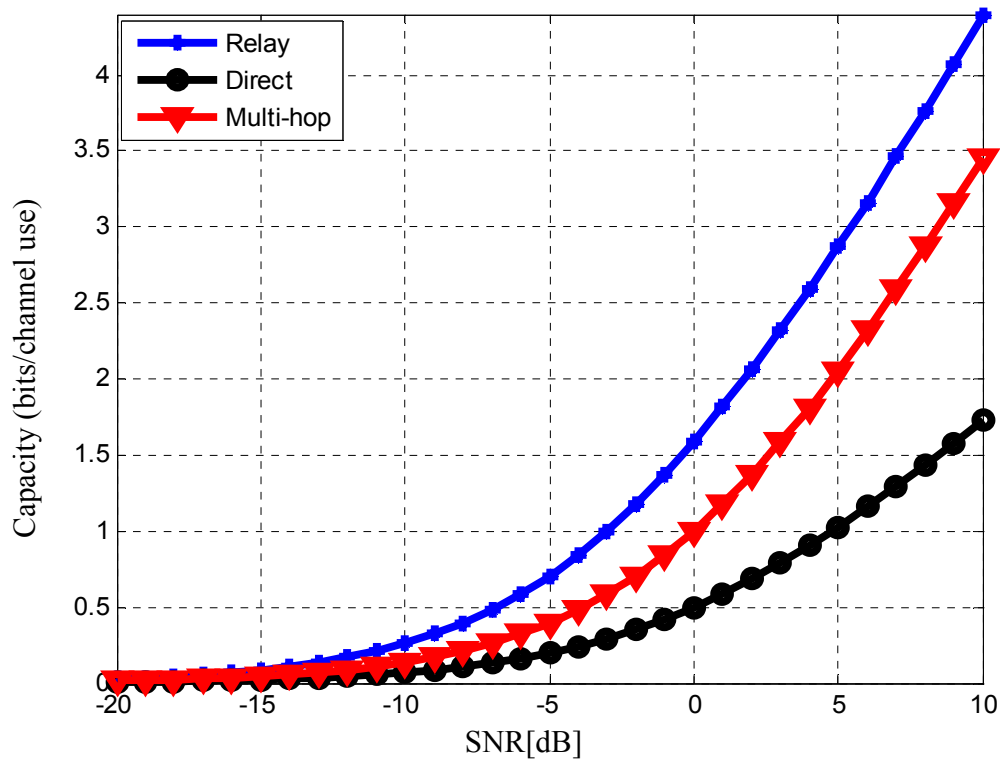


Figure 4.3: Capacity for Three Transmissions

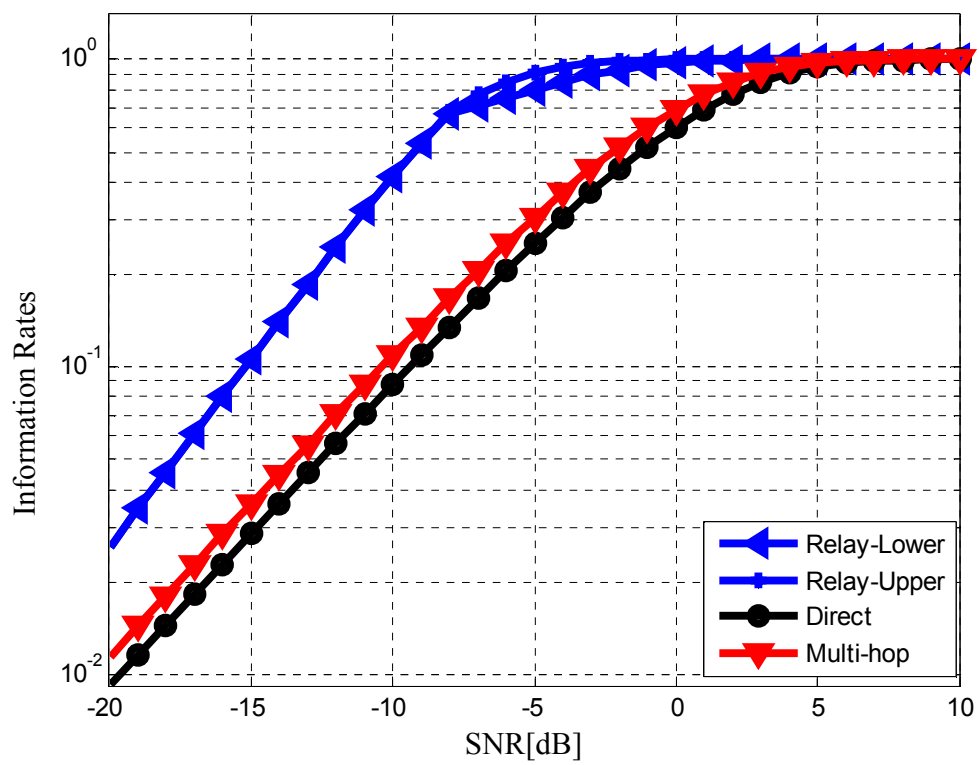


Figure 4.4: Information Rates for Three Transmissions

4.1.3 Iterative LDPC Decoding for Relay Channels

Low-Density Parity-Check Codes (LDPC) were first discovered by Gallager in 1962 and rediscovered by Mackay in 1999. Recently, it has received a lot of attention lately due to its excellent error-correcting capability and simple to implement decoding algorithms [43]. LDPC codes were shown to demonstrate the properties of good codes capable of asymptotically approaching Shannon limit (With an appropriate degree distribution will come arbitrarily close to the capacity of the channel). They have a threshold within 0.0045dB of the Shannon limit of Additive White Gaussian Noise (AWGN) channel (At BER 10^{-6} and block length 10^7) [24]. With coding gain approaching Shannon limit and lower hardware complexity than Turbo codes, LDPC has been considered by a number of next generation communication standards.

During the transmission of the first block, the source node (N_S) encodes u^0 with a code rate of $R=1/2$ and sends x_S^0 to both relay (N_R) and destination (N_D). Then relay node decodes x_S^0 and decodes it into \hat{u}^0 . In the second block, x_S^1 , the codeword for u^1 , is transmitted to both relay and destination. The relay node decodes x_S^1 into \hat{u}^1 , but at the same time, it encodes \hat{u}^0 and gets x_R^1 , which is sent to destination. As a result, the destination node receives the superposition of x_S^1 and x_R^1 . In summary, in the block i , where $i=0, 1 \dots B$ and B is the number of blocks, source encodes u^i and transmits the coded bits x_S^i to both relay and destination nodes. Relay node both decodes current codeword, and encodes the previous codeword into x_R^i to send to destination. Destination receives the superposition of two signals from source and relay nodes and given $B+1$ received blocks, the destination node tries to decode the message bits u^i . This process is shown in Figure 4.5, where N_S , N_R , N_D denotes source, relay and destination node, respectively. There is no rate loss here, since the last message block is only encoded and transmitted by the source node, that is relay node do not contribute in transmission of the last block. Therefore, there is no rate loss here i.e., $B+1$ message blocks are transmitted in $B+1$ time slots.

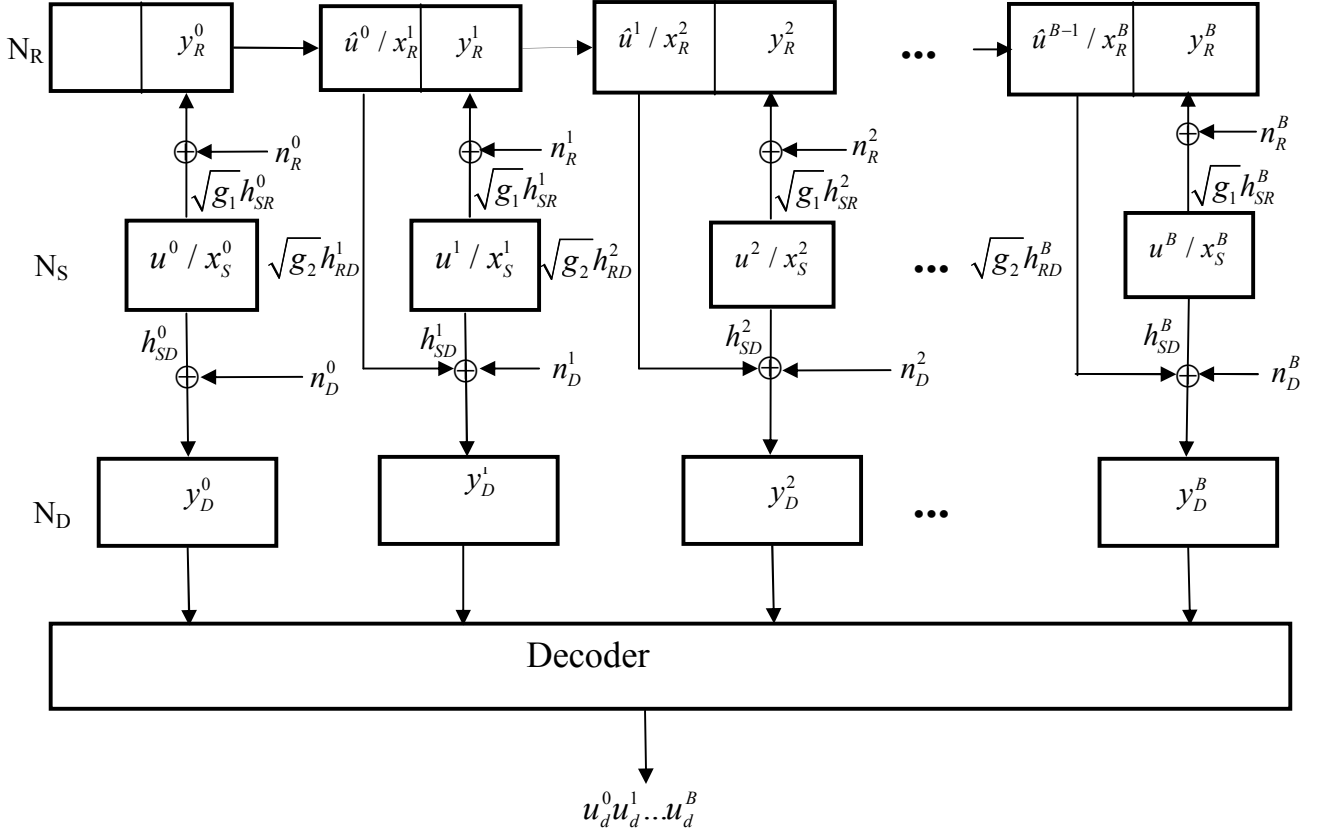


Figure 4.5: Block Diagram of the coding scheme for the relay channels

The general decoding procedure is illustrated in Figure 4.6. First $B+1$ MAP detectors are used to find the log-likelihood ratios (LLRs) for the coded bits from both the source and the relay nodes, and these LLRs are sent to appropriate LDPC decoders. The i^{th} LDPC decoder takes the soft information $L(x_S^i)$ and $L(x_R^{i+1})$ from i^{th} and $(i+1)^{\text{th}}$ channel MAP detectors, respectively, and calculates the extrinsic information, $E(x_S^i)$ and $E(x_R^{i+1})$ which are sent back to the same two channel MAP detectors. This decoding process is similar to the idea of turbo equalization (TE) proposed to reduce the intersymbol interference (ISI) [45]. The final hard decisions are made by the LDPC decoders after a number of iterations. All the channel MAP detectors calculate LLR values concurrently, and thus are implemented in parallel, and also the LDPC decoders operate in parallel. But, MAP detectors and LDPC decoders exchange the soft information serially.

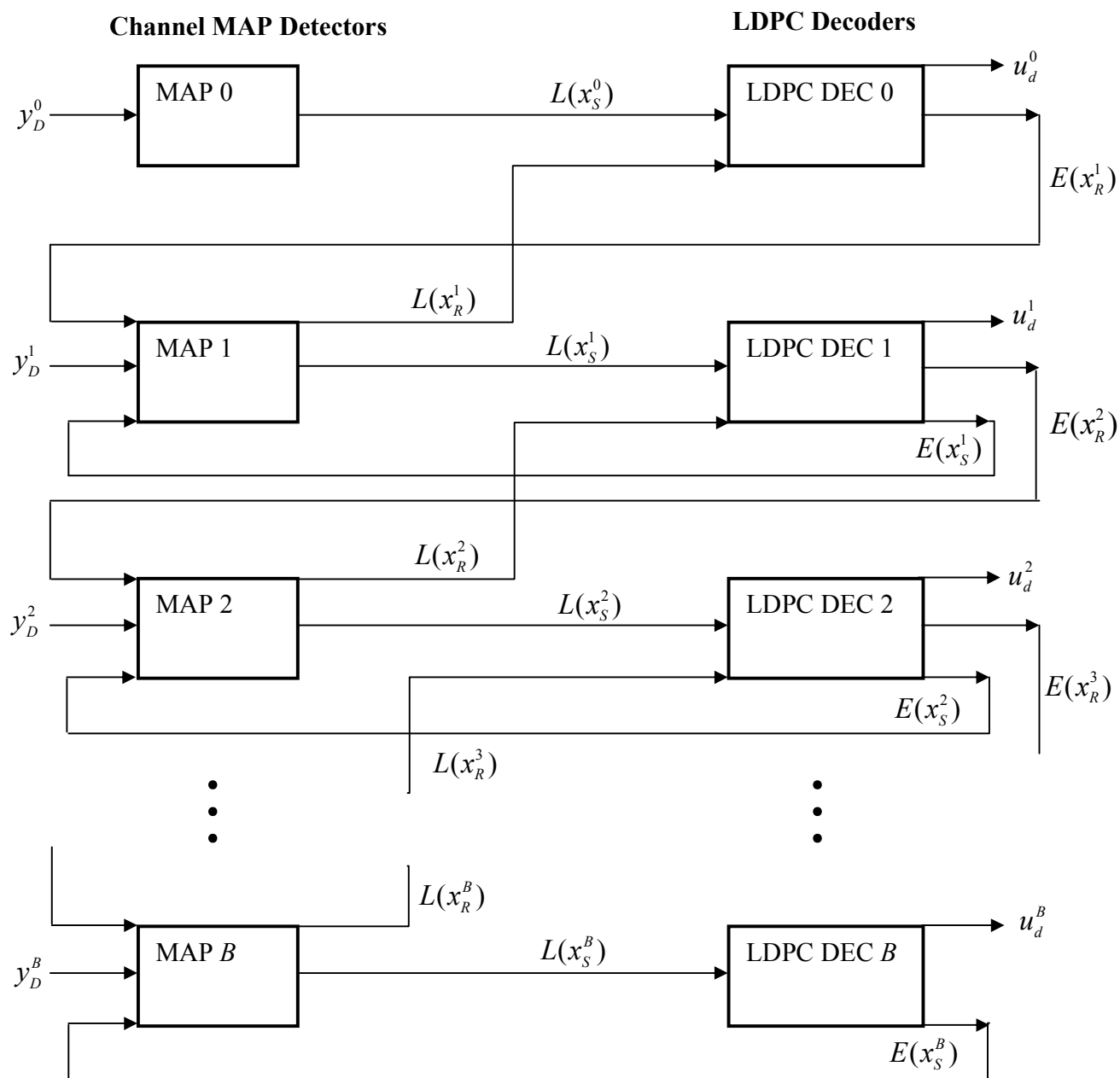


Figure 4.6: Block Diagram of the Decoder

To briefly describe the soft input soft output MAP detector,

$$LLR = \Delta(x_S) = \log \frac{p(x_S = 1 | y_D)}{p(x_S = 0 | y_D)} = \log \frac{p(y_D | x_S = 1, x_R = 0)p_{1,0} + p(y_D | x_S = 1, x_R = 1)p_{1,1}}{p(y_D | x_S = 0, x_R = 0)p_{0,0} + p(y_D | x_S = 0, x_R = 1)p_{0,1}} \quad (4.9)$$

where $p_{i,j} = p(x_S = i)p(x_R = j)$ with i and j taking values 0 or 1. $\Delta(x_S)$ and $\Delta(x_R)$ are LLRs for the coded bits from the source and relay node, respectively. Similarly, the LLR for x_R is computed.

Due to the fact that *a priori* information about x_S and x_R is available, which can be obtained from an outer decoder, $p_{i,j}$ can be updated, and the soft information passed to the outer decoder is given by

$$L(x_i) = \Delta(x_i) - \log \frac{p(x_i = 1)}{p(x_i = 0)}, i = S, R \quad (4.10)$$

The soft information $L(x_S)$, $L(x_R)$ provided by the source and the relay nodes, respectively are combined by summing up the likelihood information from the source and the relay corresponding to the same data block. Then, the combined soft information is sent to the decoder, which is implemented using the log-domain belief propagation (BP) algorithm. The extrinsic information sent back to the detector is

$$E(x_S) = L_{dec} - L(x_S), \quad E(x_R) = L_{dec} - L(x_R) \quad (4.11)$$

where L_{dec} is the total LLR for each bit obtained by belief propagation.

A priori probabilities are found using extrinsic information obtained from decoders and is passed to the detector for the next iteration.

$$p(x_S = 1) = \frac{e^{E(x_S)}}{1 + e^{E(x_S)}} \text{ and } p(x_R = 1) = \frac{e^{E(x_R)}}{1 + e^{E(x_R)}} \text{ for source and relay nodes, respectively.}$$

4.1.4 Simulation Results

We now present several simulation results. The information block of length 1000 was first encoded with LDPC regular \mathbf{H} (matrix taken from Mackay library) with rate 1/2 and codeword of block length 2000 is created. 1000 consecutive blocks are considered. The encoded codeword was modulated using BPSK assigning -1 to digit 0 and 1 to digit 1 and sent through the Rayleigh fading channel to the both relay and destination. At the relay node, two techniques are employed which are DF and EF. In DF scheme, received signal was decoded by using LDPC decoding and again re-encoded the signal with LDPC codes with rate 1/2 and transmitted it to the destination. On the other hand, in EF scheme, the information transmitted is extracted using

$$x_R = \text{sign}(\sqrt{g_1} h_{SR} x_S + n_R) \quad (4.12)$$

where h_{SR} is the channel coefficient between source and relay node, which is considered as 1 when AWGN channel is considered and zero-mean complex Gaussian random variable with unit variance when Rayleigh fading channel is considered.

Today's multimedia communication applications include delivery of video, data over IP, wireless basestation, and medical applications, which require high data rates and low latency, specifically for full-duplex communication that involves streaming data like voice. Lower latency puts tight requirements on the number of acceptable bit errors in serial transmission. Our acceptable target BER is chosen as 10^{-5} , since wireline serial transmission typically has a BER in the 10^{-10} to 10^{-12} range, whereas most radio systems are in the 10^{-3} to 10^{-6} range [47]. For example, the Wireless Lan (WLAN) cards used by DELL computers require a BER of better than 10^{-5} for both 802.11a, 802.11b and 802.11g standards [48]. The BER that gives a good quality for voice applications is 10^{-4} , but BER of 10^{-5} , is better and common. For Voip communication, packet loss and voice frame loss are unacceptable at BER larger than 10^{-5} . Moreover, the quality of service (Qos) parameters specified in the 3rd Generation Partnership Project (3GPP) considers

10^3 - 10^{-7} , as an acceptable BER constraint for real time applications in satellite, vehicular and portable, handheld wireless devices [49].

In Figure 4.7, we simulated the channel models for both direct transmission, multi-hop transmission and single relay transmission for Rayleigh fading channel using Monte-Carlo simulation and plotted the Bit Error Rates (BER) performances at various SNR values. The relay node performs DF technique to extract the codeword and destination node performs 2 global iterations (iteration between MAP detector and LDPC decoder), and 100 inner LDPC iterations. The channel gain g_1 is 4 dB and g_2 is 4 dB. As it is seen in Figure 4.7, relay transmission outperforms direct and multi-hop transmission. For example, at BER 10^{-5} , there is a gain of about 1 dB over the multihop transmission and about 5 dB over the direct transmission.

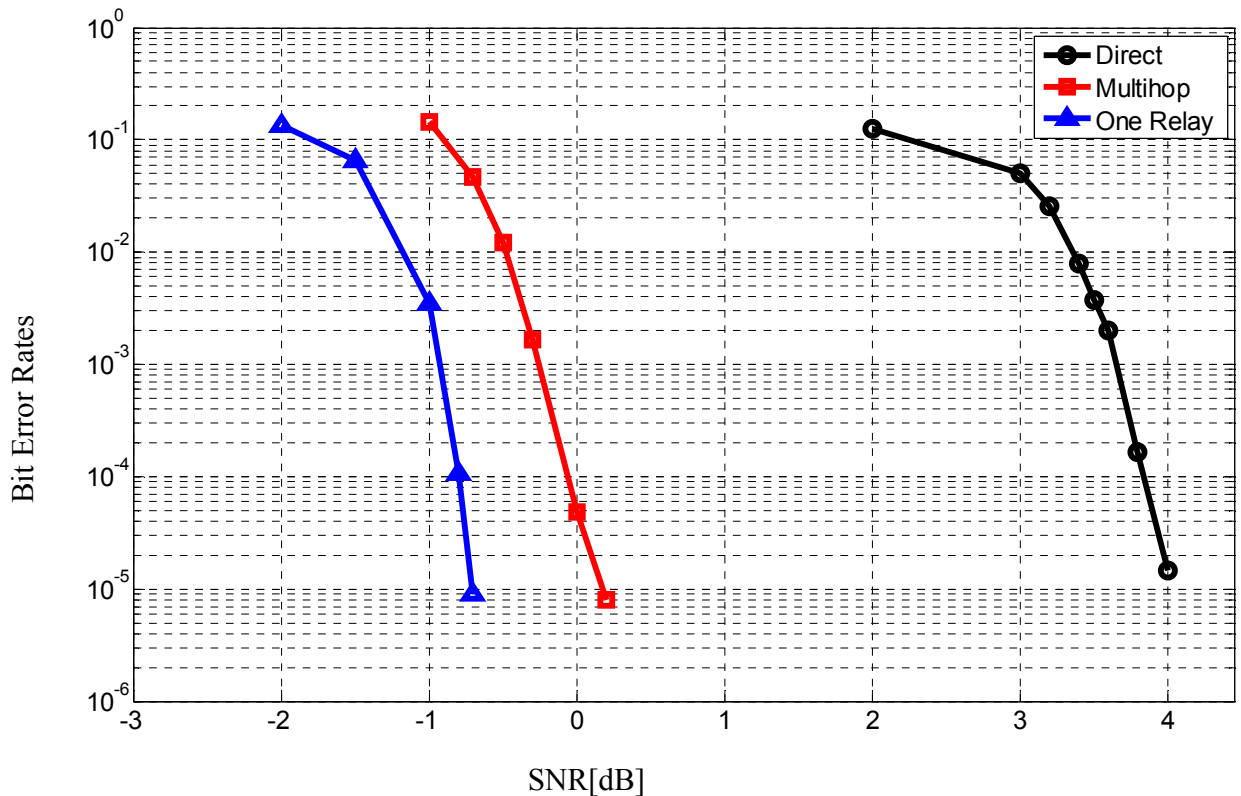


Figure 4.7: Bit error rate for three transmissions using LDPC decoding

The intuition of the above result is that multi-hop transmission outperforms direct transmission over fading channels due to path-loss gain. And relay transmission outperforms multi-hop transmission due to diversity gain. Thus, the relay transmission requires less power to achieve a certain BER relative to the direct and multi-hop transmission [50].

In addition, we simulated the single relay channel for different number of global iterations using DF and EF technique. At the destination, transmitted codeword was extracted using iterative decoding. The number of global iteration taken as one, two, and three; since further iterations would not improve the performance significantly, so small number of iterations is enough [20]. The number of inner iterations (local iterations) within the LDPC decoder is 100. The channel gain g_1 is 4 dB and g_2 is 4 dB.

In Figure 4.8, EF technique is used at relay nodes. As it is seen in the figure, at BER 10^{-5} the improvement between first and second global iteration is 0.8 dB, and the improvement between second and third global iteration is 0.4 dB. In Figure 4.9, DF technique is used at relay nodes. As it is seen in the figure, at BER 10^{-5} the improvement between first and second global iteration is 0.5 dB, and the improvement between second and third global iteration is 0.2 dB. Therefore, the improvement in BER as the global iteration number increases diminishes.

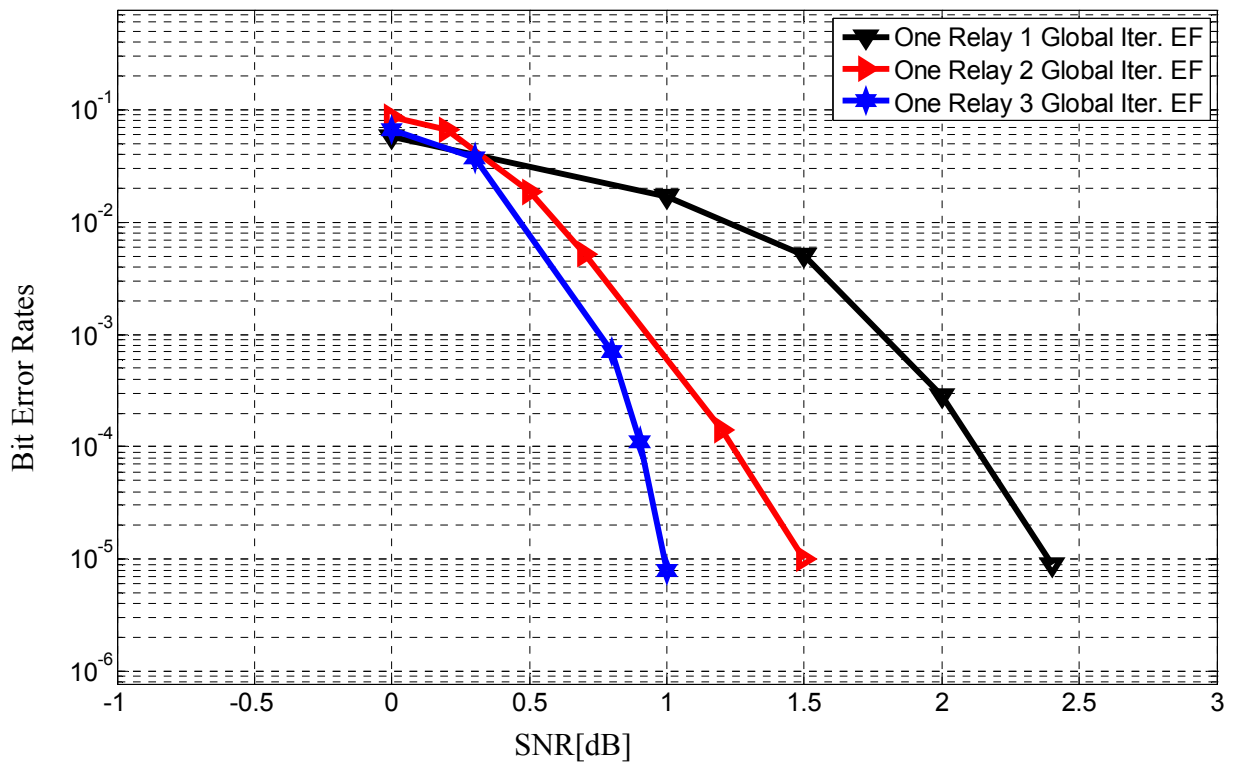


Figure 4.8: BER of single relay channel for different number of global iteration using EF

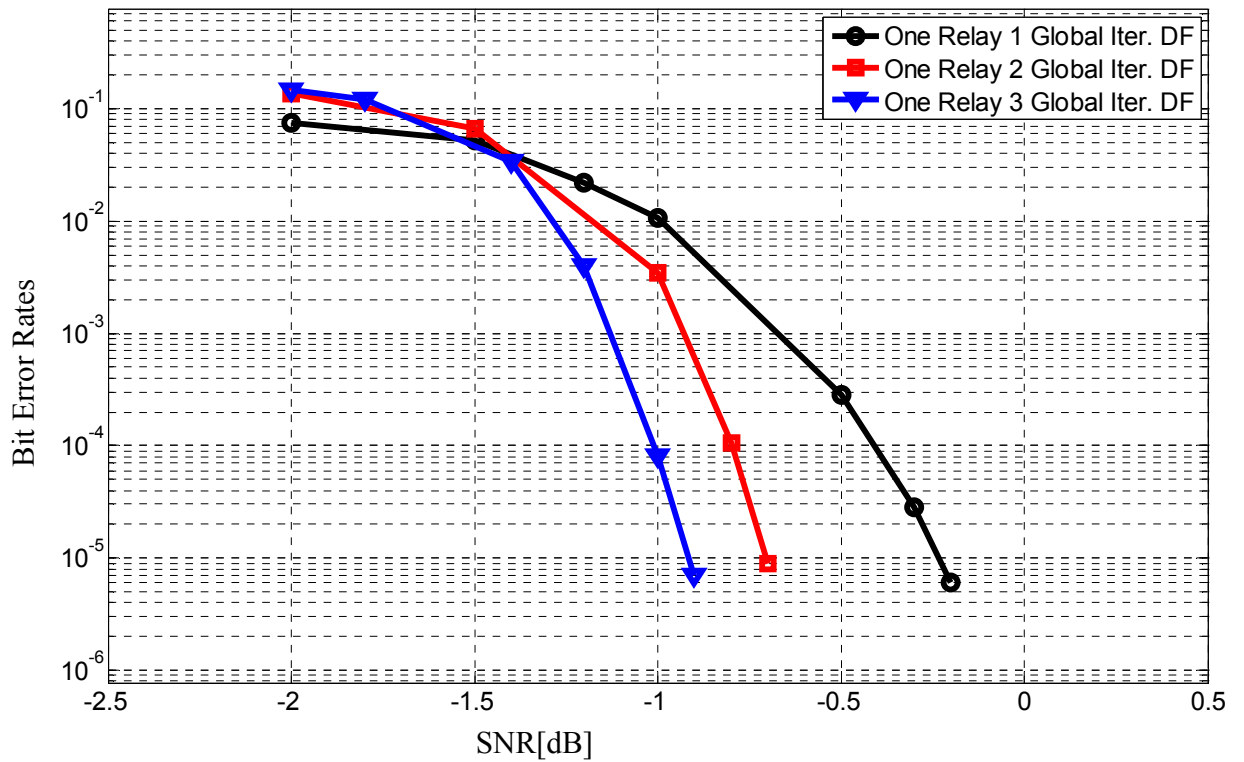


Figure 4.9: BER of single relay channel for different number of global iteration using DF

If we combine Figure 4.8 and Figure 4.9, we get Figure 4.10. As it is seen in the figure, DF technique outperforms EF technique. At BER 10^{-5} , DF is 2.6 dB better than EF for one global iteration, 2.2 dB better for two global iterations, 1.9 dB better for three global iterations.

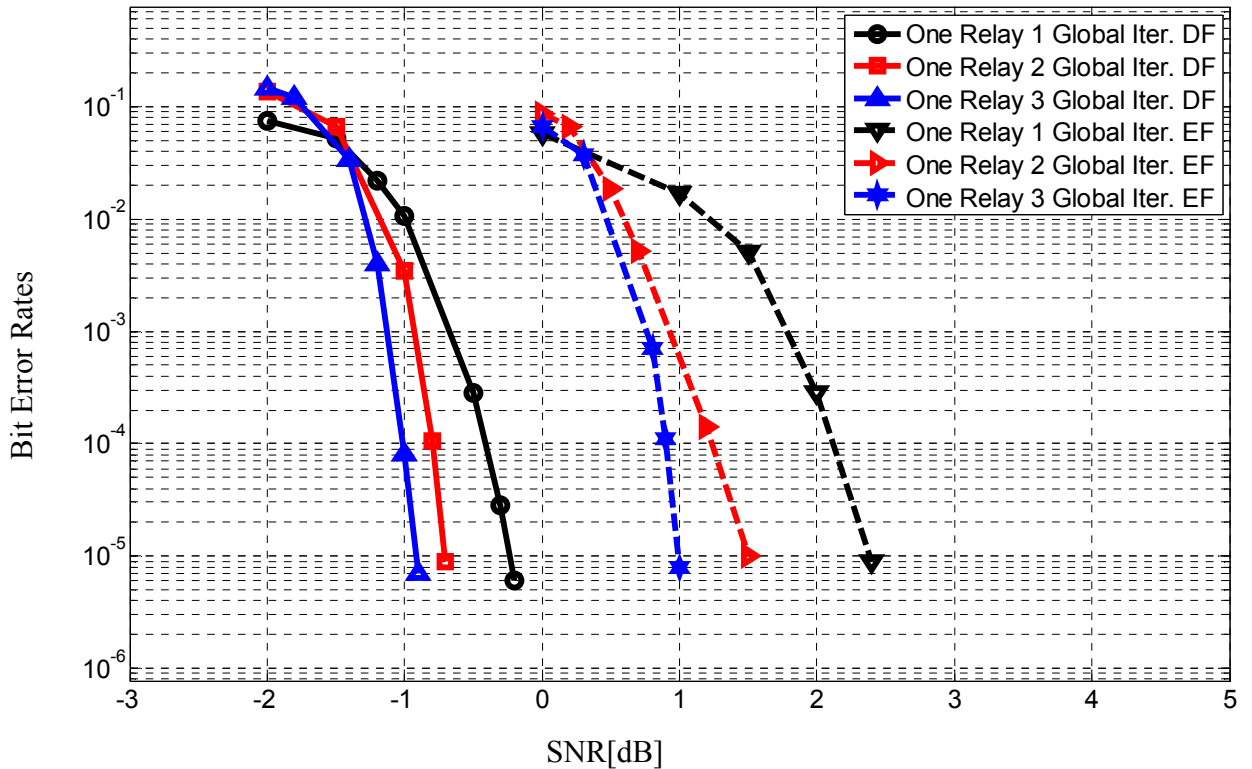


Figure 4.10: BER comparison of EF and DF techniques for different number of global iteration

In the next section, one relay channel is extended to multi-relay channels to gain some improvements in terms of BER. The iterative receiver structure of single relay channel is also adopted, but some modifications to compute the LLR values have been done. The comparison between single relay and multi-relay channel is studied through simulations.

4.2 Multiple Relay Channels

The propagation loss from source node to the destination node can attenuate the signals beyond detection. One way to deal with this problem is to pass the transmitted signal through two or more relay sensors. The transmission model is shown in Figure 4.11.

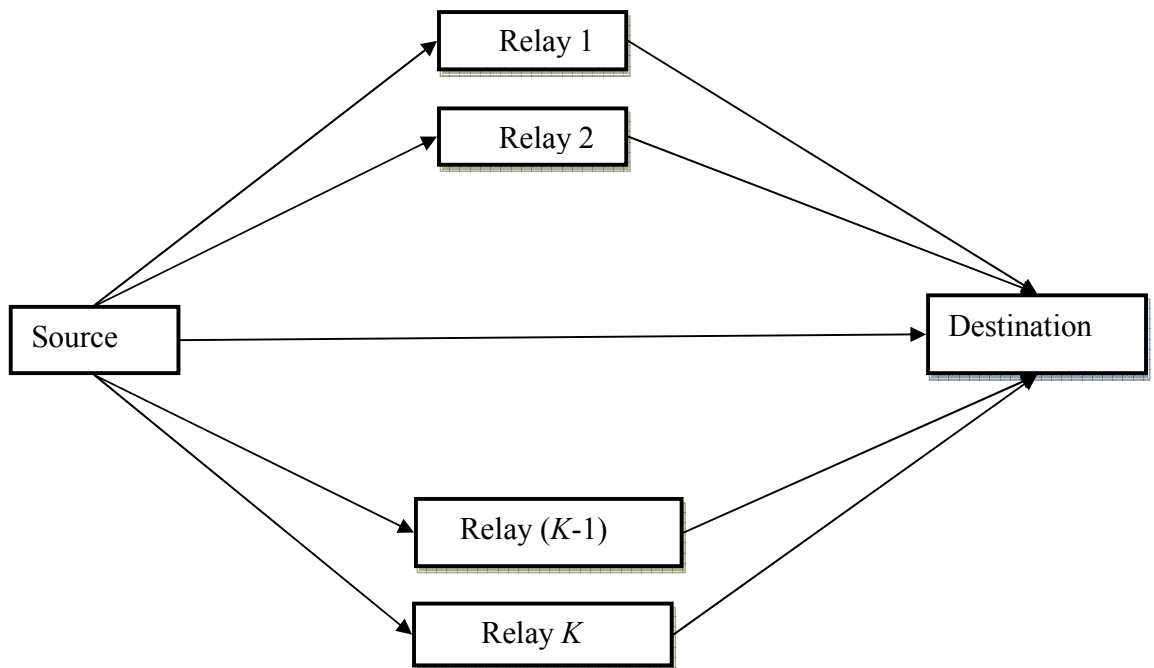


Figure 4.11: Multiple Relaying Systems

The received signal at the relay nodes are

$$y_{R_k} = \sqrt{g_1} h_{SR_k} x_S + n_{R_k} \quad (4.13)$$

where $k=1, 2, \dots, K$ and K is the number of relays. h_{SR_k} is the Rayleigh channel coefficient between source and k^{th} relay node, which is assumed as zero-mean complex Gaussian

random variable with unit variance. n_{R_k} is AWGN term for the k^{th} relay node, with zero mean and variance $N_0 / 2$.

The received signal at the destination node is given by

$$y_D = h_{SD}x_S + \sqrt{g_2}h_{R_1D}x_{R_1} + \sqrt{g_2}h_{R_2D}x_{R_2} + \dots + \sqrt{g_2}h_{R_KD}x_{R_K} + n_D \quad (4.14)$$

where h_{R_kD} is the Rayleigh channel coefficient between k^{th} relay node and destination, which is assumed as zero-mean complex Gaussian random variable with unit variance. n_D is AWGN term for the destination node, with zero mean and variance $N_0 / 2$.

The important point is that the transmission power of one relay is P_0 / K , so the total relay transmission power is P_0 , which is similar to single relay channels, where relay transmits with power P_0 .

4.2.1 Iterative LDPC Decoding for Multiple Relay Channels

Decoding process at the receiver can be extended from single relay to multiple relays easily. Source encodes u^i and transmits the coded bits x_S^i ($i=0, 1 \dots B$) to both relay nodes and destination node, where B is the total block number and i is the i^{th} block to be transmitted. k^{th} relay node both decodes current codeword, and encodes the previous codeword into $x_{R_k}^i$ ($k=1, 2 \dots K$) to send to destination, where K is the number of relays. Destination receives the superposition of signals from source and K relay nodes. Given $B+1$ received blocks, the destination tries to decode the message bit u^i

The general decoding procedure is illustrated in Figure 4.12. First $B+1$ MAP detectors are used to calculate the log-likelihood ratios (LLRs) for the coded bits from both the

source and the relay nodes, and these LLR values are sent to appropriate LDPC decoders. The i^{th} LDPC decoder takes the soft information

$L[x_S^i]$ from i^{th} and $L(x_{R_1}^{i+1}), L(x_{R_2}^{i+1}), \dots, L(x_{R_K}^{i+1})$ from $(i+1)^{th}$ channel MAP detectors, and calculates the extrinsic information, $E[x_S^i]$ and $E(x_{R_1}^{i+1}), E(x_{R_2}^{i+1}), \dots, E(x_{R_K}^{i+1})$ which are sent back to the same two channel MAP detectors. The final hard decisions are made by the outer decoders after a number of iterations. As it is mentioned for one relay channel, the channel MAP detectors and the LDPC decoders also operate in parallel for multiple relay channels and detectors and decoders exchange the soft information serially.

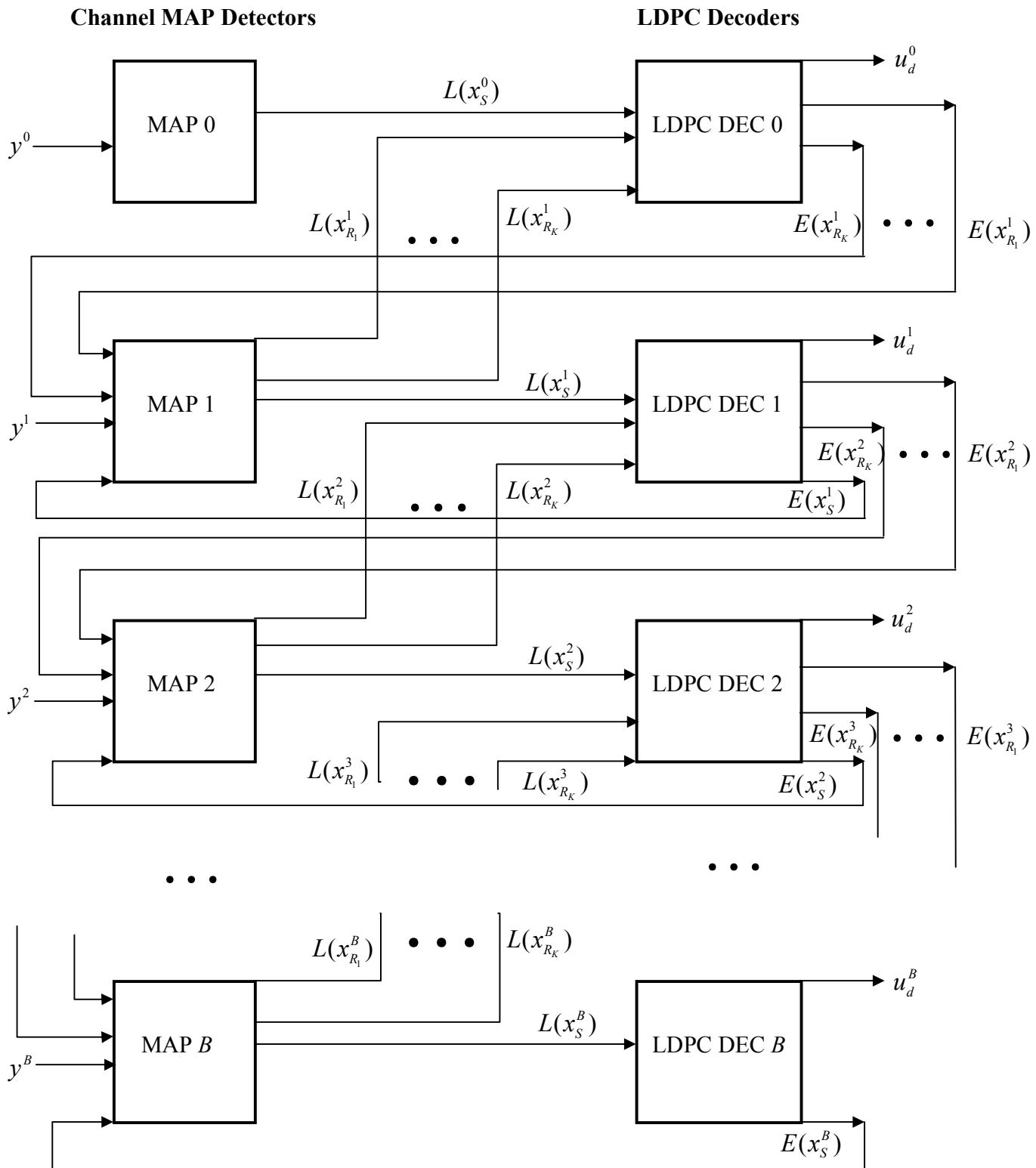


Figure 4.12: Block Diagram of the Decoder for Multiple Relays

To briefly describe the soft input soft output MAP detector,

$$\begin{aligned}
LLR = \Delta(x_S) = \log \frac{p(x_S = 1 | y_D)}{p(x_S = 0 | y_D)} &= \log \frac{p(y_D | x_S = 1, x_{R_1} = 0, x_{R_2} = 0, \dots, x_{R_K} = 0)p_{1,0,0,\dots,0} + \dots}{\dots + p(y_D | x_S = 1, x_{R_1} = 1, x_{R_2} = 1, \dots, x_{R_K} = 1)p_{1,1,\dots,1}} \\
&= \log \frac{p(y_D | x_S = 0, x_{R_1} = 0, x_{R_2} = 0, \dots, x_{R_K} = 0)p_{0,0,0,\dots,0} + \dots}{\dots + p(y_D | x_S = 0, x_{R_1} = 1, x_{R_2} = 1, \dots, x_{R_K} = 1)p_{0,1,\dots,1}}
\end{aligned} \tag{4.15}$$

where $p_{x_S x_{R_1} x_{R_2} \dots x_{R_K}}$ is the joint probability of the signals transmitted at the source and relay nodes. Similarly, the LLR for x_{R_k} ($k=1, 2 \dots K$) is computed. By assuming that $x_{R_1}, x_{R_2}, \dots, x_{R_K}$ are independent, which is justified by the use of random interleavers, LLR for the source and relay nodes are expressed as

$$\begin{aligned}
LLR = \Delta(x_S) = \log \frac{p(x_S = 1 | y_D)}{p(x_S = 0 | y_D)} &= \log \frac{\sum_{x_{R_1}, x_{R_2}, \dots, x_{R_K}} p(y_D | x_S = 1, x_{R_1}, x_{R_2}, \dots, x_{R_K}) \prod_{i=1}^K p(x_{R_i})}{\sum_{x_{R_1}, x_{R_2}, \dots, x_{R_K}} p(y_D | x_S = 0, x_{R_1}, x_{R_2}, \dots, x_{R_K}) \prod_{i=1}^K p(x_{R_i})} + \log \frac{p(x_S = 1)}{p(x_S = 0)}
\end{aligned} \tag{4.16}$$

Suppose we have a priori information about $x_S, x_{R_1}, x_{R_2}, \dots, x_{R_K}$ which can be obtained from LDPC decoders, then $p_{x_S x_{R_1} x_{R_2} \dots x_{R_K}}$ is updated and the soft information passed to the LDPC decoders is given by

$$L(x_S) = \Delta(x_S) - \log \frac{p(x_S = 1)}{p(x_S = 0)} \tag{4.17}$$

and

$$L(x_{R_k}) = \Delta(x_{R_k}) - \log \frac{p(x_{R_k} = 1)}{p(x_{R_k} = 0)} \tag{4.18}$$

for both source and relay nodes, respectively.

The soft information provided by source and relay nodes are summed up and combined information is sent to the LDPC decoder, which is implemented using log-domain belief propagation algorithm. The extrinsic information sent back to the detector is calculated as

$$E(x_{R_k}^i) = L_{dec} - L(x_{R_k}^i) \quad (4.19)$$

and

$$E(x_S^i) = L_{dec} - L(x_S^i) \quad (4.20)$$

for both source and relay nodes, respectively, where L_{dec} is the total LLR for each bit obtained from LDPC decoder.

A priori probabilities are found using extrinsic information obtained from decoders and passed to the detector for the next iteration.

$$p(x_S = 1) = \frac{e^{E(x_S)}}{1 + e^{E(x_S)}} \text{ and } p(x_{R_k} = 1) = \frac{e^{E(x_{R_k})}}{1 + e^{E(x_{R_k})}} \text{ for source and relay nodes, respectively}$$

4.2.2 Simulation Results

We now present simulation results. The information block of length 1000 was first encoded with LDPC regular \mathbf{H} (matrix taken from Mackay library) with rate 1/2 and codeword of block length 2000 is created. 10000 consecutive blocks are considered. The encoded codeword was modulated using BPSK assigning -1 to digit 0 and 1 to digit 1. We simulated the channel models for one relay, two relay and three relay transmissions for Rayleigh fading channel using DF and EF protocol and plotted the BER performances at various SNR values. In DF scheme, received signal was decoded by using LDPC decoding and again re-encoded the signal with LDPC codes with rate 1/2 and transmitted it to the destination. On the other hand, in EF scheme, the information transmitted is extracted using

$$x_{R_k} = \text{sign}(\sqrt{g_1} h_{SR_k} x_S + n_{R_k}), \text{ for } k=1, 2 \dots K \quad (4.21)$$

At the destination, transmitted codeword was extracted using iterative LDPC decoding. The inner iteration of LDPC decoder is 100. Channel gains g_1 and g_2 are both 4 dB. We have simulated the channel for single, two and three relays using DF and EF protocol for different number of global iterations. In Figure 4.13, we have used DF protocol and as it

is seen in the figure, there is an improvement in BER as relay number increases. To be specific, at BER 10^{-5} for two global iterations, increasing the number of relays from one to two provides us with 3.1 dB BER gain and from two to three provides us with 1.1 dB BER gain. In addition, for two relays the gain obtained by increasing the global iteration from two to three is 0.1 dB, which is very inconsiderable. Therefore, there is no need to increase the global iteration number.

In Figure 4.14, we have used EF protocol and as it is seen in the figure, there is an improvement in BER as relay number increases. To be specific, at BER 10^{-5} for two global iterations, increasing the number of relays from one to two provides us with 4.9 dB BER gain and from two to three provides us with 1.4 dB BER gain. Similar to the DF case, for two relays the gain obtained by increasing the global iteration from two to three is 0.1 dB, which is very inconsiderable. Therefore, there is no need to increase the global iteration number.

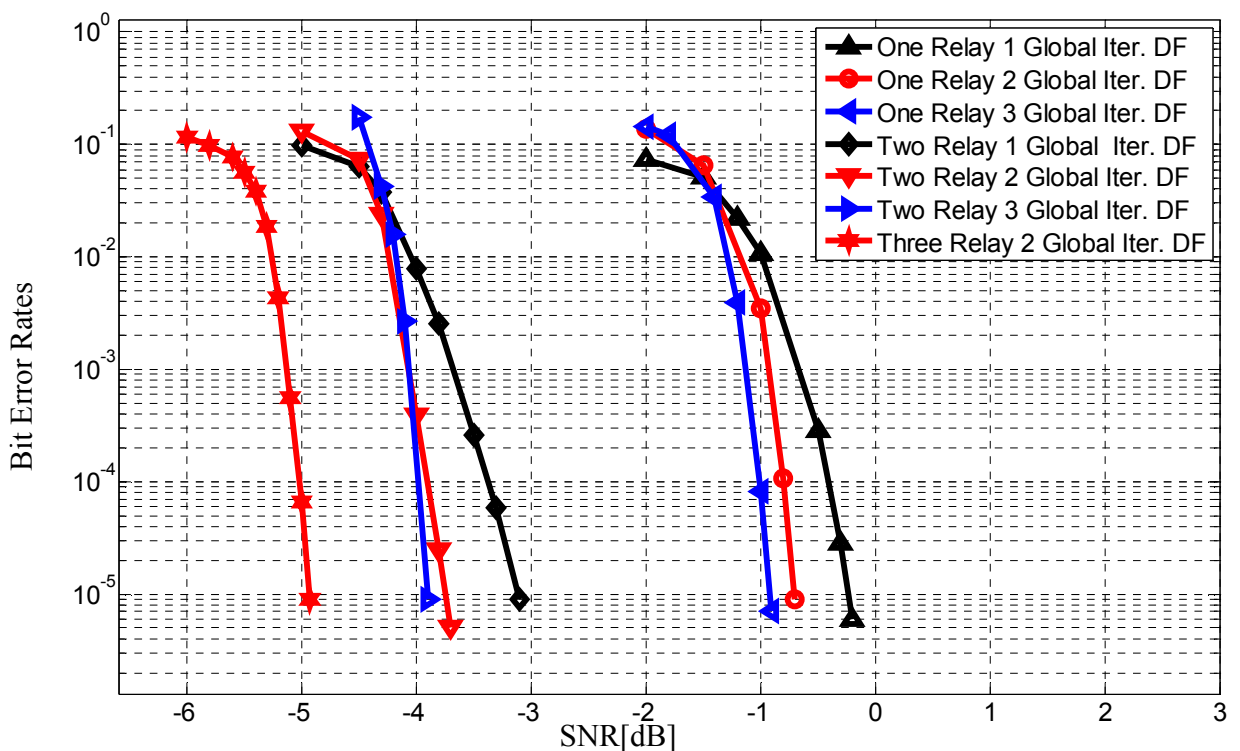


Figure 4.13: Bit Error Rate for one, two and three relays using DF

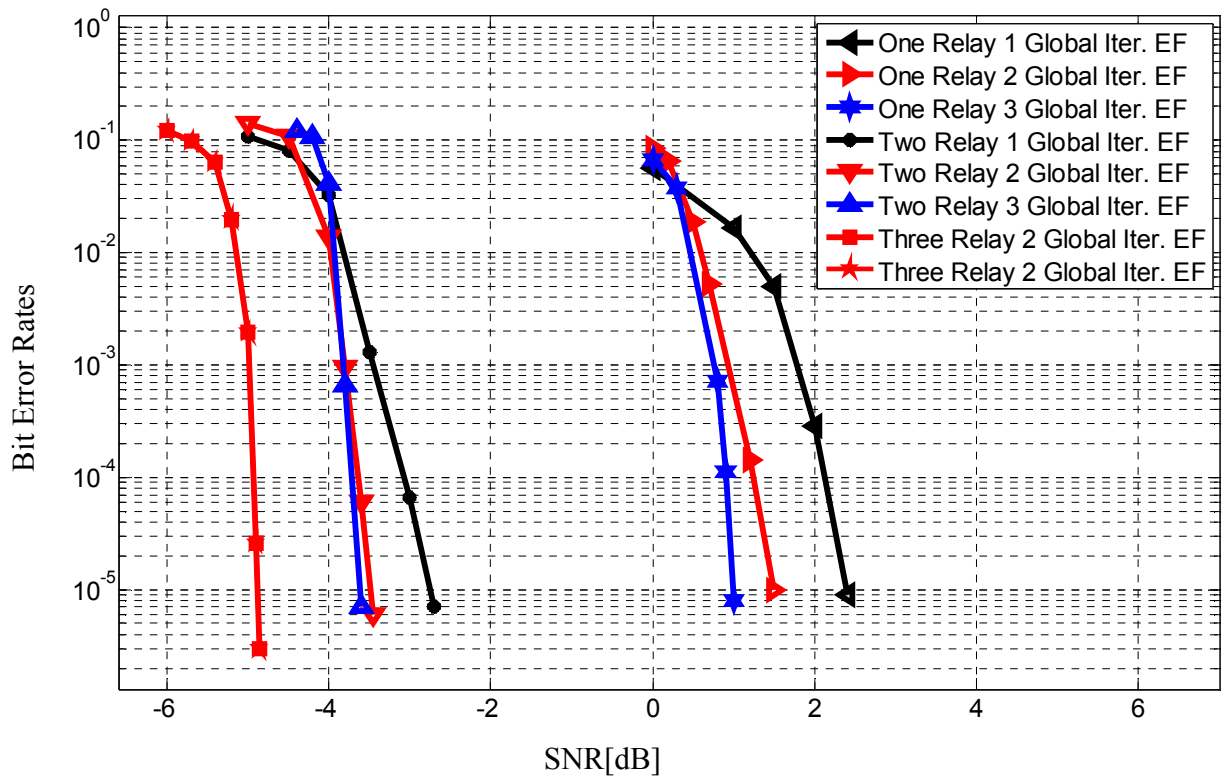


Figure 4.14: Bit Error Rate for one, two and three relays using EF

If we combine Figure 4.13 and Figure 4.14 to compare the performances of DF and EF protocols, we get Figure 4.15. As it is seen in the figure, DF protocol outperforms EF protocol. For two relays, the gain obtained by DF technique compared to EF is 0.4 dB for one global iteration, 0.3 dB for two global iterations and 0.2 dB for three global iterations at BER 10^{-5} . Moreover, for three relay network, the gain is less than 0.1 dB at BER 10^{-5} .

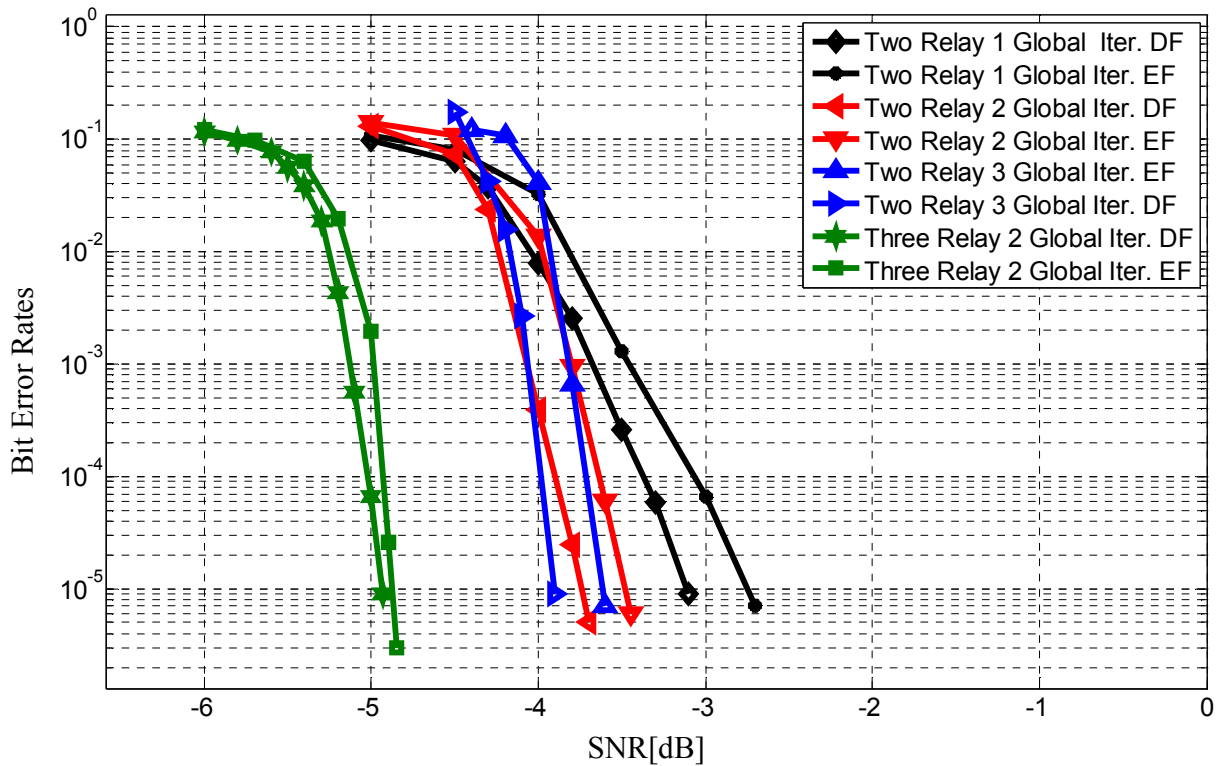


Figure 4.15: BER comparison of EF and DF techniques for multi-relay channels

We have not considered the multi-hop case where the source message is conveyed to the destination through K nodes. Each node gets the source message from previous node and delivers to the next node. Employing multi-hop technique leads to the propagation of error [51]. For example, if the first link between source and first relay node is degraded, then the error decoding performance of the first relay becomes worse, and thereby the undetected errors of the first relay propagates to the destination through the other relay nodes. In contrast, in multi-relay channels, even if the link between source and one of the relay nodes is degraded, other relays can help the source transmit its data. As a result, multi-relay scheme outperforms multi-hop scheme.

Next, we comment on the assumptions in our simulations and say how much it would differ in real life applications and in what aspects

- 1) We considered Rayleigh fading in our simulations, since it is most applicable signal propagation model when relay lies in the non-line-of-sight (NLOS) scenario of both the source and the destination, which is the situation for urban environments. But, in practical propagation environments, these assumptions may not hold true. In the future work part, a relay channel model which can take into account both LOS and NLOS propagation environments should be proposed.
- 2) We also ignored the effect of the location of the relay and effect of power allocation on the system performance in our analysis, which remains as a future work.
- 3) In commercial wireless communication system, most wireless devices function in time division duplexing (TDD) mode that can not transmit and receive at the same time in the same frequency band [52]. This scheme is called half-duplex system. Although full-duplex scheme can be implemented, the design of full-duplex radios are not too favourable since the design of such radios require accurate interference cancellation between transmitted and received signals.

It is good to have improvements as we increase the relay number, but improvement comes with increased complexity to calculate LLR values using MAP detector. Therefore, in the next section two sub-optimal detectors are investigated to decrease the computational complexity of MAP detector. A comparative study of the performance of these two detectors is presented.

5. Low Complexity Iterative Soft Detection

In many practical communication systems, data is transmitted through a channel where multiple-access interference (MAI) and ISI are present and pose an obstacle for reliable communication in multipath channels. Therefore, redundant bits are added to the original data using an error correction code at the transmitter to mitigate those problems. The receiver tries to extract the transmitted data using equalization and decoding. Joint equalization and decoding faces important developments, one of which information is exchanged back and forth between the decoder and equalizer iteratively, until convergence is achieved.

In this thesis, an iterative receiver structure is used for decoding multi-relay information in a LDPC coded system. The receiver consists of two soft input soft output modules that exchange information iteratively. At each iteration, extrinsic information resulting from one module is used as a priori information for the other module. In the iterative receiver, the detector provides the log likelihood ratio (LLR) of symbols. Hence MAP detector is optimal, and thus desirable. Unfortunately, the computational complexity of this detector grows exponentially as relay number increases. Especially, in multi-relay case, the detector calculates LLR values for source and relay nodes iteratively. Therefore, the high computational complexity of the optimal detectors has motivated the study of a number of computationally suboptimal and efficient detectors. In [53], the minimum square error (MMSE) detector with soft interference cancellation (SIC), referred to as MMSE-SIC detector is proposed. But, the fact that MMSE-SIC involves matrix inversion; it still requires a high complexity and processing delay. Thus, other various sub-optimal, but less complex detectors, which perform worse, compared to MAP detector are proposed [54]. In [55], Taylor series are considered to approximate the LLR directly to find computationally efficient detectors for the iterative receiver.

Moreover, in [56] MAP detector is approximated under the Central Limit Theorem (CLT) assumption.

5.1 Approximation based on Taylor Expansion

We approximate the LLR directly by using Taylor series to find computationally efficient detectors. This approach differs from the existing approaches in [53]-[54], where LLR is obtained by an indirect approach.

(In this chapter, results are obtained for vector case. They can easily be extended to scalar case with minor modifications.)

Soft information passed to the LDPC decoder for the source data is expressed as

$$L(x_S) = \Delta(x_S) - \log \frac{p(x_S = 1)}{p(x_S = 0)} \quad (5.1)$$

where $\Delta(x_S)$ is calculated in (4.16). Then

$$L(x_S) = \log \frac{\sum_{\mathbf{X}_R} p(\mathbf{y}_D | x_S = 1, \mathbf{X}_R) \Pr(\mathbf{X}_R)}{\sum_{\mathbf{X}_R} p(\mathbf{y}_D | x_S = 0, \mathbf{X}_R) \Pr(\mathbf{X}_R)}, \quad (5.2)$$

where $\mathbf{X}_R = [x_{R_1} \ x_{R_2} \ \dots \ x_{R_K}]$ and $x_{R_k} \in \{+1, -1\}$. x_{R_k} is the binary symbol of the k^{th} relay node

There are 2^K binary vectors in the set \mathbf{X}_R , where K is the relay number. Therefore, the complexity to calculate the a posteriori probability of x_S is $O(2^K)$. It is easily seen that, as relay number increases, the computational complexity increases.

First consider

$$\begin{aligned} \sum_{\mathbf{X}_R} p(\mathbf{y}_D | x_S = 1, \mathbf{X}_R) \Pr(\mathbf{X}_R) &\propto \sum_{\mathbf{X}_R} e^{-\frac{1}{N_0} \|\mathbf{y}_D - \sqrt{P_S} \mathbf{h}_{SD} - \sqrt{g_2} \sqrt{P_R} \mathbf{H}_{RD} \mathbf{X}_R^T\|^2} \Pr(\mathbf{X}_R) \\ &= E_{\mathbf{X}_R} [e^{-\frac{1}{N_0} \|\mathbf{y}^+ - \sqrt{g_2} \sqrt{P_R} \mathbf{H}_{RD} \mathbf{X}_R^T\|^2}] \end{aligned} \quad (5.3)$$

where $\mathbf{H}_{RD} = [\mathbf{h}_{R_1D} \ \mathbf{h}_{R_2D} \ \dots \ \mathbf{h}_{R_KD}]$ and $\mathbf{y}^+ = \mathbf{y}_D - \sqrt{P_S} \mathbf{h}_{SD}$.

\mathbf{h}_{R_kD} denotes the channel coefficient for k^{th} relay node-destination link, \mathbf{h}_{SD} denotes the channel coefficient between source and destination. P_S is the transmission power from source to destination and $P_R = \frac{P_S}{K}$ is the transmission power from relay node to destination, which is assumed as equal for each relay node.

Let $v^+(\mathbf{X}_R) = e^{-\frac{1}{N_0} \|\mathbf{y}^+ - \sqrt{g_2} \sqrt{P_R} \mathbf{H}_{RD} \mathbf{X}_R^T\|^2}$, then using Taylor series it is shown that

$$v^+(\mathbf{X}_R) = v^+(\hat{\mathbf{X}}_R) + \nabla_{v^+}^T(\hat{\mathbf{X}}_R)(\mathbf{X}_R - \hat{\mathbf{X}}_R) + \dots \quad (5.4)$$

where ∇_{v^+} is the gradient of $v^+(\mathbf{X}_R)$ which is given as

$$\nabla_{v^+}(x) = \left[\frac{\delta v^+(x)}{\delta x_1} \ \frac{\delta v^+(x)}{\delta x_2} \ \dots \ \frac{\delta v^+(x)}{\delta x_K} \right] \text{ and } \hat{\mathbf{X}}_R = E[\mathbf{X}_R], \text{ where } E[\cdot] \text{ is the expectation}$$

operator.

We can show that

$$E[v^+(\mathbf{X}_R)] = v^+(\hat{\mathbf{X}}_R) + E[\nabla_{v^+}^T(\hat{\mathbf{X}}_R)(\mathbf{X}_R - \hat{\mathbf{X}}_R)] + \dots = v^+(\hat{\mathbf{X}}_R) + 0 + \dots$$

where the first term order becomes zero.

This Taylor series leads to the following approximation:

$$\sum_{\mathbf{X}_R} p(\mathbf{y}_D | x_S = 1, \mathbf{X}_R) \Pr(\mathbf{X}_R) \approx e^{-\frac{1}{N_0} \|\mathbf{y}^+ - \sqrt{g_2} \sqrt{P_R} \mathbf{H}_{RD} E[\mathbf{X}_R]^T\|^2} \quad (5.5)$$

With the same approach above, we can approximate $\sum_{\mathbf{X}_R} p(\mathbf{y}_D | x_S = 0, \mathbf{X}_R) \Pr(\mathbf{X}_R)$. The approximate LLR is given as

$$L(x_S) \approx \log \frac{e^{-\frac{1}{N_0} \|\mathbf{y}^+ - \sqrt{g_2} \sqrt{P_R} \mathbf{H}_{RD} E[\mathbf{X}_R]^T\|^2}}{e^{-\frac{1}{N_0} \|\mathbf{y}^- - \sqrt{g_2} \sqrt{P_R} \mathbf{H}_{RD} E[\mathbf{X}_R]^T\|^2}} \quad (5.6)$$

where $\mathbf{y}^- = \mathbf{y}_D + \sqrt{P_S} \mathbf{h}_{SD}$.

Then LLR is approximated by

$$L(x_S) \triangleq 4 \frac{\sqrt{P_S} \mathbf{h}_{SD}^T}{N_0} (\mathbf{y}_D - \sqrt{g_2} \sqrt{P_R} \mathbf{H}_{RD} E_{\mathbf{X}_R}[\mathbf{X}_R]^T) \quad (5.7)$$

Using the same approach, we can also calculate LLR for relay nodes. For example, LLR for relay node 1 is

$$L(x_{R_1}) \triangleq 4 \frac{\sqrt{g_2} \sqrt{P_R} \mathbf{h}_{R_1 D}^T}{N_0} (\mathbf{y}_D - \mathbf{H}_R E_{\mathbf{X}}[\mathbf{X}]^T) \quad (5.8)$$

where $\mathbf{X} = [x_S \ x_{R_2} \ x_{R_3} \ \dots \ x_{R_K}]$ and $\mathbf{H}_R = [\sqrt{P_S} \mathbf{h}_{SD} \ \sqrt{g_2} \sqrt{P_R} \mathbf{h}_{R_2 D} \ \dots \ \sqrt{g_2} \sqrt{P_R} \mathbf{h}_{R_K D}]$

The channels gains (g_2) between relay nodes and destination are assumed as equal. This can be justified by the fact that the distance between relay nodes and destination node is equal, so the path loss gain is the same for all relays.

Hence, first Soft Cancellation method is applied on received signal, $\mathbf{y}_D - \mathbf{H}_R E_X[\mathbf{X}]^T$ and then the resulting vector is multiplied with $\sqrt{g_2} \sqrt{P_R} \mathbf{h}_{R_1 D}$ and first order approximation of LLR is obtained. This detector is called the matched filter (MF) detector with SIC, referred to as the MF-SIC detector, in [57]. The equation (5.7) does not contain a matrix inversion, so it is computationally more efficient than the MMSE-SIC detector in [53].

The BER comparison for MAP detector and sub-optimal detector obtained by Taylor expansion is shown in Figure 5.1-Figure 5.2 for two relay network for different number of global iterations.

For both figures, the information block of length 1000 was first encoded with LDPC regular \mathbf{H} (matrix taken from Mackay library) with rate 1/2 and codeword of block length 2000 is created. The codeword is sent through Rayleigh fading channel and at relay nodes DF or EF technique is used. At the destination node, transmitted codeword was extracted using iterative LDPC decoding. The inner iteration of LDPC decoder is 100. Channel gains g_1 and g_2 are both 4 dB.

As it is shown in Figure 5.1, the performance of the detector obtained by Taylor expansion is 0.8 dB worse than MAP detector for one global iteration at BER 10^{-5} . Figure 5.2 compares the performance of sub-optimal detector obtained by Taylor expansion for two global iterations. Sub-optimal detector performs 1 dB worse when relay nodes use DF technique and 1.2 dB worse when EF technique is used at relay nodes.

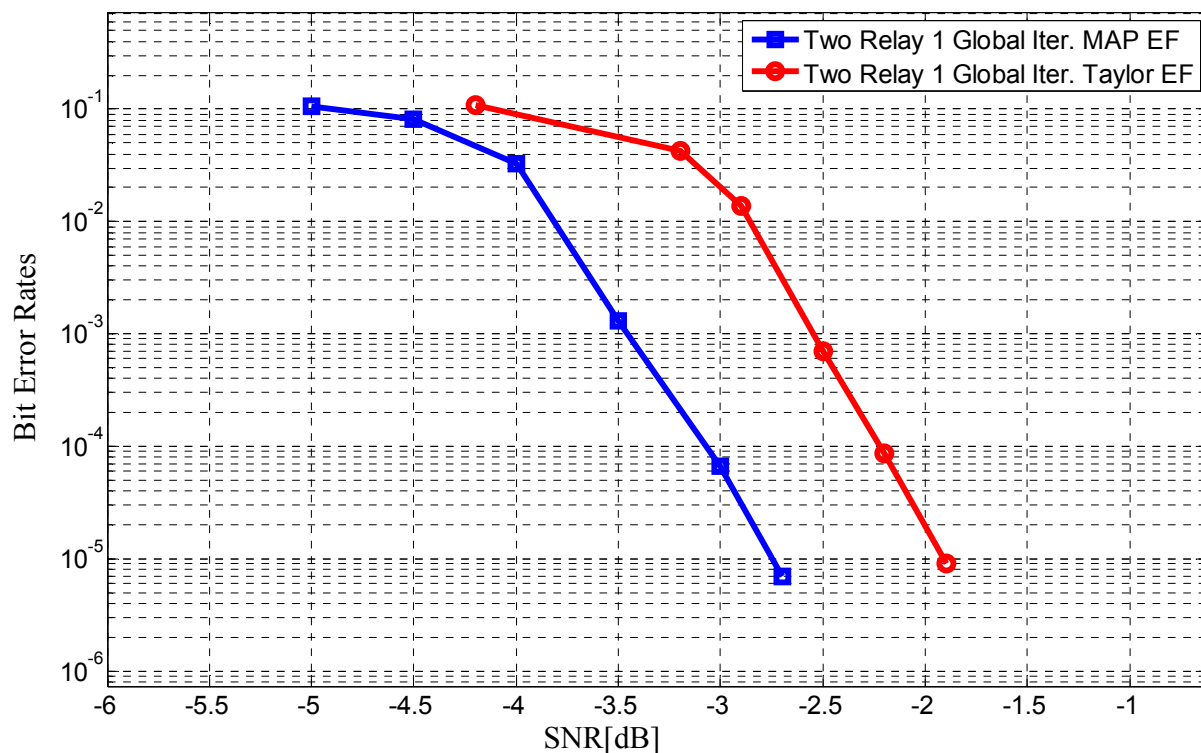


Figure 5.1: BER comparison of MAP detector and sub-optimal detector obtained by Taylor expansion for 1 global iteration

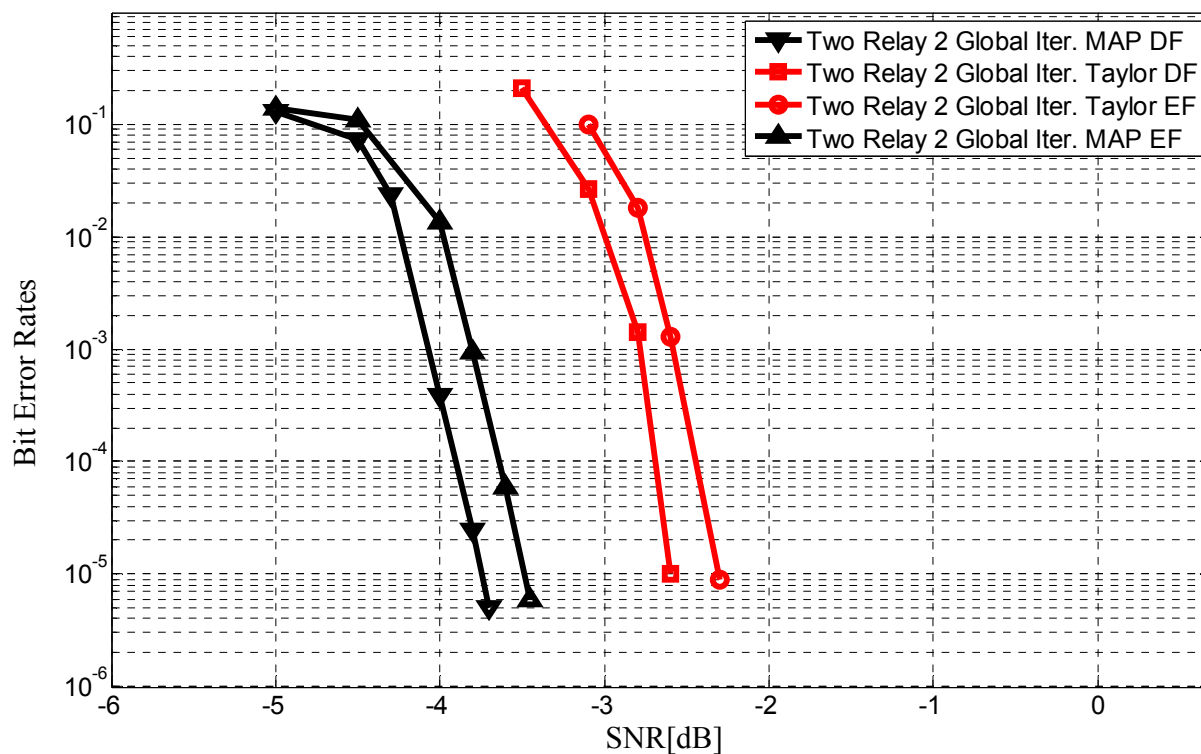


Figure 5.2: BER comparison of MAP detector and sub-optimal detector obtained by Taylor expansion for 2 global iterations

5.2 Approximation based on Central Limit Theorem (CLT)

In this section, Gaussian approximation based on the CLT is considered to find the LLR, as the sum of interfering signals caused by relay transmissions can be approximated by a Gaussian random process for large number of relay nodes [56].

To calculate the soft information passing to the LDPC decoder for the source node, in (5.3)

$$\sum_{\mathbf{X}_R} p(\mathbf{y}_D | x_S = 1, \mathbf{X}_R) \Pr(\mathbf{X}_R) \approx E_{\mathbf{X}_R} [e^{-\frac{1}{N_0} \|\mathbf{y}^+ - \mathbf{H}_{RD} \mathbf{X}_R^T\|^2}]$$

where $\mathbf{H}_{RD} = [\sqrt{g_2} \sqrt{P_R} \mathbf{h}_{R_1D} \quad \sqrt{g_2} \sqrt{P_R} \mathbf{h}_{R_2D} \quad \dots \quad \sqrt{g_2} \sqrt{P_R} \mathbf{h}_{R_KD}]$ is found.

Let $\mathbf{u}_S = \mathbf{H}_{RD} \mathbf{X}_R^T = \hat{\mathbf{u}}_S + \mathbf{e}_S$

where $\hat{\mathbf{u}}_S = E_{\mathbf{X}_R} [\mathbf{u}_S] = \mathbf{H}_{RD} E_{\mathbf{X}_R} [\mathbf{X}_R^T]$ and $\mathbf{e}_S = \mathbf{H}_{RD} (\mathbf{X}_R^T - E_{\mathbf{X}_R} [\mathbf{X}_R^T])$

It follows that

$$E_{\mathbf{X}_R} [e^{-\frac{1}{N_0} \|\mathbf{y}^+ - \mathbf{H}_{RD} \mathbf{X}_R^T\|^2}] = E_{\mathbf{e}_S} [e^{-\frac{1}{N_0} \|\mathbf{v}^+ - \mathbf{e}_S\|^2}], \text{ where } \mathbf{v}^+ = \mathbf{y}^+ - \hat{\mathbf{u}}_S \quad (5.9)$$

Assumption: When number of relay nodes is large, based on CLT, \mathbf{e}_S is assumed as zero mean Gaussian random variable with the covariance matrix

$$\mathbf{R}_S = E[\mathbf{e}_S \mathbf{e}_S^T] = \mathbf{H}_{RD} E_{\mathbf{X}_R} [\tilde{\mathbf{X}} \tilde{\mathbf{X}}^T] \mathbf{H}_{RD}^T, \text{ where } \tilde{\mathbf{X}} = \mathbf{X}_R^T - E_{\mathbf{X}_R} [\mathbf{X}_R^T] \quad (5.10)$$

Under this assumption,

$$L(x_S) = \hat{L}(x_S)^{(clt)} \cong 4\sqrt{P_S} \mathbf{h}_{SD}^T (\mathbf{R}_S + N_0 \mathbf{I})^{-1} \mathbf{y}_S, \text{ where } \mathbf{y}_S = \mathbf{y}_D - \hat{\mathbf{u}}_S \quad (5.11)$$

Hence, as relay number increases, $\overset{\Delta}{L}(x_S)^{(clt)}$ can approach $L(x_S)$ given in (5.2).

The direct derivation of (5.11) for the general vector case is the following:

$$E_{\mathbf{e}_S} [e^{-\frac{1}{N_0} \|\mathbf{v}^+ - \mathbf{e}_S\|^2}] = C e^{(-\frac{1}{N_0} \|\mathbf{v}^+\|^2)} \int e^{(-\mathbf{e}_S^H \mathbf{Q}_S^{-1} \mathbf{e}_S + \frac{2}{N_0} \Re((\mathbf{v}^+)^H \mathbf{e}_S))} d\mathbf{e}_S \quad (5.12)$$

where C is a normalizing constant and $\mathbf{Q}_S^{-1} = \mathbf{R}_S^{-1} + \frac{1}{N_0} \mathbf{I}$

Since $-\mathbf{e}_S^H \mathbf{Q}_S^{-1} \mathbf{e}_S + \frac{2}{N_0} \Re((\mathbf{v}^+)^H \mathbf{e}_S) = -(\mathbf{e}_S - \mathbf{z}^+)^H \mathbf{Q}_S^{-1} (\mathbf{e}_S - \mathbf{z}^+) + (\mathbf{z}^+)^H \mathbf{Q}_S^{-1} \mathbf{z}^+$ where $\mathbf{z}^+ = \frac{1}{N_0} \mathbf{Q}_S \mathbf{v}^+$, we have

$$C \int e^{(-\mathbf{e}_S^H \mathbf{Q}_S^{-1} \mathbf{e}_S + \frac{2}{N_0} \Re((\mathbf{v}^+)^H \mathbf{e}_S))} d\mathbf{e}_S = C' e^{\frac{1}{N_0} (\mathbf{v}^+)^H \mathbf{Q}_S \mathbf{v}^+},$$

where C' is a constant. Then, we have

$$E_{\mathbf{e}_S} [e^{-\frac{1}{N_0} \|\mathbf{v}^+ - \mathbf{e}_S\|^2}] = C' e^{(-\frac{1}{N_0} \|\mathbf{v}^+\|^2 + \frac{1}{N_0^2} (\mathbf{v}^+)^H \mathbf{Q}_S \mathbf{v}^+)} = C' e^{(-\frac{1}{N_0} (\mathbf{v}^+)^H \hat{\mathbf{Q}}_S \mathbf{v}^+)} \quad (5.13)$$

where $\hat{\mathbf{Q}}_S = \mathbf{I} - \frac{1}{N_0} \mathbf{Q}_S$

If we carry out eigendecomposition of \mathbf{Q}_S , we get $\mathbf{Q}_S = \mathbf{E}_S \mathbf{\Lambda}_S \mathbf{E}_S^H$, where $\mathbf{E}_S = [\mathbf{e}_{S,1} \ \mathbf{e}_{S,2} \dots \ \mathbf{e}_{S,N}]$ and $\mathbf{\Lambda}_S = \text{Diag}\{\lambda_{S,1} \ \lambda_{S,2} \dots \ \lambda_{S,N}\}$. $\mathbf{e}_{S,n}$ and $\lambda_{S,n}$ are the n^{th} eigenvector and eigenvalue of \mathbf{Q}_S .

As a result,

$$\begin{aligned} \hat{\mathbf{Q}}_S &= \mathbf{I} - \frac{1}{N_0} \mathbf{Q}_S = \mathbf{I} - \frac{1}{N_0} (\mathbf{R}_S^{-1} + \frac{1}{N_0} \mathbf{I})^{-1} \\ &= \mathbf{I} - \frac{1}{N_0} \mathbf{E}_S (\mathbf{\Lambda}_S^{-1} + \frac{1}{N_0} \mathbf{I})^{-1} \mathbf{E}_S \\ &= N_0 (\mathbf{R}_S + N_0 \mathbf{I})^{-1} \end{aligned} \quad (5.14)$$

Substituting (5.13) and (5.14) into (5.9), we get

$$L(x_S) = \hat{L}(x_S)^{clt} \triangleq 4(\sqrt{P_S} \mathbf{h}_{SD}^T [\mathbf{R}_S + N_0 \mathbf{I}]^{-1} \mathbf{y}_S) \quad (5.15)$$

It is shown in (5.15) that LLR for CLT detector can be calculated with a lower complexity. Actually, the major complexity of the detector is due to matrix inversion which has the complexity $O(N^3)$, whereas the MAP detector has $O(2^K)$. In [56], it is shown that the approximate MAP detector which is obtained under the assumption based on the CLT becomes the well-known MMSE-SIC detector proposed in [53].

The BER comparison of MAP detector and sub-optimal detector obtained CLT assumption is shown in Figure 5.3 and Figure 5.4 for two relay network for different number of global iterations.

For both figures, the information block of length 1000 was first encoded with LDPC regular \mathbf{H} (matrix taken from Mackay library) with rate 1/2 and codeword of block length 2000 is created. The codeword is sent through Rayleigh fading channel and at relay nodes DF or EF technique is used. At the destination node, transmitted codeword was extracted using iterative LDPC decoding. The inner iteration of LDPC decoder is 100. Channel gains g_1 and g_2 are both 4 dB.

As it is shown in Figure 5.3, the performance of the detector obtained by CLT assumption is about 1 dB worse than MAP detector for one global iteration at BER 10^{-5} . Figure 5.4 compares the performance of sub-optimal detector obtained by CLT assumption for two global iterations. Sub-optimal detector performs about 1.3 dB worse when relay nodes use DF technique at BER 10^{-5} and 1.5 dB worse when EF technique is used at relay nodes for BER 10^{-4} .

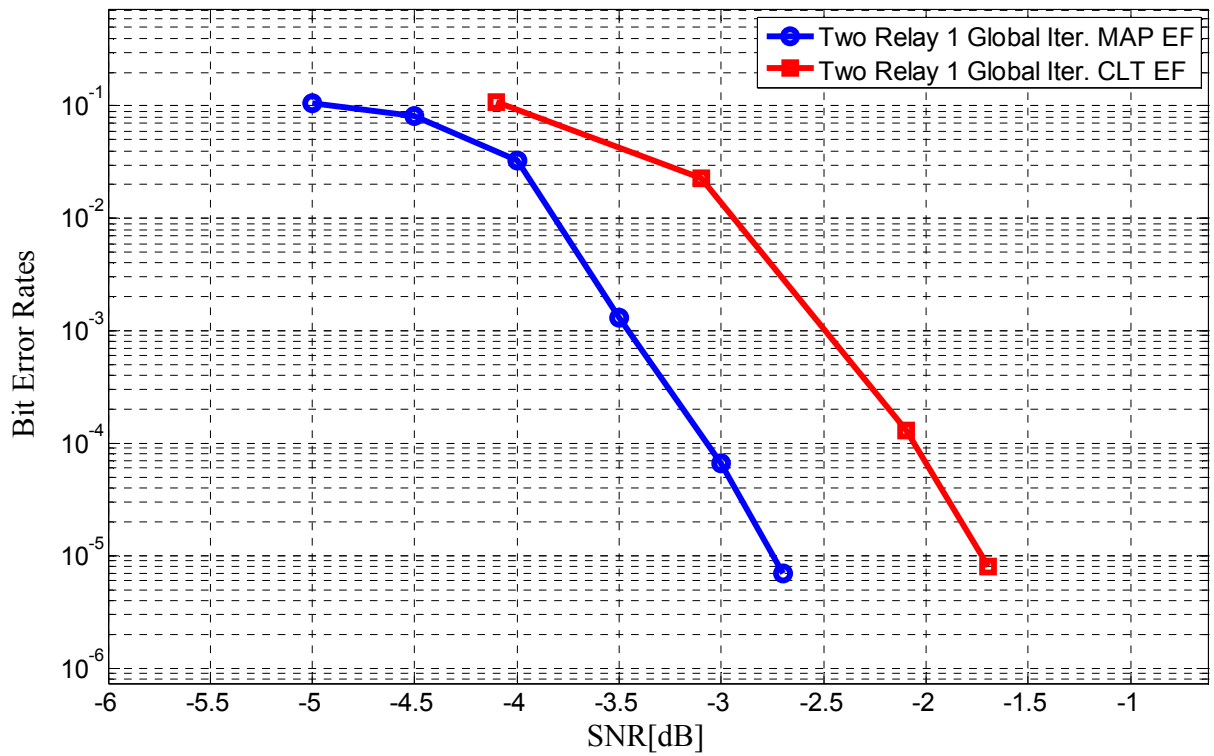


Figure 5.3: BER comparison of MAP detector and sub-optimal detector obtained by CLT assumption for 1 global iteration

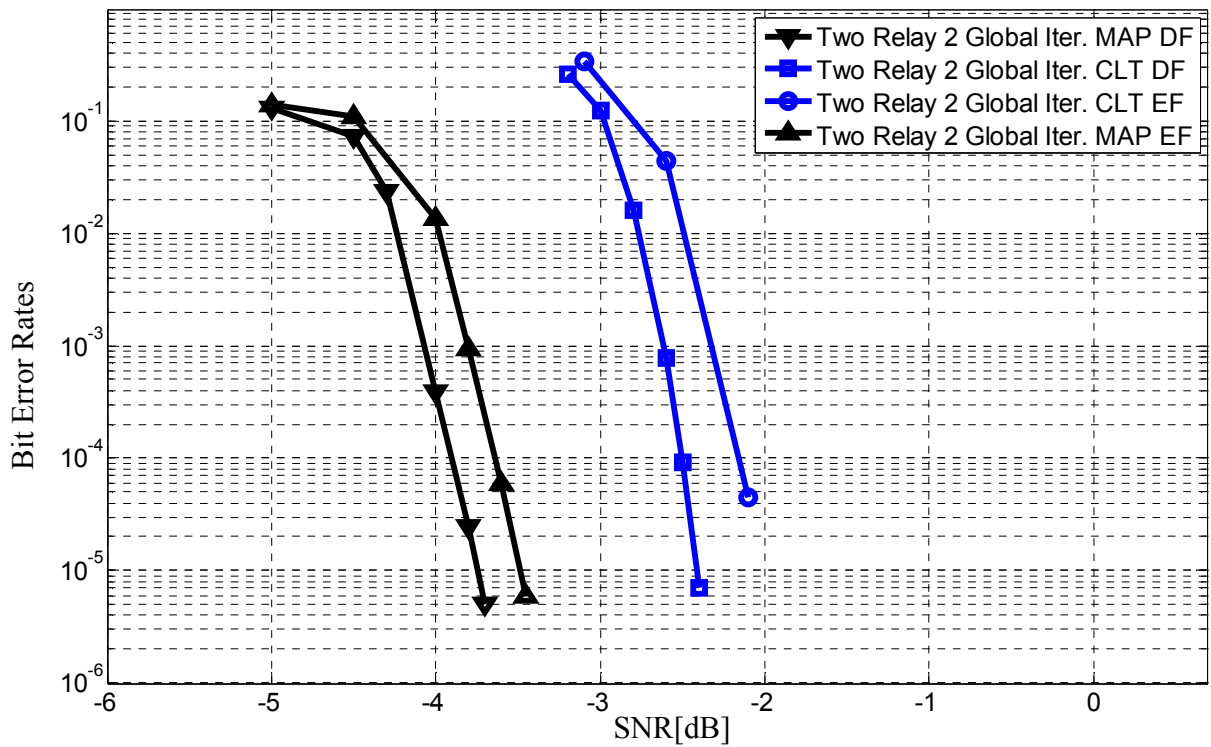


Figure 5.4: BER comparison of MAP detector and sub-optimal detector obtained by CLT assumption for 2 global iterations

As it is mentioned above, the computation of Taylor detector is similar to MF-SIC detector, while CLT detector becomes MMSE-SIC detector. Therefore, comparing the Taylor detector and CLT detector is similar to comparing MF-SIC and MMSE-SIC detectors.

MF-SIC detector does not contain a matrix inversion, so it is computationally more efficient than the MMSE-SIC detector. The main computational complexity of the MMSE-SIC detector is due to the matrix inverse in the computation of the MMSE filter, which is $O(N^3)$, whereas the computational complexity of the MF-SIC detector is $O(N^2)$ [58]. In [59], MF-SIC detector is compared to the MMSE-SIC detector for MIMO/OFDM systems using two global iterations. It is observed that MF-SIC requires only 10–30 % computation of the MMSE-SIC. In other words, employing MF-SIC enables to achieve 70–90 % reduction of computational complexity of MMSE-SIC. However, [60] also pointed out that the MF approximation is certainly not suitable for the case in which no a priori information is available, e.g. at the initial detection stage and it is shown in [57] MMSE-SIC generally provides a higher spectral efficiency than the MF-SIC.

For our relay case, the performances of the sub-optimal detectors obtained by Taylor expansion and CLT assumption are compared in Figure 5.5. As it is seen in the figure, detector obtained through Taylor expansion is about 0.2 dB better than detector obtained by CLT assumption at BER 10^{-5} when DF technique is used and 0.3 dB better at BER 10^{-4} when EF technique is used. The reason for this gap is that the sub-optimal detector approximated using CLT assumption is identical to the minimum mean square error (MMSE) detector with soft interference cancellation (SIC) proposed in [53] and MMSE detector works better at conditions that the interference is higher. For two relay network, the interference is not high enough. Therefore, if we increase the interference by increasing the relay number, the detector of CLT assumption outperforms the detector of Taylor expansion as it is shown in Figure 5.6. For eight relay network, sub-optimal detector based on CLT assumption is about 0.1 dB better than sub-optimal detector based on Taylor expansion for both one and two global iteration.

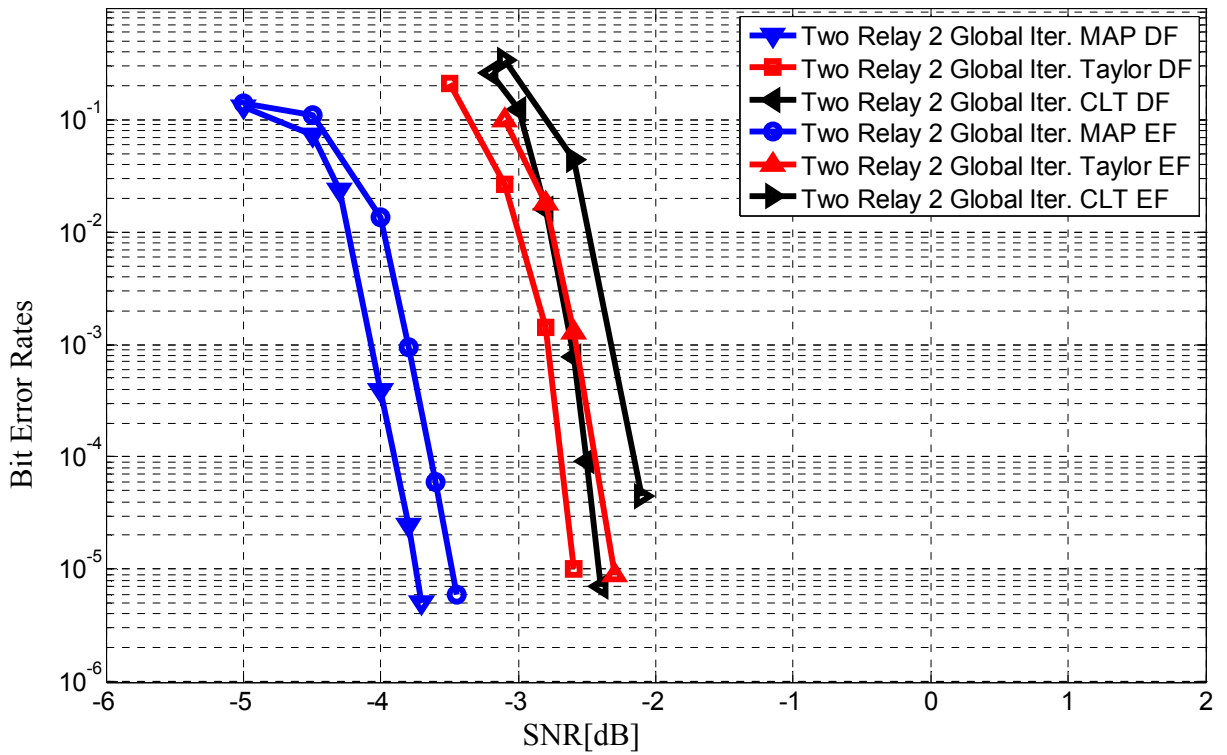


Figure 5.5: Comparison of sub-optimal detectors obtained by Taylor expansion and CLT assumptions for two relay network.

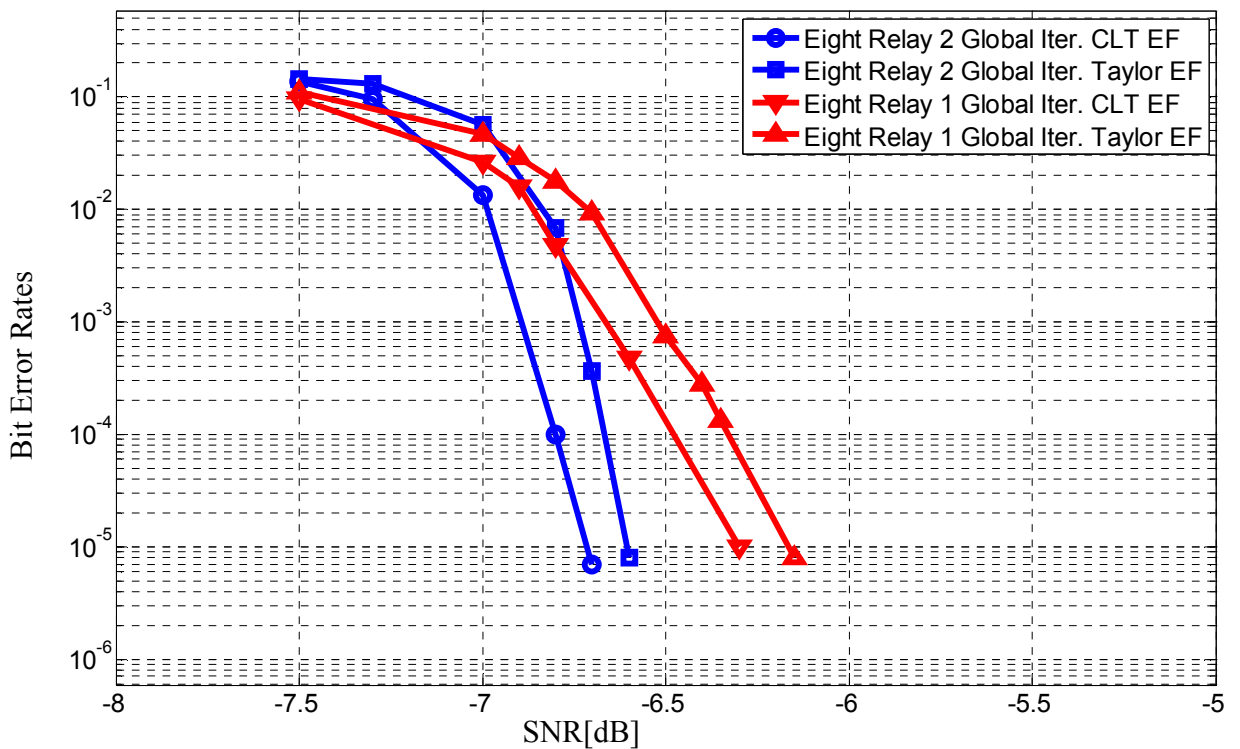


Figure 5.6: Comparison of sub-optimal detectors obtained by Taylor expansion and CLT assumptions for eight relay network.

The next section discusses the reason why sub-optimal detectors perform worse than MAP detector, and provides a technique to improve the performance of these detectors.

5.3 Soft Decorrelating Detection (SODED)

In [61], Robertson et. al has shown that when a sub-optimal detector is used instead of the MAP detector, some degradation is observed on the AWGN channel. Several papers have appeared recently that tried to find the reason behind the poor performance of sub-optimal detectors compared to the MAP [62]-[67] It is demonstrated in these papers that the reliability values at the output of the sub-optimal detectors are larger than the values at the output of MAP decoder, leading degradation. In [68], it is argued that the main reason for this degradation due to large reliability values is mostly the *high correlation* between the intrinsic information (input to the detector) and extrinsic information (output of the detector).

This correlation leads to overestimation of the extrinsic information estimated by the detector compared to its true value. The intuition behind this overestimation is that the extrinsic information passed from the detector to decoder should provide *new* information to the decoder. However, due to this high correlation, part of the extrinsic information passing to the decoder is already known to this decoder. But the receiving decoder treats all of this extrinsic value as *new* information. That results in a redundancy in the exchanged information, leading to exaggerated extrinsic information at the output of the detector.

It is clear that the intrinsic and extrinsic information of the detector must be decorrelated before the extrinsic information is passed on to the LDPC decoder. And to alleviate this problem, the authors in [68] propose to use two attenuators, one applied to the immediate output of the detector (a posteriori probability) and another applied to the extrinsic information before it is passed on to the decoder

Now let us denote the actual detector output by L_{app} and the corresponding extrinsic information by L_{ext} . The correlation between L_{ext} and intrinsic information (L_{int}) is generally assumed as weakly correlated, and thus L_{ext} is expressed as:

$$L_{ext} = L_{app} - L_{int} \quad (5.16)$$

However, the correlation between L_{int} and L_{ext} is rather strong.

(Note that the intrinsic value of the detector is the extrinsic value of the LDPC decoder)

The variables L_{int} and L_{ext} are correlated Gaussian random variables with means m_i , m_e and variances σ_i^2 , σ_e^2 , respectively. Assuming $x_S = +1$ is transmitted, the joint conditional probability density function (pdf) $P(L_{ext}, L_{int} | x_S = 1)$ is then given as

$$P(L_{ext}, L_{int} | x_S = 1) = \frac{1}{2\pi\sigma_i\sigma_e\sqrt{1-\rho^2}} \cdot \exp\left(-\frac{1}{2(1-\rho^2)} \left[\frac{(L_{ext} - m_e)^2}{\sigma_e^2} + \frac{(L_{int} - m_i)^2}{\sigma_i^2} \right]\right) \cdot \exp\left(\frac{\rho(L_{ext} - m_e)(L_{int} - m_i)}{\sigma_i\sigma_e(1-\rho^2)}\right) \quad (5.17)$$

where ρ is the correlation coefficient given by,

$$\rho = \frac{E[(L_{ext} - m_e)(L_{int} - m_i)]}{\sigma_i\sigma_e} \quad (5.18)$$

Similarly, when Assuming $x_S = -1$ is transmitted, the joint conditional probability density function (pdf) $P(L_{ext}, L_{int} | x_S = -1)$ is then given as

$$P(L_{ext}, L_{int} | x_S = -1) = \frac{1}{2\pi\sigma_i\sigma_e\sqrt{1-\rho^2}} \cdot \exp\left(-\frac{1}{2(1-\rho^2)} \left[\frac{(L_{ext} + m_e)^2}{\sigma_e^2} + \frac{(L_{int} + m_i)^2}{\sigma_i^2} \right]\right) \cdot \exp\left(\frac{\rho(L_{ext} + m_e)(L_{int} + m_i)}{\sigma_i\sigma_e(1-\rho^2)}\right) \quad (5.19)$$

Using Bayes' rule, L_{app} can be calculated as

$$\begin{aligned}
L_{app}^{true} &= \ln \frac{P(x_S = +1 | L_{int}, L_{ext})}{P(x_S = -1 | L_{int}, L_{ext})} \\
&= \ln \frac{\exp\left(-\frac{1}{2(1-\rho^2)} \left[\frac{(L_{ext} - m_e)^2}{\sigma_e^2} + \frac{(L_{int} - m_i)^2}{\sigma_i^2} \right]\right) \cdot \exp\left(\frac{\rho(L_{ext} - m_e)(L_{int} - m_i)}{\sigma_i \sigma_e (1-\rho^2)}\right)}{\exp\left(-\frac{1}{2(1-\rho^2)} \left[\frac{(L_{ext} + m_e)^2}{\sigma_e^2} + \frac{(L_{int} + m_i)^2}{\sigma_i^2} \right]\right) \cdot \exp\left(\frac{\rho(L_{ext} + m_e)(L_{int} + m_i)}{\sigma_i \sigma_e (1-\rho^2)}\right)} \\
&= -\frac{1}{2(1-\rho^2)} \left[\frac{(L_{ext} - m_e)^2}{\sigma_e^2} + \frac{(L_{int} - m_i)^2}{\sigma_i^2} - \frac{(L_{ext} + m_e)^2}{\sigma_e^2} - \frac{(L_{int} + m_i)^2}{\sigma_i^2} \right] \\
&\quad + \frac{\rho(L_{ext} - m_e)(L_{int} - m_i)}{\sigma_i \sigma_e (1-\rho^2)} - \frac{\rho(L_{ext} + m_e)(L_{int} + m_i)}{\sigma_i \sigma_e (1-\rho^2)} \\
&= -\frac{1}{2(1-\rho^2)} \left[-\frac{4L_{ext}m_e}{\sigma_e^2} - \frac{4L_{int}m_i}{\sigma_i^2} \right] + \frac{\rho(-2L_{ext}m_i - 2L_{int} - m_e)}{\sigma_i \sigma_e (1-\rho^2)} \\
&= L_{ext} \left[\frac{2m_e}{\sigma_e^2} \frac{1}{(1-\rho^2)} - \frac{2\rho m_i}{\sigma_i \sigma_e (1-\rho^2)} \right] + L_{int} \left[\frac{2m_i}{\sigma_i^2} \frac{1}{(1-\rho^2)} - \frac{2\rho m_e}{\sigma_i \sigma_e (1-\rho^2)} \right] \\
&= L_{ext} \cdot \frac{1}{1-\rho^2} \left[\frac{2m_e}{\sigma_e^2} - \rho \frac{2m_i}{\sigma_i \sigma_e} \right] + L_{int} \cdot \frac{1}{1-\rho^2} \left[\frac{2m_i}{\sigma_i^2} - \rho \frac{2m_e}{\sigma_i \sigma_e} \right] \\
&= L_{ext} \cdot \frac{1}{1-\rho^2} \left[r_e - \rho r_i \frac{\sigma_i}{\sigma_e} \right] + L_{int} \cdot \frac{1}{1-\rho^2} \left[r_i - \rho r_e \frac{\sigma_e}{\sigma_i} \right]
\end{aligned}$$

where $r_e = \frac{2m_e}{\sigma_e^2}$ and $r_i = \frac{2m_i}{\sigma_i^2}$

$$= aL_{ext} + bL_{int} \tag{5.20}$$

where $a = \frac{1}{1-\rho^2} (r_e - \rho r_i \frac{\sigma_i}{\sigma_e})$ and $b = \frac{1}{1-\rho^2} (r_i - \rho r_e \frac{\sigma_e}{\sigma_i})$

Substituting (5.16) into (5.20) yields

$$L_{app}^{true} = a(L_{app} - L_{int}) + bL_{int} \quad (5.21)$$

and consequently extrinsic information passing to LDPC decoder is

$$L_{ext} = L_{app}^{true} - L_{int} = (a+1-b) \left[\frac{a}{a+1-b} L_{app} - L_{int} \right] = c[dL_{app} - L_{int}] \quad (5.22)$$

where $c=a+1-b$ and $d=a/(a+1-b)$

As a result, to make L_{ext} and L_{int} uncorrelated, the output of the detector should be multiplied by d and then the the intrinsic information must be subtracted, and finally the difference should be scaled by c as it is seen in Figure 5.7

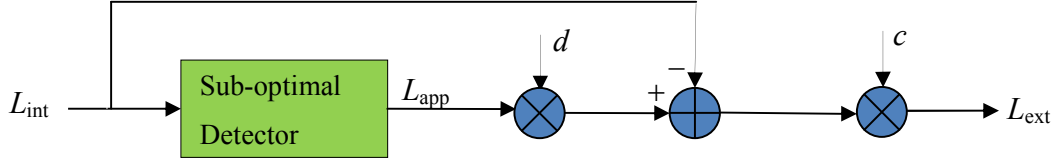


Figure 5.7: Soft Decorrelating Detection (SODED)

These attenuators depend on the means and variances of the intrinsic and extrinsic information of the detector, as well as the correlation between them. Therefore, they should be updated for every received data frame at every iteration. To compute the mean and variance of intrinsic information is very easy, which is obtained from LDPC decoder and it does not incur a high complexity, whereas computing the mean and variance of extrinsic information incurs a processing delay.

The mean and variance of intrinsic for both source and relay transmission are calculated as

$$m_i(x_l) = (1) \frac{e^{L_{int}^l}}{1 + e^{L_{int}^l}} + (-1) \left(\frac{1}{1 + e^{L_{int}^l}} \right) = \tanh\left(\frac{L_{int}^l}{2}\right) \quad (5.23)$$

$$\begin{aligned} \sigma_i^2(x_l) &= (1)^2 \left(\frac{e^{L_{int}^l}}{1 + e^{L_{int}^l}} \right) + (-1)^2 \left(\frac{1}{1 + e^{L_{int}^l}} \right) - m_i^2(x_l) \\ &= 1 - m_i^2(x_l) \end{aligned} \quad (5.24)$$

where $l = S$ or R_k , denoting source or k^{th} relay node. L_{int}^S and $L_{int}^{R_k}$ are a priori information provided by LDPC decoders, for source and k^{th} relay node, respectively.

To calculate the mean and variance of extrinsic information, we use following calculations.

First define

$$\mathbf{X} = [x_S \ x_{R_1} \ x_{R_2} \ \dots \ x_{R_K}]^T \quad (5.25)$$

We first form soft estimates of the code bits of source and all relay nodes, based on the a priori information provided by LDPC decoders.

$$\tilde{\mathbf{X}} = E[\mathbf{X}] = [\tilde{x}_S \ \tilde{x}_{R_1} \ \tilde{x}_{R_2} \ \dots \ \tilde{x}_{R_K}]^T \quad (5.26)$$

where $\tilde{x}_S = \tanh(L_{int}^S / 2)$ and $\tilde{x}_{R_k} = \tanh(L_{int}^{R_k} / 2)$

Define

$$\tilde{\mathbf{X}}_l = \tilde{\mathbf{X}} - \tilde{x}_l \mathbf{e}_l = [\tilde{x}_S \ \tilde{x}_{R_1} \ \tilde{x}_{R_2} \ \dots \ \tilde{x}_{R_{l-1}} \ 0 \ \tilde{x}_{R_{l+1}} \ \dots \ \tilde{x}_{R_K}]^T \quad (5.27)$$

where $l=1,2,\dots,K+1$. \mathbf{e}_l is a zero vector of size $(K+1)$, except l^{th} entry, which is 1. x_l denotes l^{th} entry of \mathbf{X} matrix, which is source or relay node transmission and \tilde{x}_l denotes the expectation of x_l .

The received signal at the destination node is given by

$$\mathbf{y}_D = \mathbf{H}\mathbf{X} + \mathbf{n}_D \quad (5.28)$$

where \mathbf{H} denotes $N \times (K+1)$ channel coefficient matrix between relay nodes and destination. \mathbf{n}_D denotes the $N \times 1$ zero mean complex noise with covariance matrix $\sigma^2 \mathbf{I}$.

For source and all relay nodes, a soft interference cancellation is performed on the output \mathbf{y}_D .

$$\mathbf{y}_l = \mathbf{y}_D - \mathbf{H}\tilde{\mathbf{X}}_l = \mathbf{H}(\mathbf{X} - \tilde{\mathbf{X}}_l) + \mathbf{n}_D \quad (5.29)$$

Next, in order to further suppress the residual interference in \mathbf{y}_l , an instantaneous linear filter \mathbf{w}_l is applied to \mathbf{y}_l , to obtain

$$z_l = \mathbf{w}_l^T \mathbf{y}_l \quad (5.30)$$

\mathbf{w}_l is chosen to minimize the mean square error between the code bit x_l and the filter output z_l

$$\mathbf{w}_l = \arg \min_{\mathbf{w}} E[\|x_l - \mathbf{w}_l^T \mathbf{y}_l\|^2] = \arg \min_{\mathbf{w}} (\mathbf{w}_l^T E[\mathbf{y}_l \mathbf{y}_l^T] \mathbf{w}_l - \mathbf{w}_l^T E[x_l \mathbf{y}_l] - E[x_l \mathbf{y}_l]^T \mathbf{w}_l) \quad (5.31)$$

where the expectation is taken with respect to transmissions other than x_l and noise.

Using (5.29), we have

$$E[\mathbf{y}_l \mathbf{y}_l^T] = \mathbf{H}\mathbf{\Lambda}_l \mathbf{H}^T + \sigma^2 \mathbf{I} \quad (5.32)$$

$$E[x_l \mathbf{y}_l] = \mathbf{H}\mathbf{e}_l = \mathbf{h}_D \quad (5.33)$$

where \mathbf{h}_D denotes the channel coefficient between the node, transmitting x_l and destination. In addition, covariance matrix is denoted as

$$\begin{aligned}\Lambda_l &= \text{cov}\{\mathbf{X} - \tilde{\mathbf{X}}_l\} \\ &= \text{diag}\{1 - \tilde{x}_S^2, 1 - \tilde{x}_{R_1}^2, 1 - \tilde{x}_{R_2}^2, \dots, 1 - \tilde{x}_{R_{l-1}}^2, 1, 1 - \tilde{x}_{R_{l+1}}^2, \dots, 1 - \tilde{x}_{R_K}^2\}\end{aligned}\quad (5.34)$$

Substituting (5.32) and (5.33) into (5.31), the linear filter for CLT detector is

$$\mathbf{w}_l = [\mathbf{H}\Lambda_l\mathbf{H}^T + \sigma^2\mathbf{I}]^{-1}\mathbf{h}_D \quad (5.35)$$

It is shown in [60], [70] that linear filter \mathbf{w}_S for MF-SIC, which is similar to Taylor detector is

$$\mathbf{w}_l = \frac{1}{\sigma^2 + \mathbf{h}_D^T\mathbf{h}_D}\mathbf{h}_D \quad (5.36)$$

Using (5.29) and (5.30), the mean, μ_l , and variance, v_l^2 , of the filter output, z_l , is calculated in a different approach used in [53]. Conditioning on the code bit x_l gives us

$$\begin{aligned}\mu_l &= E[z_l | x_l = x] = E[\mathbf{w}_l^T \mathbf{y}_l | x_l = x] \\ &= \mathbf{w}_l^T E[\mathbf{y}_l | x_l = x] = \mathbf{w}_l^T \mathbf{H} E[\mathbf{X} - \tilde{\mathbf{X}}_l | x_l = x] \\ &= \mathbf{w}_l^T \mathbf{H} \mathbf{x} \\ &= \mathbf{h}_D^T [\mathbf{H}\Lambda_l\mathbf{H}^T + \sigma^2\mathbf{I}]^{-1} \mathbf{h}_D\end{aligned}\quad (5.37)$$

where \mathbf{x} is a vector of zeros, except entry l , which is x .

$$\begin{aligned}v_l^2 &= \text{var}(z_l | x_l = x) = \mathbf{w}_l^H E[\mathbf{y}_l^H \mathbf{y}_l | x_l = x] \mathbf{w}_l - \mu_l^2 \\ &= \mathbf{h}_D^T [\mathbf{H}\Lambda_l\mathbf{H}^T + \sigma^2\mathbf{I}]^{-1} \mathbf{h}_D - \mu_l^2 \\ &= \mu_l - \mu_l^2\end{aligned}\quad (5.38)$$

for CLT detector.

$$\mu_l = E[z_l x_l | x_l = x] = \frac{\mathbf{h}_D^T \mathbf{h}_D}{\mathbf{h}_D^T \mathbf{h}_D + \sigma^2} \quad (5.39)$$

$$v_l^2 = E[z_l^2] - E[z_l]^2 = \mathbf{w}_l^T (\sigma^2\mathbf{I} + \mathbf{H}\Lambda_l\mathbf{H}^T - \mathbf{h}_D\mathbf{h}_D^T) \mathbf{w}_l \quad (5.40)$$

for Taylor detector.

The authors in [69], [71] examine the behaviour of multiple access-interference (MAI) at the output of the MMSE detector under various asymptotic conditions, including: large signal-to-noise ratio; small and large numbers of users. The environment of orthogonal signaling with additive white Gaussian noise is considered, similar to our relaying case. It is demonstrated that the conditional distribution of the MAI-plus-noise is approximately Gaussian in many cases of interest and the non-Gaussian portion of the MAI-plus-noise vanishes, thereby yielding a Gaussian distribution for the overall interference term.

As a result, the second order statistics we found in (5.37) and (5.38) describe the distribution of the output of the filter, z_l which is Gaussian distributed, i.e

$$z_l \sim N_c(u_l x_l, v_l^2)$$

Then the extrinsic information delivered by the filter is

$$\begin{aligned} L_{ext}(x_l) &= \log \frac{p(z_l | x_l = +1)}{p(z_l | x_l = -1)} \\ &= -\frac{(z_l - \mu_l)^2}{v_l^2} + \frac{(z_l + \mu_l)^2}{v_l^2} = \frac{4\Re\{z_l \mu_l\}}{v_l^2} \end{aligned} \quad (5.41)$$

The mean and variance of extrinsic information for both source and relay transmission is calculated as

$$m_e(x_l) = E[L_{ext}(x_l)] = \frac{4\mu_l}{v_l^2} E[z_l] = \frac{4\mu_l^2}{v_l^2} x_l \quad (5.42)$$

$$\sigma_e^2(x_l) = \text{var}(L_{ext}(x_l)) = \left(\frac{4\mu_l}{v_l^2}\right)^2 \text{var}(z_l) = \frac{8\mu_l^2}{v_l^2} \quad (5.43)$$

Hence, extrinsic information has a Gaussian distribution of the form

$$L_{ext}(x_l) \sim N\left(\frac{4\mu_l^2}{v_l^2} x_l, \frac{8\mu_l^2}{v_l^2}\right)$$

In [56], Choi used the correlation mapping technique between the information bit and estimated information bit to analyze the performance of iterative receivers, which gives similar results as extrinsic information transfer (EXIT) charts [72].

We employ empirical correlation coefficient technique for intrinsic and extrinsic information of the detector, which is given by

$$\hat{\rho} = \frac{1}{K+1} \left(\frac{L_{int}^S L_{ext}^S - m_i^S m_e^S}{\sigma_i^S \sigma_e^S} + \frac{L_{int}^{R_1} L_{ext}^{R_1} - m_i^{R_1} m_e^{R_1}}{\sigma_i^{R_1} \sigma_e^{R_1}} + \dots + \frac{L_{int}^{R_K} L_{ext}^{R_K} - m_i^{R_K} m_e^{R_K}}{\sigma_i^{R_K} \sigma_e^{R_K}} \right)$$

$$= \frac{1}{K+1} \left(\frac{L_{int}^S \frac{4\Re\{z_S \mu_S\}}{v_S^2} - \tanh\left(\frac{L_{int}^S}{2}\right) \frac{4\mu_S^2}{v_S^2} x_S}{\sqrt{1 - \tanh\left(\frac{L_{int}^S}{2}\right)^2} \sqrt{\frac{8\mu_S^2}{v_S^2}}} + \frac{L_{int}^{R_1} \frac{4\Re\{z_{R_1} \mu_{R_1}\}}{v_{R_1}^2} - \tanh\left(\frac{L_{int}^{R_1}}{2}\right) \frac{4\mu_{R_1}^2}{v_{R_1}^2} x_{R_1}}{\sqrt{1 - \tanh\left(\frac{L_{int}^{R_1}}{2}\right)^2} \sqrt{\frac{8\mu_{R_1}^2}{v_{R_1}^2}}} + \dots \right)$$

$$\dots + \frac{L_{int}^{R_K} \frac{4\Re\{z_{R_K} \mu_{R_K}\}}{v_{R_K}^2} - \tanh\left(\frac{L_{int}^{R_K}}{2}\right) \frac{4\mu_{R_K}^2}{v_{R_K}^2} x_{R_K}}{\sqrt{1 - \tanh\left(\frac{L_{int}^{R_K}}{2}\right)^2} \sqrt{\frac{8\mu_{R_K}^2}{v_{R_K}^2}}} \right) \quad (5.44)$$

where L_{int}^S and $L_{int}^{R_k}$ are intrinsic information for source and k^{th} relay node, respectively. L_{ext}^S and $L_{ext}^{R_k}$ are extrinsic information for source and k^{th} relay node, respectively. σ_i^S and $\sigma_i^{R_k}$ are standart deviations for source and k^{th} relay node, respectively. σ_e^S and $\sigma_e^{R_k}$ are standart deviations for source and k^{th} relay node, respectively. $K+1$ comes from K relay nodes and one source node.

We can use (5.44) to estimate the correlation coefficient, since as K approaches infinity, equation (5.44) approaches to

$$\begin{aligned}
& \lim_{K \rightarrow \infty} \frac{1}{K+1} \left(E \left[\frac{L_{int}^S L_{ext}^S - m_i^S m_e^S}{\sigma_i^S \sigma_e^S} + \frac{L_{int}^{R_1} L_{ext}^{R_1} - m_i^{R_1} m_e^{R_1}}{\sigma_i^{R_1} \sigma_e^{R_1}} + \dots + \frac{L_{int}^{R_K} L_{ext}^{R_K} - m_i^{R_K} m_e^{R_K}}{\sigma_i^{R_K} \sigma_e^{R_K}} \right] \right) \\
&= \lim_{K \rightarrow \infty} \frac{1}{K+1} \left(E \left[\frac{L_{int}^S L_{ext}^S - m_i^S m_e^S}{\sigma_i^S \sigma_e^S} \right] + E \left[\frac{L_{int}^{R_1} L_{ext}^{R_1} - m_i^{R_1} m_e^{R_1}}{\sigma_i^{R_1} \sigma_e^{R_1}} \right] + \dots + E \left[\frac{L_{int}^{R_K} L_{ext}^{R_K} - m_i^{R_K} m_e^{R_K}}{\sigma_i^{R_K} \sigma_e^{R_K}} \right] \right) \\
&= \lim_{K \rightarrow \infty} \frac{1}{K+1} \left(\frac{E[L_{int}^S L_{ext}^S] - m_i^S m_e^S}{\sigma_i^S \sigma_e^S} + \frac{E[L_{int}^{R_1} L_{ext}^{R_1}] - m_i^{R_1} m_e^{R_1}}{\sigma_i^{R_1} \sigma_e^{R_1}} + \dots + \frac{E[L_{int}^{R_K} L_{ext}^{R_K}] - m_i^{R_K} m_e^{R_K}}{\sigma_i^{R_K} \sigma_e^{R_K}} \right) \\
&= \lim_{K \rightarrow \infty} \frac{1}{K+1} (\rho_S + \rho_{R_1} + \dots + \rho_{R_K})
\end{aligned} \tag{5.45}$$

Using mean and variance values of intrinsic and extrinsic information and the correlation coefficient between intrinsic and extrinsic information, we calculate the values of c and d in (5.22).

We simulated the channel for Rayleigh fading channel using two relay nodes. At the source node, 1000 bit data information is encoded with rate $\frac{1}{2}$ LDPC code and at the relay nodes EF technique is used. Channel gains g_1 and g_2 are both 4 dB. At the destination node, iterative decoding where two global iterations are performed is used.

As it is observed in Figure 5.8, SODED-Taylor detector improves the performance by about 0.8 dB relative the sub-optimal detector obtained by Taylor expansion at BER 10^{-5} . Moreover, the performance gap between SODED-Taylor and MAP detector is 0.3 dB. The situation is similar for CLT case, in which SODED-CLT detector improves the performance by about 1 dB relative the sub-optimal detector obtained by CLT assumption at BER 10^{-4} , as is shown in Figure 5.9. And the performance gap between SODED-CLT and MAP detector is 0.5 dB.

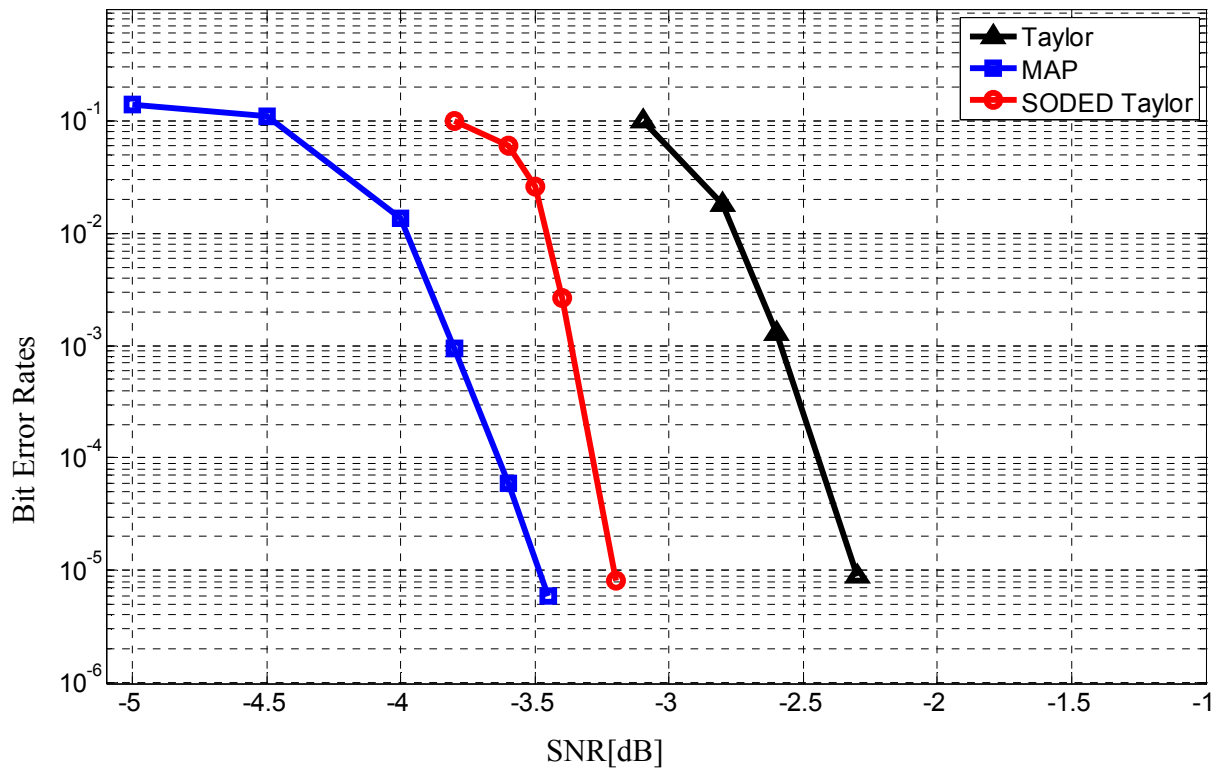


Figure 5.8: BER Comparison of MAP, Taylor and SODED-Taylor detectors

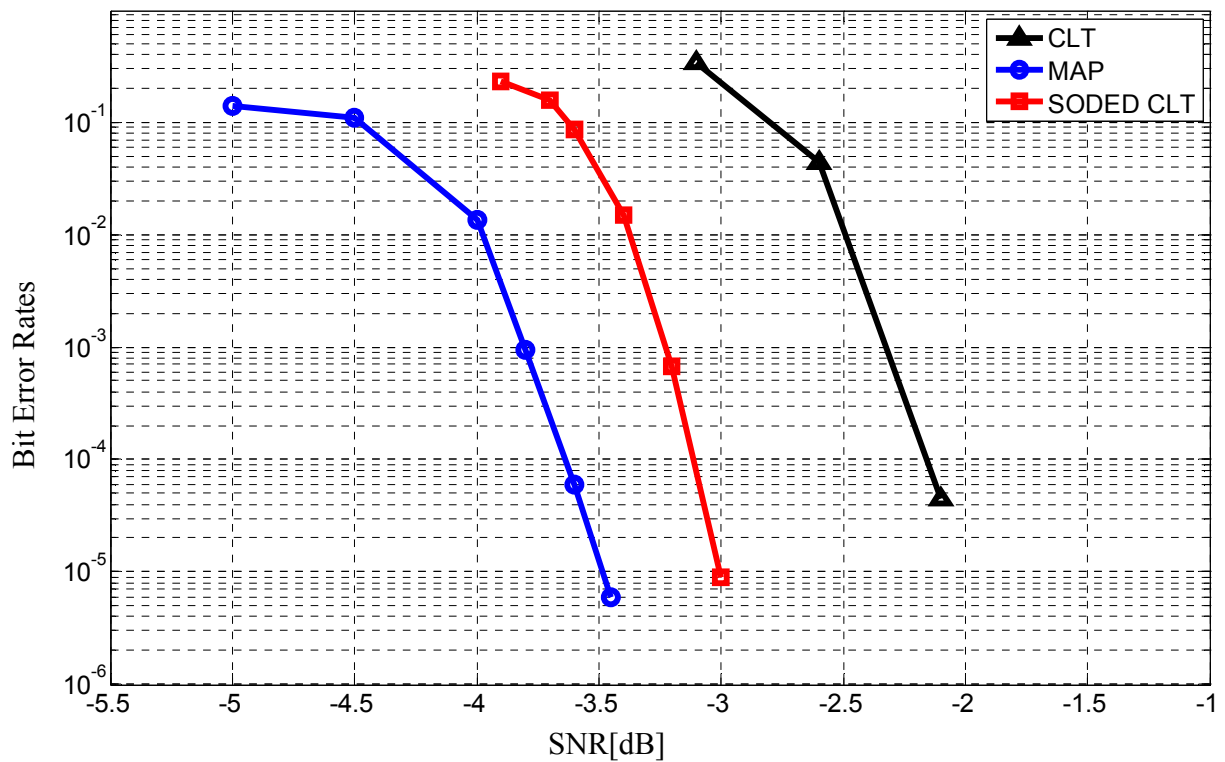


Figure 5.9: BER Comparison of MAP, CLT and SODED-CLT

6. Conclusion

In this thesis, we worked on the simulation of a wireless relay channel, where single relay case is considered. In addition to the channel simulation, we evaluated capacity and information rates, which were useful for comparing single relay channel to direct and multi-hop transmissions. It was shown that relay channels outperform other two transmission schemes. Furthermore, in relay channel the destination observes a superposition of the transmitted codewords from the source and the relay nodes. Therefore, we studied the iterative decoding process, where we had implemented MAP and outer decoders using LDPC soft decision decoding to extract the codeword received by destination.

One relay channel was extended to multiple relay channels and the iterative receiver technique is improved for multiple relay case. In all our simulations, 1000 bit data bit was encoded with rate $\frac{1}{2}$ LDPC codes and sent through Rayleigh fading channels. At the destination, 100 inner LDPC iterations is used and the channel gains g_1, g_2 are both 4 dB. Simulations demonstrated that as the relay number increases, there is a SNR gain. Moreover, it was shown that the SNR gain for both single and multi-relay case also depends on the global iteration number between MAP detector and LDPC decoder. To be specific, for 2 global iteration case, increasing the number of relays from one to two provides us with 3.1 dB BER gain for DF protocol, 4.9 dB BER gain for EF protocol and increasing the number of relays from two to three provides us with 1.1 dB BER gain for for DF protocol, 1.4 dB BER gain for EF protocol at BER 10^{-5} .

Using MAP detector incurs a high computational complexity, as the relay number increases. To alleviate this problem, we investigated two approximations. First, Taylor expansion was considered to approximate MAP detector and a sub-optimal MF-SC detector is observed. It was observed that this sub-optimal detector performs 0.8 dB worse than MAP detector for one global iteration and about 1.1 dB worse for two global iterations. And then, CLT assumption was used to approximate MAP detector and it was

shown that as relay number increases, it approached the performance of MAP and is similar to MMSE-SC. It was demonstrated in simulations that this sub-optimal detector performs 1.1 dB worse than MAP detector for one global iteration and about 1.4 dB worse for two global iterations.

For two relay network, CLT detector worked about 0.3 dB worse than Taylor detector, since CLT detector performs better for large relay numbers, where high interference channel is obtained. Therefore, as we increase the relay number from two to eight, CLT detector is about 0.1 dB better than Taylor detector, since interference also increases with the relay number.

We briefly examined the correlation between intrinsic and extrinsic information of sub-optimal detectors and observed that it is very high. Therefore, to decrease the correlation between these two values, two attenuators are put at the end of sub-optimal detectors. It was observed that as we decorrelated those, we got a better performance. Particularly, for two relay network where relay nodes use EF technique and destination node performs two global iterations, SODED-Taylor detector improves the performance by 0.8 dB BER 10^{-5} and SODED-CLT improves the performance about 1 dB at BER 10^{-4} .

6.1 Future Work

Extensions of this work are possible in the following directions:

- The concept of multi relay nodes with single antennas in relay networks can be generalized to cooperative networks in general. This would pave the way for efficient, wireless peer-to-peer networks. Various cooperation protocols could be established based on different performance goals, such as minimization of the download time, spectral efficiency, minimization of interference, etc.

- The concept of multi relay nodes with single antennas in relay networks can be generalized to multi relay nodes with multiple antennas, since MIMO systems contribute system performance in an efficient way.
- We considered Rayleigh fading in our simulations, which does not consider line-of-sight (LOS) scenario of both the source and the destination for the relay node. But, in practical propagation environments, these assumptions may not hold true. In the future work part, a relay channel model which can take into account both LOS and non-line-of-sight (NLOS) propagation environments should be proposed.
- We also assumed that relay nodes have the same power constraint and transmit with the same transmission power. Using power allocation technique and splitting the total relay transmission power smartly between relay nodes to achieve higher capacity, remains as a future work
- We considered full-duplex multi-relay scheme, where accurate interference cancellation between transmitted and received signals is difficult to achieve. Therefore, extending our work, into half-duplex schemes, which is favorable for current commercial wireless communications systems, remains as a future work.

REFERENCES

- [1] A. J. Goldsmith, *Wireless Communications*, Cambridge, UK: Cambridge University Press, 2005.
- [2] J.G. Andrews, A. Ghosh, and R. Muhamed, *Fundamentals of WiMAX: Understanding Broadband Wireless Networking*, Prentice Hall, 2007.
- [3] W.C. Jakes, *Microwave Mobile Communications*, New York: Wiley, 1974.
- [4] J.G. Proakis, *Digital Communications*, Fourth Edition, McGraw-Hill, 2001
- [5] S.M. Alamouti, "A simple transmit diversity technique for wireless communications," *IEEE Journal on Selected Areas in Communications*, vol. 16, pp. 1451-1458, October 1998.
- [6] H. Jafarkhani, V. Tarokh and A.R. Calderbank, "Space-time block codes from orthogonal designs," *IEEE Trans. Information Theory*, vol. 45, pp. 1456-1467, July 1999
- [7] N. Seshadri, V. Tarokh and A.R. Calderbank, "Space-time codes for high data rate wireless communication: Performance criterion and code construction," *IEEE Trans. Information Theory*, vol. 44, pp. 744-765, March 1998.
- [8] E.C. van der Meulen, "Three-terminal communication channels," *Advanced Applied Probability*, vol. 3, pp. 120–154, 1971.
- [9] T. Unger and A. Klein, "Cooperative MIMO Relaying with Distributed Space-Time Block Codes," *Personal, Indoor and Mobile Radio Communications, IEEE 17th International Symposium on*, pp.1-5, Sept. 2006.
- [10] C.K. Lo, S. Vishwanath, and R.W. Heath, Jr., "Rate Bounds for MIMO Relay Channels Using Precoding," in *Proc. of the IEEE GLOBECOM*, pp. 1172-1176, St. Louis, MO, November 2005.
- [11] T.E. Hunter and A. Nosratinia, "Cooperative diversity through coding," in *Proc. IEEE Int. Symp. Info. Theory*, p. 220, Lausanne, Switzerland, July 2002.
- [12] A. Stefanov and E. Erkip, "Cooperative space-time coding for wireless networks," *IEEE Trans. Commun.*, vol. 53, no. 11, pp. 1804–1809, Nov. 2005.
- [13] R. Nabar, H. Bolcskei, and F. Kneubuhler, "Fading relay channels: Performance limits and space-time signal design," *IEEE Journal on Selected Areas in Communications*, vol. 22, no. 6, pp. 1099-1109, August 2004.
- [14] Z. Zhang and T.M Duman, "Capacity-approaching turbo coding and iterative decoding for relay channels," *IEEE Trans. Commun.*, vol.53, no.11, pp. 1895-1905, Nov. 2005.
- [15] ———, "Capacity approaching turbo coding for half duplex relaying," in *Proc. IEEE Int. Symp. on Info. Theory*, pp. 1888–1892, Adelaide, Australia, Sept. 2005.
- [16] Z. Liu, V. Stankovic, and Z. Xiong, "Wyner-Ziv coding for the half duplex relay channel," in *Proc. IEEE Intl. Conf. on ASSP*, Philadelphia, PA, Mar. 2005, pp. 1113–1116.
- [17] M.A. Khojastepour, N. Ahmed, and B. Aazhang, "Code design for the relay channel and factor graph decoding," in *Proc. Asilomar Conf. On Signals, Systems and Computers*, Pacific Grove, California, Nov. 2004, pp. 2000–2004.

- [18] A. Chakrabarti, A. Baynast, A. Sabharwal, and B. Aazhang, "LDPC code design for half-duplex decode-and-forward relaying," in *Proc. Allerton Conf.*, Illinois, Sept. 2005.
- [19] P. Razaghi and W. Yu, "Bi-layer LDPC codes for the relay channel," in *Proc. Intl. Conf. on Commun.*, Istanbul, Turkey, June 2006
- [20] J. Hu and T.M. Duman, "Low Density Parity Check Codes over Wireless Relay Channels," *IEEE Trans. on Wireless Communications*, vol. 6, no. 9, pp. 3384-3394, Sep. 2007.
- [21] R.G. Gallager, "Low-Density Parity-Check codes," Ph.d thesis, MIT Press, Cambridge, MA, 1963.
- [22] D.J.C. MacKay, "Good error-correcting codes based on very sparse matrices," *IEEE Trans. Inform. Theory*, vol.45, no.2, pp.399-431, 1999.
- [23] N. Wiberg, "Codes and decoding on general graphs," Ph.d thesis, Linkoping University, Linkoping, Sweden, December 1996.
- [24] S.Y. Chung, G.D. Forney, T.J. Richardson, and R. Urbanke, "On the Design of Low-Density Parity-Check Codes within 0.0045 dB of the Shannon Limit," *IEEE Communications Letters*, vol.5, no.2, pp.58-60, Feb. 2001.
- [25] T. Richardson and R. Urbanke, "The capacity of low-density parity-check codes under message-passing decoding," *IEEE Transactions on Information Theory*, vol.42, no.2, pp.599-618, 2001.
- [26] European Telecommunications Standards Institute (ETSI). Digital Video Broadcasting (DVB) Second generation framing structure for broadband satellite applications; *EN 302 307 V1.1.1*. www.dvb.org.
- [27] M. Luby, M. Mitzenmacher, A. Shokrollahi, and D. Spielman, "Efficient erasure correcting codes," *IEEE Transactions on Information Theory*, vol. 47, no. 2, Feb. 2001
- [28] M. Tanner, "A recursive approach to low complexity codes," *IEEE Trans. Inform. Theory*, vol.27, no. 5, Sep. 1981
- [29] T. Richardson, A. Shokrollahi, and R. Urbanke, "Design of provably good low-density parity-check codes," *IEEE Trans. Inform. Theory*, vol. 47, pp. 619-637, Feb. 2001
- [30] T. Richardson and R. Urbanke, "Efficient encoding of low-density parity- check codes," *IEEE Trans. on Information Theory*, vol. 47, no. 2, Feb. 2001
- [31] W. E. Ryan, "An Introduction to LDPC Codes," in *CRC Handbook for Coding and Signal Processing for Recording Systems* (B. Vasic, ed.) CRC Press, 2004.
- [32] A. Sendonaris, E. Erkip, and B. Aazhang, "User cooperation diversity: Part I and Part II," *IEEE Trans. Commun.*, vol. 51, no. 11, pp. 1927-1948, Nov. 2003.
- [33] J.N. Laneman, D. N. C. Tse, and G.W. Wornell, "Cooperative diversity in wireless networks: Efficient protocols and outage behavior," *IEEE Trans. Inf. Theory*, vol. 50, no. 12, pp. 3062-3080, Dec. 2004.
- [34] T.M. Cover and A.E. Gamal, "Capacity theorems for the relay channel," *IEEE Trans. Inf. Theory*, vol. 25, no. 5, pp. 572-584, Sept. 1979.

- [35] A. Chakrabarti, A. De Baynast, A. Sabharwal, and B. Aazhang, "Half-duplex estimate-and-forward relaying: bounds and code design," in *IEEE International Symposium on Information Theory (ISIT '06)*, pp. 1239-1243, Seattle, Wash, USA, July 2006.
- [36] T.E. Hunter and A. Nosratinia, "Diversity through coded cooperation," *IEEE Trans. on Wireless Communications*, vol. 5, pp. 283-289, Feb. 2006.
- [37] T. Hunter, S. Sanayei, and A. Nosratinia, "Outage analysis of coded cooperation," *IEEE Trans. on Information Theory*, vol. 52, no. 2, pp. 375-391, February 2006.
- [38] P. Mitran, H. Ochiai, and V. Tarokh, "Space-time diversity enhancements using collaborative communications," *IEEE Trans. on Information Theory*, vol. 51, no.6, pp. 2041-2057, June 2005.
- [39] B. Zhao and M. Valenti, "Distributed turbo coded diversity for relay channel," *IEEE Electronics Letters*, vol. 39, no. 10, pp. 786-787, May 2003.
- [40] M. Janani, A. Hedayat, T. Hunter, and A. Nosratinia, "Coded cooperation in wireless communications: Space-time transmission and iterative decoding," *IEEE Trans. Signal Process.* vol.52, no.2, pp.362-371, Feb. 2004.
- [41] M.R. Souryal and B.R. Vojcic, "Cooperative turbo coding with time-varying rayleigh fading channels," in *Proc. Intl. Conf. on Commun.*, Paris, France, June 2004, pp. 356-360.
- [42] Z. Liu, V. Stankovic, and Z. Xiong, "Wyner-Ziv coding for the half duplex relay channel," in *Proc. IEEE Intl. Conf. on ASSP*, Philadelphia, PA, Mar. 2005, pp. 1113-1116.
- [43] D. Burshtein, M. Krivelevich, S. Litsyn, and G. Miller, "Upper Bounds on the Rate of LDPC Codes," *IEEE Trans. Inf. Theory*, vol. 48, no. 9, September 2002.
- [44] S. Chae and Y. Park, "Low Complexity Encoding of Regular Low Density Parity Check Codes," *IEEE Vehicular Technology Conference*, vol.3, pp. 1822-1826, Oct. 2003.
- [45] D. Raphaeli and Y. Zarai, "Combined turbo equalization and turbo decoding," in *Proc. IEEE Global Commun. Conf.*, vol. 2, Nov. 1997, pp. 639-643.
- [46] C. Douillard, M. Jezequel, C. Berrou, A. Picart, P. Didier, and A. Glavieux, "Iterative correction of intersymbol interference: Turbo equalization," *Eur. Trans. Telecomm.*, vol. 6, pp. 507-511, Sept./Oct. 1995.
- [47] Wireless Tech. Info, available at <http://www.zytrax.com/tech/wireless/soup.html>
- [48] Specifications of DELL WLAN card, available at <http://support.ap.dell.com/support/edocs/network/p44970/en/specs.htm>
- [49] 3GPP TS 22.105 – Services and service capabilities (Release 8) – January 2007, available at http://www.arib.or.jp/IMT-2000/V710Dec08/5_Appendix/Rel8/22/22105-840.pdf
- [50] C. Carbonelli, S.H. Chen and U. Mitra, "Error propagation analysis for underwater cooperative multi-hop communications," *Ad Hoc Networks*, vol. 7, no. 4, pp. 759-769, June 2009.
- [51] J. Boyer, D.D. Falconer, and H. Yanikomeroglu, "Multihop Diversity in Wireless Relaying Channels," *IEEE Trans. Comm.*, vol. 3, no. 6, pp. 1963-1968, 2004.

- [52] M.A. Khojastepour, A.S., B. Aazhang, “ Lower Bounds on the Capacity of Gaussian Relay Channel,” 38th annual conference on information sciences and systems, Princeton, New Jersey, March 2004
- [53] X. Wang and H.V. Poor, “Iterative (turbo) soft interference cancellation and decoding for coded CDMA,” *IEEE Trans. Commun.*, vol. 47, pp. 1046-1061, July 1999
- [54] M. Tuchler, A. Singer, and R. Koetter, “Minimum mean squared error equalization using *a priori* information,” *IEEE Trans. Sig. Proc.*, vol. 50, pp. 673-683, Mar. 2002.
- [55] J. Choi, “Low complexity MAP detection using approximate LLR for CDMA iterative receivers,” *IEEE Communications Letters*, vol. 10, no. 5, May 2006.
- [56] J. Choi, “A correlation based analysis for approximate MAP detectors and iterative receivers,” *IEEE Trans. Wireless Communications*, vol. 6, no. 5, pp. 1764-1773, May 2007.
- [57] K. Li and X. Wang, “EXIT chart analysis of turbo multiuser detection,” *IEEE Trans. Wireless Commun.*, vol. 4, pp. 300-311, Jan. 2005.
- [58] R. Böhnke, D. Wübben, V. Kühn, and K.D. Kammeyer, "Reduced complexity MMSE detection for BLAST architectures," in *Proceedings of IEEE Global Telecommunications Conference (GLOBECOM '03)*, vol. 4, pp. 2258-2262, San Francisco, Calif, USA, December 2003.
- [59] T. Ito, X. Wang, Y. Kakura, et al., “Performance comparison of MF and MMSE combined iterative soft interference canceller and V-BLAST technique in MIMO/OFDM systems,” *Proceedings of the IEEE 58th. Vehicular Technology Conference - VTC 2003* 1:488-492, 2003
- [60] M. Tüchler, R. Koetter, and A. C. Singer, “Turbo equalization: principles and new results”, *IEEE Tans. Signal Process.*, vol. 50, no.5, pp.754-756, May 2002.
- [61] P. Robertson, E. Villebrun, and P. Hoeher, “A comparison of optimal and sub-optimal MAP decoding algorithms operating in the log domain,” in *Proc. IEEE Int. Conf. Communications (ICC)*, 1995, pp. 1009–1013
- [62] L. Papke, P. Robertson, and E. Villerbrun, “Improved decoding with the SOVA in a parallel concatenated (turbo-code) scheme,” in *Proc. IEEE Int. Conf. Communications (ICC)*, Jun. 1996, pp. 102–106.
- [63] G. Colavolpe, G. Ferrari, and R. Raheli, “Extrinsic information in iterative decoding: A unified view,” *IEEE Trans. Commun.*, vol. 49, no. 12, pp. 2088–2094, Dec. 2001.
- [64] D.W. Kim, T.W. Kwon, J.R. Choi, and J. J. Kong, “A modified two-step SOVA-based turbo decoder with a fixed scaling factor,” in *Proc. IEEE ISCAS*, vol. 4, May 2000, pp. 37–40.
- [65] S. Papaharalabos, P. Sweeney, and B. G. Evans, “Improvements in SOVA-based decoding for turbo codes,” *Electron. Lett.*, vol. 39, no. 19, pp. 1391–1392, Sep. 2003.
- [66] L. Lin and R.S. Cheng, “Improvements in SOVA-based decoding for turbo codes,” in *Proc. IEEE Int. Conf. Communications (ICC)*, Montreal, QC, Canada, Jun. 1997, pp. 1473–1478.
- [67] Z.Wang and K. Parhi, “High performance, high throughput turbo/SOVA decoder design,” *IEEE Trans. Commun.*, vol. 51, no. 4, pp. 570–579, Apr. 2003

- [68] A.Ghrayeb and C.X. Huang, "Improvements in SOVA-based decoding for turbo-coded storage channels", *IEEE Trans. on Magnetics*, vol. 41, no. 12, pp. 4435-4442, December 2005
- [69] H.V. Poor and S. Verd'u, "Probability of error in MMSE multiuser detection," *IEEE Trans. Inform. Theory*, vol. IT-43, pp. 858–871, May 1997.
- [70] H. Omori, T. Asai, and T. Matsumoto, "A matched filter approximation for SC/MMSE iterative equalizers", *IEEE Commun. Lett.*, vol. 5, no.7, pp.310-312, July 2001.
- [71] J. Zhang, E.K.P. Chong, and D.N.C. Tse, "Output MAI distributions of linear MMSE multiuser receivers in DS-CDMA systems," *IEEE Trans. Inform. Theory*, pp. 1128–1144, Mar. 2001.
- [72] S.T. Brink, "Convergence behavior of iterative decoded parallel concatenated codes," *IEEE Transactions on Communications*, vol. 49, pp. 1727– 1737, Oct. 2001.
- [73] K.T(John) Sun, and J. Choi, "Selective detection in an iterative soft-interference cancellation receiver," in *Proc. Asia-Pacific Conf. Comm., APCC 2005*, Oct. 2005, pp.1005-1008.